The role of miR-16
in embryonic brain development

Dissertation zur Erlangung des akademischen Grades

Doktor der Naturwissenschaften

Am Fachbereich Biologie

der Johannes Gutenberg-Universität Mainz

vorgelegt von

Frau Laura Schlichtholz

geb. am 14. Juni 1992 in Freiburg im Breisgau

Mainz, 2021

Dekan: Prof. Dr. Eckhard Thines

1. Berichterstatter: PD Dr. Jennifer Winter

Table of content

Abstract

Micro RNAs (miRNAs) are key players in post transcriptional gene regulatory processes. Upon binding to specific recognition sites harbored mainly in the 3'untranslated regions of their target mRNAs, miRNAs either mediate degradation of these target mRNAs or their translational inhibition (O'Brien et al. 2018). Due to the considerably large number of genes targeted by miRNAs, it is not surprising that they also play a role during brain development. Many aspects of neurogenesis and neuronal migration are controlled by miRNAs and consequently, the misregulation of miRNAs can lead to impairments in these processes. In this study, a miRNA expression analysis was performed to access the miRNA expression profile of the murine embryonic brain at different developmental stages. Based on that, the effect of miR-16 on embryonic brain development was studied in more detail. MiR-16 is part of the miR-15 miRNA family. Other members of this miRNA family have already been shown to be important during embryonic brain development, the role of miR-16, however, remained unclear. To study the exact role of miR-16 in these developmental processes in more detail, a general description of the phenotype caused by miR-16 overexpression was made. For this, miR-16 was overexpressed in vivo in the embryonic neocortex of the mouse brain by in utero electroporation, followed by a range of antibody stainings with different neuronal cell markers. This analysis revealed that miR-16 is an important regulator of neural differentiation. In addition, mRNA sequencing of miR-16 overexpressing neuronal cells was performed to reveal potential target genes of this miRNA. One of the predicted targets, *Wee1*, was validated by performing luciferase reporter assays, western blot analyses and RT-qPCR. Taken together, this study gives an overview of miRNA expression profiles during murine brain development and reveals miR-16 as important regulator of embryonic neurogenesis. Furthermore, the checkpoint kinase *Wee1* was identified as a target of miR-16.

Zusammenfassung

Mikro RNAs (miRNAs) sind wichtige Einflussfaktoren der post-transkriptionell stattfindenden Genregulation. Durch translationale Repression oder Degradierung von mRNA, können miRNAs die Genexpression ihrer Zielgene regulieren (O'Brien et al. 2018). Aufgrund der hohen Anzahl an Genen, die einer Regulation durch miRNAs unterliegen, ist es nicht erstaunlich, dass einige Aspekte der Neurogenese und der Entwicklung des Gehirns ebenfalls von miRNAs reguliert werden. Vielmehr kann ein großer Anteil der neuronalen Entwicklungsstörungen im embryonalen Cortex auf miRNA Fehlregulationen zurückgeführt werden. In dieser Arbeit wurde das miRNA Expressionsprofil im sich entwickelnden, embryonalen Gehirn mittels miRNA Sequenzierung genauer betrachtet. Darauf aufbauend, wurde der Effekt von miR-16 auf die embryonale Gehirnentwicklung genauer untersucht. MiR-16 ist Teil der miR-15 miRNA Familie. In der Vergangenheit konnte gezeigt werden, dass miRNAs aus dieser Familie wichtige Rollen in regulatorischen Prozessen der embryonalen Gehirnentwicklung spielen. Um die Rolle und Targets von miR-16 in diesen regulatorischen Prozessen genauer zu untersuchen, wurde eine mRNA Sequenzierung von mit miR-16 überexprimierten, neuronalen Zellen durchgeführt. *Wee1*, eines der vorhergesagten Targets von miR-16 wurde darauffolgend mittels Luciferase Reporter Assays, Western Blot Analysen und RT-qPCR validiert. Darüber hinaus wurde eine generelle Beschreibung des durch miR-16 Überexpression hervorgerufenen Phänotyps im sich entwickelnden Gehirn vorgenommen. Hierfür wurde miR-16 mittels In Utero Elektroporation im embryonalen Maushirn überexprimiert um anschließend Antikörperfärbungen mit einer Auswahl an neuronalen Zellmarkern durchzuführen. Zusammengefasst gibt diese Studie einen Überblick über die generelle Expression von miRNAs im sich entwickelnden Gehirn und beschreibt miR-16 als möglichen Regulator der embryonalen Gehirnentwicklung. Darüber hinaus wurde die Checkpoint Kinase *Wee1* als wichtiges Target von miR-16 identifiziert und der in vivo durch miR-16 Fehlregulation verursachte Phänotyp wurde beschrieben.

Introduction

1. The developing brain

The brain is one of the most fascinating and complex organs of the human body. A lot of research has been done to figure out how this complex machinery works and how it develops from embryonic stages up to adulthood. Human brain development starts at around week 3 of gestation and proceeds at least until postnatal adolescent stages of development (Stiles et al., 2010). Recent studies even suggest, that the brain´s development is not completed until the third decade of a human´s life (Gibb et al., 2018). One of the most prominent structures of the mammalian brain is the so-called neocortex. This 2-5 mm thick layer of cells lies on the surface of the brain and is part of one of the most important information processing networks of the human body (Stiles et al., 2010).

Size, mass and complexity of the human neocortex increased over the course of evolution so that now it has become the center of the vast cognitive abilities that distinguishes mankind from other mammals (Rakic, 2009). The cortical development from reptiles to the modern human species *Homo sapiens*, came along with a broad variety of changes in the structure of the brain. One of them was the formation of folds and ridges within the cortex, so called gyri (Armstrong et al., 1995). This enabled the cortical surface to increase its number of neurons and to expand to a bigger over all area, which is associated with higher cognitive performances. Most rodents, including mice lack these cortical folds and ridges and are therefore referred to as being “lissencephalic” (Sun et al., 2014).

Even though cortical size and mass do not necessarily correlate with cognitive function and behavioral intelligence in all species, it has been suggested that in humans, cortex size is of major significance concerning brain function and intelligence performance. In line with this assumption, patients suffering from syndromes associated with smaller or enlarged brains, referred to as micro- or macrocephaly, display a wide range of cognitive deficits (Hanzlik et al., 2017). To get a better perception of the brain as a whole and to shed more light on the complex process of brain development, the following chapter

will discuss the origin of brain tissue in the body and the different stages of neurodevelopment.

1.1. Stages of neurodevelopment

Brain development starts, when a first brain like structure emerges from the neural tube. This structure consists of 3 vesicles: The prosen-, mesen- and rhombencephalon, which are the embryonic precursors of the later for-, mid- and hindbrain (Stiles et al., 2010). During further developmental stages, the prosencephalon divides into the telencephalon and the diencephalon, and the rhombencephalon divides into the metencephalon and the myelencephalon (Moreno et al., 2011; Wang, 2004).

The huge diversity of neuronal cell types forming the mammalian brain mostly emerges at embryonic and early postnatal stages (Mira & Morante, 2020). In mice, neurogenesis starts around embryonic day E10 when neuroepithelial cells gradually evolve into apical radial glia cells (RGCs) (Cardénas & Borrell, 2020; Prieto-Colomina et al., 2021). This type of cells with apical-basal polarity is located in the ventricular zone of the developing brain and in the course of time directly or indirectly gives rise to all kinds of cortical neuronal cell types (Juan & Borrell, 2015). By undergoing asymmetric as well as symmetric division, radial glia cells can both self-renew the stem cell pool or produce daughter cells that are either neurons or intermediate progenitor cells (IPCs) (Kriegstein & Alvarez-Buylla, 2009). To keep the balance between the number of IPCs, neurons and RGCs in the developing brain, the process of radial glia division has to be regulated precisely (Taverna et al., 2014).

As more and more RGCs of the ventricular zone start to divide asymmetrical into intermediate progenitor cells, the subventricular zone of the brain is built gradually with an increasing number of Tbr2 positive IPCs (Sessa et al., 2008).

Whereas the basal progenitors populating the subventricular zone seem to have a multipolar morphology, the radial glia cells in the ventricular zone keep their clear apio-basal polarity and ability of self-renewal to constantly undergo symmetric and asymmetric divisions for stem cell pool maintenance or production of neurons (Buchmann et al., 2007).

Most of the basal progenitors in the intermediate zone preferentially undergo symmetrical division and by this, produce mostly neuronal daughter cells which later migrate to the outer layers of the developing brain (Noctor et al., 2008; Hevner et al., 2012).

Figure 1 depicts schemes of the different cell types of the murine and the human cortex.

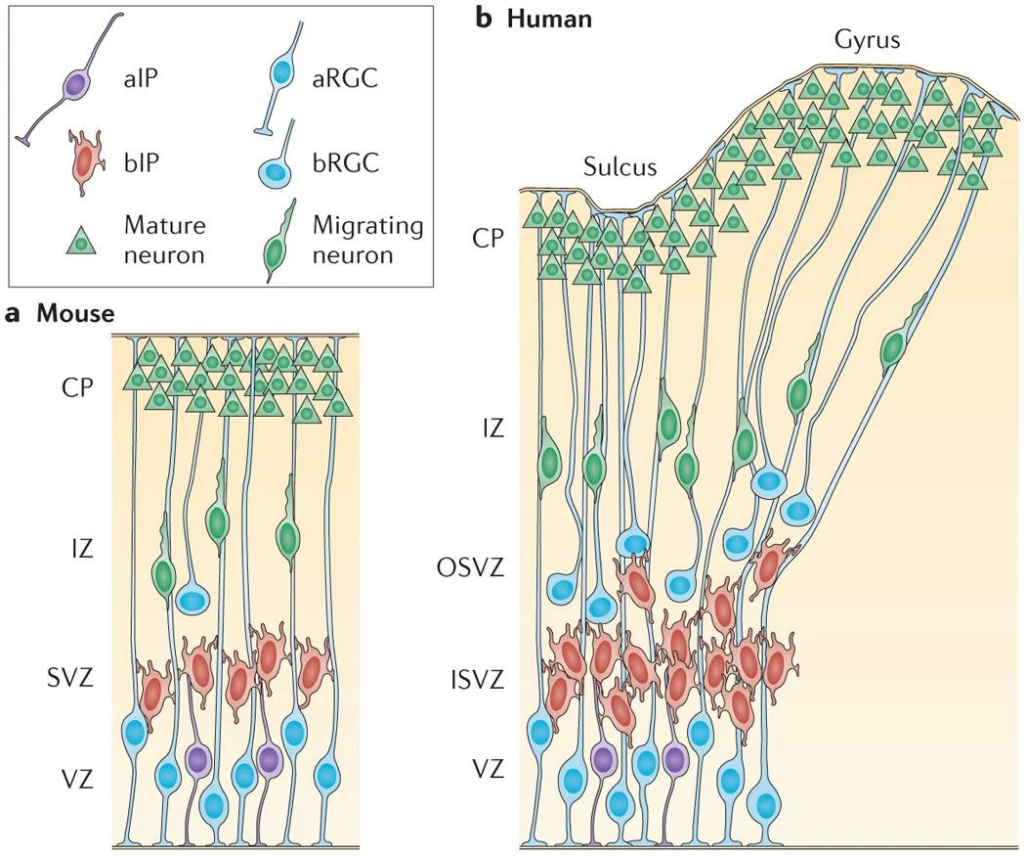

Figure 1: The developing cerebral cortex in mice and humans. aRGCs and aIPCs reside in the ventricular zone, bIPCs in the subventricular zone, bRGCs and migrating neurons in the intermediate zone and mature neurons are located in the cortical plate. (From Sun et al., 2014)

1.2. Neuronal migration

The cortex is built up in a distinctly organized structure containing 6 layers. The inside-out arrangement of cortical neurons locates the youngest neurons farthest and the oldest neurons closest to their place of origin. From bottom to top, the six layers of the cortical plate are numbered from I to VI (Cooper, 2008).

To reach their layer of destination, new born neurons have to make their way from their area of origin through already existing layers of neuronal tissue. This process is called neuronal migration. Neuronal migration can be subclassified into radial and tangential migration. In the developing cerebral cortex, radial migration is the principal mode of neuronal migration (Hatten, M.E., 1999). Neurons born in the ventricular and subventricular zone of cerebral cortex radially migrate into the cortical plate. Tangential migration on the other hand often is used by interneurons born in the ganglionic eminences to travel long, border crossing distances in the brain and is characterized by movements parallel to the surface along axons of other neurons (Marìn et al., 2001). In the case of radial migration, there are two possibilities for new born neurons to migrate out of the ventricular zone to their layers of destination. Somal translocation and neuronal migration along radial glia cells. Due to the fact, that during early phases of cortical formation newborn neurons don't have to travel long distances, somal translocation is preferentially used for migration in these stages of development (Nadarajah et al., 2002). During somal translocation, the migrating neuron extends a long process to the pial surface of the developing brain. After having attached to the outer most layer with its basal process, the soma of the migrating neuron travels towards the pial surface along this process. The end of this migration is characterized by a regression of the neuron´s process and a completed movement of the neuron out of the ventricular zone into the developing cortical plate (Miyata et al., 2001).

With proceeding brain development, the distances that have to be travelled increase and therefore, another mode of neuronal migration occurs. Referred to as "neuronal migration along RGCs", this type of migration describes the movement of neurons along long radial glia processes out of the ventricular zone into developing cortical layers. Whilst the nucleus of the RGCs neurons migrate along is still located in the ventricular zone of the developing brain, their basal processes reach out to the pial surface and attach to it. By attaching to this radial glia process, new born neurons are able to migrate into different cortical layers along the radial glia scaffold (Rakic, 1972).

The "tangential" type of neuronal migration mentioned earlier was described when the ventral telencephalon was identified as a second proliferative zone in the developing embryonic brain. This region was identified as an important source of inhibitory cortical

interneurons (Anderson et al., 2001). In comparison to radially migrating neurons which usually only have one single leading process, neurons that migrate tangentially through the developing brain display far more branched leading processes (Valiente et al., 2010). As tangential migration is mainly regulated by molecular guidance cues, tangentially migrating neurons have to rapidly react to different cues by maintaining a number of leading process branches similarly (Huang, 2009).

Cortical development is strictly regulated by so called Cajal-Retzius cells (CR cells), which have been first described in 1891 by Santiago Ramón y Cajal and Gustaf Retzius. In early stages of development, these cells have migrated tangentially into the developing cortex and form a border for other migrating neurons by being continually pushed along as the cortex grows in its inside-out manner (Soriano et al., 2005). Like this, the CR cells form the marginal zone of the developing cortex which makes them the only cells not subjected to the inside-out birth order of the remaining developing cortex (Cooper, 2008). Figure 2 shows a scheme of the adult and developing embryonic neocortex with its 6 different layers. In the context of CR cells, it is also important to shed some light on the reelin pathway. The molecular signal reelin is produced by the CR cells in the upper most layer of the developing brain and signals the migrating neurons where and when to stop their migration through the cortical layers (Bielle et al., 2005). The accuracy of reelin signaling is very important, as disruptions of this pathway lead to defects in the laminar structure and conglomerates of neurons that are unable to migrate properly to their layer of destination in the developing brain (Rice et al., 2001).

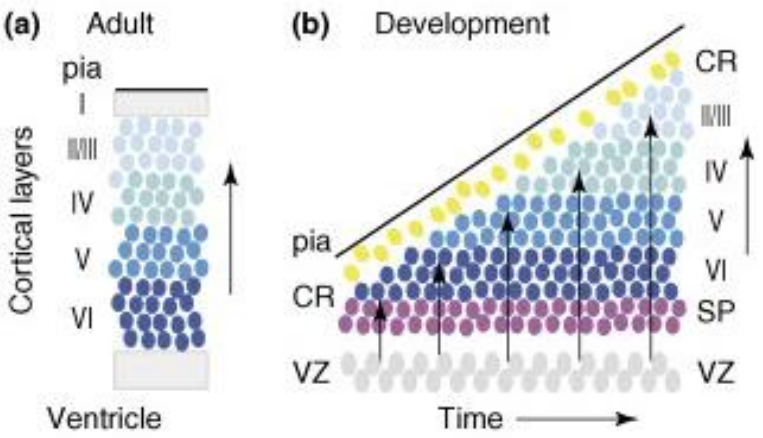

Figure 2: The six layers of the developing brain. New born neurons add themselves to the developing cortex in an inside-out manner. (From Cooper, 2008)

1.3. Different types of neurons and synaptic transmission

Young neurons develop neuronal processes in the form of axons and dendrites as soon as they arrive in their target region of the cortex. These processes allow the neurons to integrate into neuronal networks of the brain and to communicate with other, neighboring brain cells (Stiles et al., 2010). Generally, neurons consist of the cell body, referred to a soma, one single outreaching axon covered by a myelin sheath and a huge number of dendrites, that form arbor-like structures and spread out to other cells (Brown et al., 2005). Figure 3 shows a schematic drawing of a neuron. Whereas axons are that part of the nerve cell that sends information to other cells of the body, the dendritic arbors spread out to receive messages and cues from the surrounding environment including other nerve cells. To help the neuron navigate through the brain tissue, every axon exhibits growth cones at the top of its process. This growth cone helps to sample the environment for attractive and repulsive cues and assists the neuron to find the way to its target (Stiles et al., 2010).

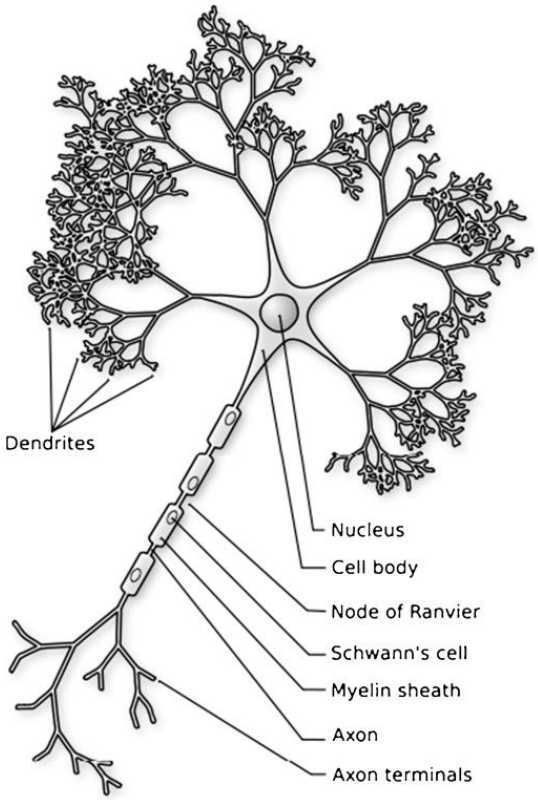

Figure 3: Schematic drawing of a neuron. (From Stiles at al., 2010)

Communication between two neurons is performed via synaptic transmission. The synapses located on the axon terminal of a signal sending neuron(presynaptic) release neurotransmitters and electrochemical cues which are recognized by receptors on the dendrites of the signal receiving neuron(postsynaptic) (Freissmuth et al., 2020).

Although all neurons respond to and send electrochemical nerve signals, there are still different types of neurons that are characterized by varying structures and functions in the central nervous system. Whilst so called sensory neurons display a bipolar shape to detect and convert different kinds of stimuli of the environment, motorneurons which are unipolar, carry signals from the central nervous system to the muscles of the body. In between these two types of neurons, a third type can be found, interneurons. Interneurons display a pseudounipolar shape with two axons connected to both the central nervous system and muscle tissue and therefore facilitate communication of the different neuronal cell types in the brain (Abraira et al., 2013).

1.4. Cell cycle and neurogenesis

As already described above, the brain emerges from a limited number on neuroepithelial and primary neuronal stem cells. The formation of neuronal networks out of these stem cells is precisely orchestrated and numerous factors regulate the division and proliferation of these cells. The eucaryotic cell cycle can be divided into four phases: M phase, G1 phase, S phase and G2 phase (Cheffer at al., 2013). G1-, S- and G2 phase are often referred to as interphase. During these phases, the DNA of the cell is duplicated in order to build a fully functional daughter cell. The division of the nucleus takes place during mitosis (M phase). Mitosis is divided into prophase, metaphase, anaphase and telophase. During prophase, the duplicated chromatin condenses and the nuclear membrane dissolves. At the two poles of the dividing cell, the spindle apparatus emerges. Metaphase is characterized by the attachment of the spindle apparatus´ microtubules to the condensed chromosomes and thereby an arrangement of the chromosomes at the equatorial level of the cell. During anaphase, the sister chromatids eventually divide from one another and move to the opposite poles of the cell, directed by the attached microtubules of the spindle apparatus. Telophase completes cell division by duplicating all remaining cellular components and organelles, referred to as cytokinesis, and by re-establishing the normal cellular shape. By the end of telophase,

the chromatids have decondensed and have returned to their loose form. After mitosis is completed, the cell moves into G1 phase to prepare for DNA replication which occurs in S phase. Subsequently, during G2 phase, the cell again prepares for another mitosis. Cells that are not dividing at the moment can also enter a resting state, referred to as G0 phase. In this state, no DNA duplication or nuclear division takes place. Most of the non-growing and non-proliferative cells of the human body reside in G0 phase (McIntosh, 2016). Figure 4 shows an overview of the different phases of the cell cycle and involved factors.

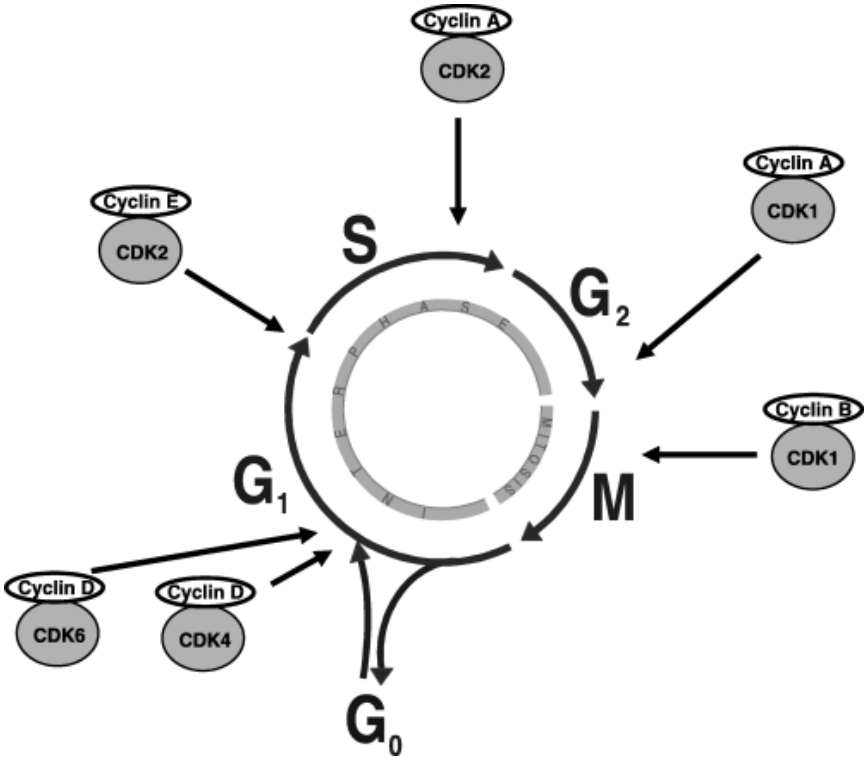

Figure 4: The cell cycle. With Mitosis, G0-, G1-, S- and G2 phase (From Vermeulen et al., 2003).

In order to maintain the correct sequence, the cell cycle is strictly regulated by a wide range of cellular proteins. One of the most important regulators of the cell cycle are cyclin dependent kinases (CDKs). These serine/threonine protein kinases are activated throughout the cell cycle and effect the cell cycle by phosphorylation of downstream targets (Morgan, 1995). CDKs are activated by specific cyclins whose levels periodically vary during different phases of the cell cycle (Pines, 1995). As depicted in figure 4, different CDKs and cyclins act on different phases of the cell cycle. Besides cyclins, CDKs can also be regulated by phosphorylation of conserved threonine and tyrosine residues.

This inactivation occurs through kinases as Wee1 and Myt1 and can be reversed by the enzyme Cdc25 (Malumbres, 2014; Lew, 1996).

To ensure that each phase of the cell cycle is conducted properly and in sequence, the cell cycle is intermitted by so called check points which enable the cell to perform quality controls of the processes that have happened so far. One main use of these checkpoints is the detection of DNA and spindle damage before and after S phase. The most important checkpoints are the G1-S and the G2-M checkpoints. At the G1-S checkpoint, cells displaying an abnormally high level of p53 are detected and arrested in their cell cycle due to possible DNA damage (Levine, 1997). p53 is a transcription factor which is known to be highly active in DNA damaged cells and which has also been shown to play a role in tumor suppression (Chen, 2016). It has been documented, that p53 enhances the transcription of a variety of genes, including *p21*, which is known to inhibit CDKs and therefore effects a cell cycle arrest of the DNA damaged cell (Ko et al., 1996). The G2-M checkpoint on the other hand is p53 independent and keeps damaged cells from entry into mitosis by simply maintaining CDK1 in its inhibited form (Zeng et al., 1998).

In order to produce new neurons in the cerebral cortex, neuronal progenitor cells have to leave the cell cycle and differentiate. Cell divisions can be classified as proliferative divisions and differentiative divisions. As already described in chapter 1.1., during symmetric proliferative division, cells divide into two identical daughter cells. Besides this, asymmetric differentiative divisions are described as another mode of division in which one neuronal stem cell divides into an identical daughter stem cell and a neuron. Neurons are terminally differentiated, postmitotic cells and therefore are not able to divide or differentiate any further (Götz el al., 2005).

Cell cycle length and phases vary dependent on the state of neurogenesis in the developing brain. During development, when increasing numbers of radial glia cells switch from proliferative to neurogenic mode to differentiate into IPCs and later neurons, the cell cycle and especially the G1 phase lengthens (Takahashi et al., 1995). The “cell cycle length” hypothesis states, that a lengthening of G1 phase induces neural stem cells to switch into neurogenic differentiation mode (Lukaszewicz et al., 2002). If the G1 phase lengthens, cell exposure to different cell fate determining factors increases, and cells switch from proliferative to neurogenic differentiation mode

(Calegari et al., 2003). Furthermore, the “cell cycle length” hypothesis states, that with increasing cell cycle length the neural stem cells first switch from symmetric, proliferative divisions to asymmetric, neurogenic divisions and finally end with symmetric, neurogenic divisions to produce two similar neuronal daughter cells (Götz el al., 2005).

2. Neurodevelopmental disorders

The last chapters gave a brief overview of the enormous complexity of brain development. In consideration of this complexity, it is no surprise, that many difficulties and problems can occur during the process of brain development. The range of neurodevelopmental disorders spans developmental brain dysfunctions, impaired motor learning and function, problems in verbal and non-verbal communication, neuropsychiatric problems and many other impairments. The Fifth edition of the Diagnostic and Statistical Manual of Mental Disorders (DSM-V; American Psychiatric Association, 2013) defines neurodevelopmental disorders as an own category and includes intellectual disabilities, autism spectrum disorder (ASD), Attention-Deficit/Hyperactivity Disorder (ADHD), schizophrenia and bipolar disorders (Vahia, 2013). According to the DSM-V, the basis of all neurodevelopmental disorders are impairments in brain function which occur with the beginning of development in prenatal stages or early childhood. (Morris-Rosendahl et al., 2020).

3. Micro RNAs

3.1. Epigenetic modulation

More than 20 years ago, the term epigenetics was described as “the study of mitotically and/or meiotically heritable changes in gene function that cannot be explained by changes in DNA sequence” (Russo et al., 1996). As cited, the term epigenetics refers to any modification to the DNA that can be inherited to daughter cells and somehow has an effect on gene activity without directly changing the DNA sequence (Weinhold, 2006). Jakovcevski et al. describe the “epigenome” as the sum of all three-dimensional structures, modifications and molecular regulations of DNA inside the cell’s nucleus (Jakovcevski et al., 2012).

Epigenetic modifications include DNA methylation, histone modifications and non-coding RNA-mediated regulation, including miRNAs (Kyzar et al., 2016). DNA methylation and histone modifications regulate gene expression by giving or denying access to the chromatin complex and therefore increasing or decreasing transcriptional processes (Krishnan et al., 2014).

The epigenetic process of DNA methylation that is best-known is driven by the attachment of a methyl group to a cytosine nucleotide. Methylated DNA is known to be suppressed in its gene expression. Other modifications such as oxidations of methylated cytosines and other have also been described (Klungland et al., 2017). Histone modification either occur in form of acetylation or methylation of histones. Just as it is the case with DNA methylations, methylated histones are markers for closed chromatin whereas acetylated histones are a mark for open chromatin and increased transcription of the affected DNA (Kumar et al., 2018). Histones have also been shown to underlie other modifications as phosphorylation and ubiquitination (Wei et al., 2017).

The third epigenetic mechanism refers to all kinds of RNA regulations by non-coding RNAs. Non coding RNAs are a group of RNAs that do not encode for proteins and are therefore not translated. They can be divided into so called housekeeping RNAs and regulatory RNAs. Regulatory RNAs can be subdivided into siRNAs, piRNAs, miRNAs and lncRNAs (Zaratiegui et al., 2007). These types of non-coding RNAs have been found to play major roles in regulation of gene expression and also cell differentiation (Wei et al., 2017). Table 1 shows an overview of the different types of non-coding RNAs and their main functions.

Name	Size	Source	Functions
siRNA	19-24 bp	ds RNA	Silent transcription gene
miRNA	19-24 bp	pri miRNA	Silent transcription gene
piRNA	26-31 bp	long single chain precurser	Transposon repression
lncRNA	>200 bp	multiple ways	Genomic imprinting

Table 1: Main non-coding RNAs in epigenetics. (Adapted from Wei et al., 2017)

siRNAs are cut from long double stranded RNA molecules into 19-24 nucleotides long fragments by the enzyme Dicer. They form a complex with AGO proteins and together with them act as transcriptional gene silencers (Moazed, 2009).

Even though miRNAs have the same size as siRNAs, their main difference is, that miRNAs, other than siRNAs are single stranded. Detailed information about miRNA biogenesis can be found in chapter 3.2. miRNAs cleave and degrade their mRNA targets by recognizing complementary 6-8 bp long sequences, so called seed sequences (Bartel, 2009). Aberrant miRNA expression profiles have been shown to affect chromatin state by suppressing chromatin remodeling enzyme activity through histone modification (Denis et al., 2011). Tumor miRNAs as miRNA-17 and miRNA-20a for example have been shown to induce the formation of heterochromatin (Gonzales et al., 2008).

piRNAs, or also Piwi-interacting RNAs, are important regulators of Piwi proteins which act as silencing factors during epigenetic regulatory processes. piRNAs originate from single chain precursors and are strongly associated with chromatin regulation and repression of RNA polymerase II transcription (Huang et al., 2013).

The rarely protein encoding class of long non coding RNAs (lncRNAs) can be divided into several categories and mainly derive from disrupted reading frames of protein coding genes or chromosomal reorganization (Ponting et al., 2009). lncRNAs have been found to be involved in the epigenetic regulation of x chromosome inactivation and genomic imprinting (Yang et al., 2015). It has also been proposed, that lncRNAs and some miRNAs interact and therefore form more complex networks of epigenetic regulation (Paraskevopoulou et al., 2016).

As the main focus of this thesis is on miRNA function during neurogenesis and brain development, in the following chapters, miRNA biogenesis as well as the effect of miRNAs on brain development and disease studied so far will be explained in more detail.

3.2. Micro RNA biogenesis and function

The first description of a micro-RNA (miRNA) was made in 1993, when the small, noncoding RNA *lin-4* was found in *Caenorhabditis elegans* (Lee et al., 1993). This miRNA was identified as a posttranscriptional regulator of lin-14. Since this discovery, miRNAs

have been found in all animals and also have been shown to be highly conserved across species (O'Brien et al., 2018).

MicroRNAs (miRNAs) are 21-23 nucleotides long, non-coding RNAs which regulate gene expression post-transcriptionally. By binding to specific recognition sequences which are mostly located in the 3´untranslated regions of target genes mature miRNAs mark mRNAs for degradation or translation inhibition (Vo et al. 2010). This gene silencing process is mediated by the RISC complex (RNA induced silencing complex) a ribonucleoprotein complex consisting of miRNAs associated with Argonaute proteins (Winter et al. 2009).

In the course of time, the importance of miRNAs has become more and more clear. They have been found to play critical roles in developmental processes and a wide range of biological processes (Fu et al., 2013). Thus, it is not surprising that many miRNAs are involved in many human diseases like for example cancer and developmental problems. Besides being expressed intracellularly, miRNAs have also been reported to act as extracellular signaling molecules which participate in cell-cell communications (Huang, 2017).

As depicted in figure 5, miRNA genes are transcribed by RNA polymerase II or III to give rise to primary miRNAs (pri-miRNAs) which are typically several hundred nucleotides long and contain a 33 base pair long hairpin stem, a flanking single stranded sequence and a terminal loop (Romero-Cordoba et al. 2014). The pri-miRNA usually is polyadenylated at the 3´end and 7-methylguanosin capped at the 5´end. The microprocessor complex formed by the ribonuclease Drosha and the dsRNA binding protein DGCR8 cleaves the pri-miRNA. The resulting precursor miRNA (pre-miRNA) translocates from the nucleus to the cytoplasm where the RNAse Dicer in complex with the double stranded RNA binding protein TRBP digests the pre-miRNA hairpin to its mature length of about 22 nucleotides. In a final step, the functional, so-called guiding strand of the miRNA duplex is loaded onto the RISC complex whose core components are the Argonaute proteins. The “passenger” strand is not included and usually degraded (Romero-Cordoba et al. 2014; Winter et al. 2009).

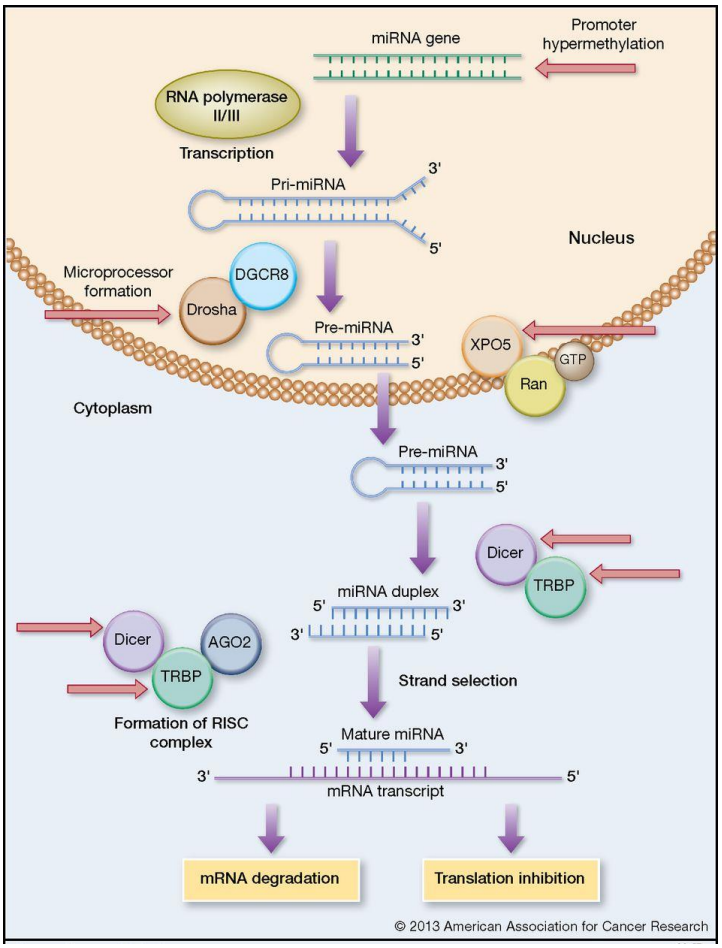

Figure 5: miRNA biogenesis. (From Mulrane et al., 2013)

Not all modes of miRNA regulation are completely understood by now. And as explained above, most studies have concentrated on the translational repression induced by miRNAs binding to the 3´UTR region of their target genes. However, miRNA binding sites have also been found in 5´UTR regions, promoter regions and even in coding sequences (Xu et al., 2014). Contrary to 5´UTR and coding sequence binding, miRNAs binding to promoter regions of target genes have been described to induce transcription (Dharap et al., 2013). *Let-7* for example has been found to induce translation during cell cycle arrest and other miRNAs seem to upregulate gene expression in quiescent cells, such as oocytes (Bukhari et al., 2016).

The effect of miRNAs on their target mRNA is not the same in every cell type. To regulate a target mRNA, one specific miRNA first has to be available in a sufficient amount at the right place. Factors like alternative polyadenylation, alternative splicing as well as secondary structures of target mRNAs have also been identified to play important roles in terms of defining targets as sensitive or in-sensitive to miRNA regulation (Blazie et al.,

2017). To overcome the problem of miRNAs not being able to successfully regulate their target mRNAs due to lacking proximity or concentrations, the cell spatially enriches mRNAs and their according miRNA-RISC complexes and therefore promotes efficient gene expression regulation (Barman et al., 2015). Genome wide analyses of the FANTOM5 (Functional Annotation of the Mammalian Genome) consortium discovered, that half of the expressed miRNAs are cell type specific and that one particular cell type usually is regulated up to 50% by a handful of "top expressed" miRNAs (Rie et al., 2017).

As already stated above, miRNAs are not only present intracellularly but are also excreted to extracellular locations. So far, miRNAs have been detected in a variety of biological fluids as for example breast milk, tears, urine, saliva and many more (O´Brien et al., 2018). Surprisingly, contrary to intracellular RNA, extracellular miRNAs have been shown to be highly stable. Besides resisting degradation at room temperature, extracellular miRNAs also seem to be insensitive to boiling and multiple freeze-thaw cycles (Chen et al., 2008). Extracellular miRNAs are either bound to proteins such as AGO2 or can be found in vesicles. This protein binding or vesicular transport is believed to protect the miRNAs from extracellular environmental influence and is said to increase the miRNAs stability (Gallo et al., 2012). In terms of cell-cell communication, miRNAs have been shown to regulate different biological functions as neurodegeneration, tumor growth and metastasis by binding to Toll-like receptors of the affected cells (Fabbri, 2018). However, the exact ways how miRNAs are secreted from cells and how particularly they act on signal-receiving cells remains poorly understood and still has to be studied in more detail.

3.3. The role of miRNAs in brain development and in disease

Since the discovery of miRNAs and their identification as post transcriptional regulators of gene expression, more and more studies have underlined the importance of miRNAs for different physiological processes in the body. MiRNAs are best known for acting as oncogenes or tumor suppressors (Peng et al., 2016). Besides this, they have also been identified as important regulators of brain growth and development. A study published in 2004 showed, that miRNAs are expressed in the entire central nervous system. Moreover, miRNAs have been found to show specific expression profiles in all kinds of cell types important for development (Sempere et al., 2004). Due to these expression

profiles, it is not surprising, that miRNAs have also been identified as important key players in the development of the cortex (Bhalala et al., 2013). As depicted in figure 6, miRNAs are involved in many neurodevelopmental processes including astrocyte and oligodendrocyte differentiation, NPC differentiation and proliferation and axonal outgrowth (Cho et al., 2019).

It has been found, for example, that miR-125 and let-7b are important regulators during astrocyte maturation and miRNAs -138, -219, -338, -199a and -145 play a role in oligodendrocyte differentiation (Shenoy et al., 2015; Letzen et al., 2010). MiRNAs -9, -124 and miRNAs of the 17-92 cluster on the other hand have been identified to be involved in axonal outgrowth and NPC differentiation and proliferation (Bian et al., 2013; Radhakrishnan & Alwin Prem Anand, 2016).

In general, a wide range of miRNAs has been shown to display specific expression patterns throughout the different stages of neurodevelopment and therefore seem to play major roles in neuronal differentiation and maturation, neuronal migration and many other processes during brain development (Sen, 2014).

Since they play a huge role in neurodevelopmental processes, it is likely, that miRNAs also act as important factors of brain malformation and disease. Many neurodegenerative diseases as Alzheimer´s and Huntington´s disease or epilepsy seem to be influenced by dysregulated miRNAs in the brain (Godlewski et al., 2019; Hussein et al., 2021). A study published in 2020 identified heritable expression profiles of six miRNAs specific to autism spectrum disorder (Ozkul et al., 2020). Furthermore, Hicks et al. proposed the possibility of using miRNAs as biomarkers for ASD as decreased levels of miRNAs have been found in the brain, blood and saliva of ASD patients (Hicks et al., 2016). The gene *MECP2* which is associated with Rett syndrome and autism also seems to underlie miRNA regulation, as a downregulation of miR-132 leads to an increased expression of this gene (Zhang et al., 2015).

In conclusion, miRNAs are involved in a great variety of brain development processes and diseases. Besides their role as potential biomarkers for ASD and other neurodevelopmental disorders, the regulatory effect of miRNAs on a wide range of

genes qualifies them as important key players in brain development and disease (Schepici et al., 2019). The following chapter will focus on the miR-15 miRNA family. This family is of special importance for the work described in this thesis, as it includes many miRNAs, amongst them miR-16, that have been found to be involved in several neurodevelopmental processes in the brain.

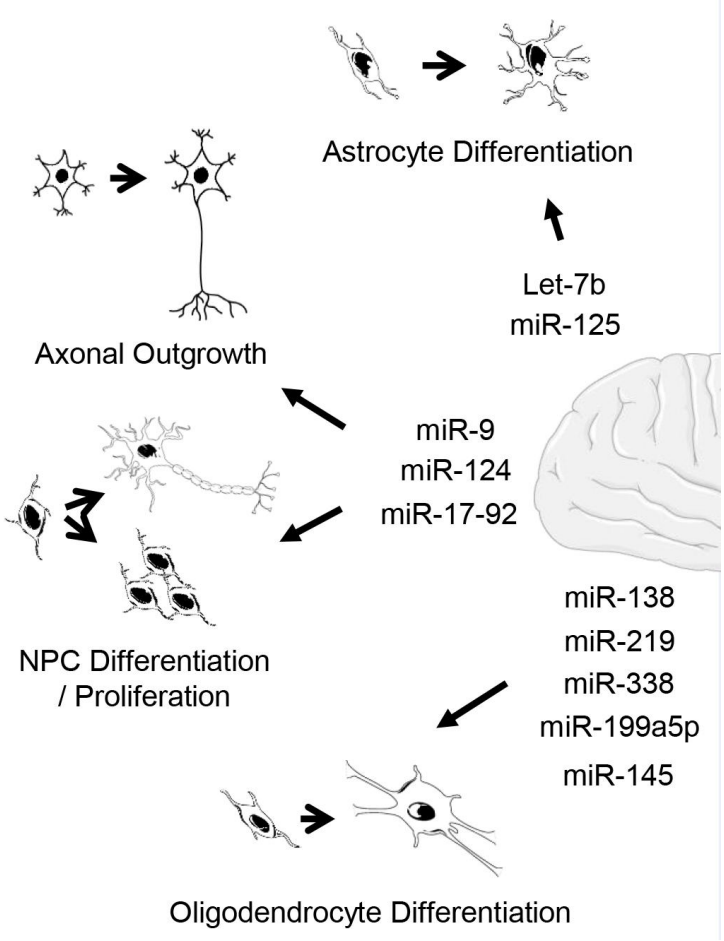

Figure 6: Roles of different miRNAs in brain development. (Adapted from Cho et al., 2019)

3.4. The miR-15 miRNA family

The miR-15 miRNA family includes miR-15a, -15b, -16, -103, -107, -195, -424, -497, -646 and miR-503 of whom the latter five are exclusively expressed in mammals. Members of the miR-15 family have been found to be involved in cardiovascular disease, cancer and also neurodegenerative diseases (Finnerty et al., 2010). Microarray profiling revealed, that miRNAs of the miR-15 family are expressed in all kinds of tissues in mostly moderate to high levels (Baskerville et al., 2005). An overview of expression levels of the different miRNAs of the miR-15 family can be seen in figure 7.

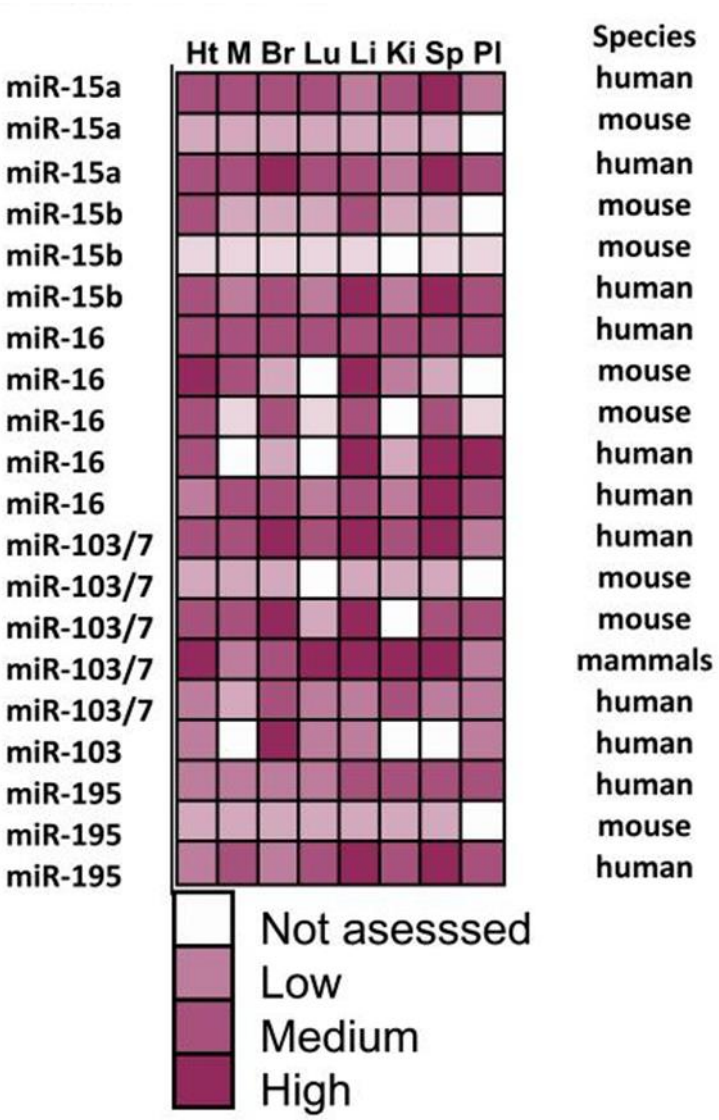

Figure 7: Expression of the miR-15 miRNA family in different tissue types. Heart (HT), skeletal muscle (M), brain (Br), lung (Lu), liver (Li), kidney (Ki), spleen (Sp) and placenta (Pl). (Adapted from Finnerty et al., 2010).

Many studies suggest a relevance of miR-15 and miR-16, both important members of the miR-15 miRNA family, in cancer dynamics. Here, miR-15 and -16 which are both encoded in the miR-15a/miR-16-1 cluster on chromosome 13 in humans and which is known to be a critical regulator of proliferation, have been found to function as tumor suppressors by controlling cell-cycle progression (Klein et al., 2010; Bonci et al., 2008; Kay et al., 2021). But miRNAs of the miR-15 family don't only play a role in cancer dynamics. They have also been identified as key factors of brain development and neurogenesis. MiR-15b for example has been shown to regulate various aspects of cortical development. It promotes cell cycle exit and neuronal differentiation by

inhibiting NPC proliferation in the developing murine neocortex (Lv et al., 2014). Others found, that downregulation of miR-15a results in stimulation of fibroblast growth factor 2 (*FGF2*) and therefore promotes NPCs differentiation and proliferation (Chen et al., 2016). The delicate role miR-15 family members play in the switch from proliferation to differentiation in B-cells has been underlined by Lindner et al. who stated, that miR-15 family members trigger differentiation-specific cell cycle arrest by repressing the crucial proliferation factors cyclins E1 and D3 (Lindner et al., 2017).

This thesis concentrates mainly on the function of miR-16. This miRNA is expressed in close proximity to miR-15a on chromosome 13 in humans and on chromosome 14 in mice (Lagos-Quintana et al., 2001). MiR-16 shares the same seed sequence with miR-15a and -15b. Just like the other miRNAs of the miR-15 family, miR-16 is also involved in a variety of biological processes within the body. The serotonin pathway in the human brain for example, crucial to prevent symptoms like depression, anxiety and suicidal behavior, is influenced by miR-16 which increases serotonin transporter expression in serotonergic cells (Baudry et al, 2010). Just as for miR-15a, miR-16 also has been found to directly target *FGF2* and furthermore, to also inhibit the mitogen-activated protein kinase signaling pathway (MAPK). The inhibitory effect of miR-16 on cell migration could also be detected, when migration assays with miR-16 overexpressing NPCs resulted in a significant reduction of migratory and invasive cells in comparison to the control. This study also stated, that silencing miR-16 results in increased proliferation in NPCs. Additionally, miR-16 seems to be more abundantly expressed in neurons than in NPCs (He et al., 2016).

Most recently, the involvement of miR-16 in lung cancer and cell cycle progression has been stated in various publications where it was found, that miR-16 targets the cell cycle checkpoint gene *Wee1* and therefore plays a crucial part in cell division (Du et al., 2021; Wang et al., 2020).

To summarize, miRNAs of the miR-15 miRNA family have been reported to be of great importance in a huge variety of biological processes in the human body. Due to its described influence in developmental processes, especially miR-16 seems to be an interesting candidate in regard to cell proliferation, cell differentiation and brain development in general.

3.5. Target genes of miR-16

As already described above, miR-16 has a wide range of target genes. In the following chapter, only the genes studied in this thesis are described in more detail.

3.5.1. Wee1

The protein kinase *Wee1* was first identified in the fission yeast *Schizosaccharomyces pombe* and is a member of the serine/threonine specific family of protein kinases (Nurse, 2004). These kinases are known to be involved in the inactivation of cyclin dependent kinase 1 (*Cdk1*) by terminal phosphorylation and therefore play a major role in cell cycle progression and mitosis entry of dividing cells (Do et al., 2013). Due to its regulatory function at the G2 checkpoint, *Wee1* is also known as "G2 checkpoint kinase" and responds to DNA damage in dividing cells by determining the timepoint of their entry into mitosis (Ghiasi et al., 2014). Numerous studies confirmed the role of *Wee1* in cancer dynamics and also identified it as potential target for tumor therapy (Du et al., 2021). A loss of *Wee1* has also been shown to result in the formation of daughter cells that are smaller than normal. This suggests, that *Wee1* also functions as part of a cell size checkpoint which prevents cells that are too small from entry into mitosis (Kellogg, 2003). *Wee1* is located on chromosome 11 in humans and on chromosome 7 in mice.

3.5.2. Cdk1

As well as *Wee1*, the cyclin dependent kinase 1 (*Cdk1*) is part of the serine/threonine family of protein kinases. *Cdk1* is conserved across all eucaryotes and plays a major role in successful completion of M-phase in the cell cycle (Brown et al., 2015). *Cdk1* is located on chromosome 10 in both humans and mice. Cdk1 does not display kinase activity on its own, it rather acts in complex with the two cyclins A and B (Desai et al., 1992). Together with its cyclins, *Cdk1* regulates mitosis entry of dividing cells (Lindqvist et al., 2009). The activity of Cdk1-cyclin B complexes on the other hand is regulated by inhibitory phosphorylation through the protein kinases *Wee1* and *Myt1* (Deibler et al., 2010). It has been found, that a loss of *Cdk1* results in highly impaired embryonic development around the blastocyst stage and high lethality rates. Other cyclin dependent kinases such as *Cdk2, Cdk4* and *Cdk6* don't seem to play such essential roles for proper cell cycle function as *Cdk1* compensates their loss by forming complexes with A, B, E and D-cyclins (Bienvenu, 2010).

3.5.3. Fbxw7

The F-box and WD repeat-containing protein 7 (*Fbxw7*) is part of the F-box protein family which is known to be involved in signal transduction and cell cycle regulation (Craig et al., 1999). Many F-box proteins have been shown to underly miRNA and RNA interference regulation in plants (Jones-Rhoades et al., 2006). The three different isoforms (FBXW7α, FBXW7β, and FBXW7γ) of *Fbxw7* in mammals localize to different subcellular compartments. They are separately expressed in the nucleoplasm (FBXW7α), the cytoplasm (FBXW7β) and the nucleus (FBXW7γ) (Welcker et al., 2004). The isoform responsible for most of the known *Fbxw7* functions is FBXW7α which is also expressed in the majority of proliferating cells. *Fbxw7* is classified as a tumor suppressor gene and targets pro-proliferative genes such as *Notch1*, *cMyc*, *mTOR* and *Jun* (Yeh et al., 2008). Mutations is *Fbxw7* are known to cause stem cell differentiation defects, chromosomal instability and inhibition in cell division. A full *Fbxw7* knockout in mice is embryonic lethal (Takada et al., 2017). *Fbxw7* is located on chromosome 4 in humans and on chromosome 3 in mice.

3.5.4. Chek1

Another important key player for cell cycle regulation is the checkpoint kinase 1 (*Chek1*). Just as *Wee1* and *Cdk1*, *Chek1* is a member of the serine/threonine family of protein kinases and also an important part of DNA damage checkpoints during the cell cycle (Zhang et al., 2014). *Chek1* was first identified in fission yeast and has homologues in *Drosophila*, *Xenopus*, mouse and human (Patil et al., 2013). By phosphorylating cell cycle regulators, as for example the earlier described *Cdk1*, *Chek1* is an essential factor of DNA damage response networks and cell cycle progression in the dividing cell (McNeely et al., 2014). The two subtypes of the checkpoint kinase, *Chek1* and *Chek2* respond to different types of DNA damage. *Chek1* identifies a multitude of DNA damages, including damage induced by UV light as well as virus infections. C*hek2* on the other hand primarily responds to double DNA strand breaks (Ben-Yehoyada et al., 2009). Due to its roles in DNA damage control and cell cycle progression, *Chek1* also is an important target for cancer therapies. It has been found, that cancer cells often display mis regulation of *Chek1* (Verlinden et al., 2007). *Chek1* is located on chromosome 11 in humans and on chromosome 9 in mice.

3.5.5. Taf15

The nuclear protein TATA-binding protein-associated factor 2N (*Taf15*) is a member of the FET RNA- and DNA binding family of proteins (Morohoshi et al., 1998). The FET protein family includes fused in sarcoma (*FUS*), Ewing sarcoma breakpoint region 1 (*EWS*) and *Taf15* (Therrien et al., 2016). It has been shown, that FET proteins play a role in post-transcriptional as well as transcriptional gene regulation. *Taf15* and the other FET proteins have also been linked to neurodegenerative diseases such as amyotrophic lateral sclerosis (Therrien et al., 2014). Furthermore, it has also been shown, that *Taf15* is involved in post-transcriptional regulations of oncogenes and together with miRNAs plays a role in cell proliferation (Ballarino et al., 2013). Taf15 is located on chromosome 17 in humans and on chromosome 11 in mice.

4. Purpose of this Thesis

As already stated in the previous chapters, brain development is a complex field that underlies a huge variety of different regulators and impacts. On the posttranscriptional level, miRNAs have been shown to also contribute to the conglomerate of impacts and regulators controlling brain development.

The exact mechanisms and pathways with which miRNAs effect embryonic brain development have not been studied in detail so far and studies about the effect of miRNAs on the embryonic developing brain by now have only scratched the surface, leaving a lot of space for further and deeper research in this topic.

Besides identifying miR-16 as possible key regulator in the developing brain, this thesis wants to elucidate the phenotype induced by mis-regulation of this miRNA in detail. By applying overexpression and knockdown approaches in the mouse model in vivo, the effects of miR-16 on prenatal brain development will be studied and resulting phenotypes will be described.

Another goal of this work is to identify genes that are known to be involved in brain development and are targeted by miR-16. This question will be addressed with an mRNA sequencing approach of murine cortical neurons that have been electroporated with miRNA-16 in vivo.

Beyond that, a general expression analysis of miRNAs in the developing brain will be made by conducting miRNA sequencing. This experiment will shed more light on the diversity of expression patterns of miRNAs along different stages and cell types of brain development.

Material

1. Cell lines and animal models

Cell line	Growth/cultivation media
Human embryonic kidney cells 293 (HEK293)	DMEM 1x high glucose + 1% Penicillin/Streptomycin + 10% Fetal bovine serum (FBS)
Neuroblastoma cells (N2A)	DMEM 1x high glucose + 1% Penicillin/Streptomycin + 10% Fetal bovine serum (FBS)
Mouse Hippocampal Neuronal cell line (Ht22)	DMEM 1x high glucose + 1% Penicillin/Streptomycin + 10% Fetal bovine serum (FBS)
Mouse cortical neurons	48 ml Neurobasal media + 1 ml Glutamax + 1ml B27
Mouse neural progenitor cells (NPCs)	48 ml Neurobasal media + 1 ml Glutamax + 1ml B27(without Vit A) + 5 µl EGF (Stock 100 µg/ml) + 1µl FGF (Stock 100 µg/ml)

Table 2: List of used cell lines.

Mouse line	Origin
C57BL/6JRj	Janvier Labs. France
NMRI	Janvier Labs, France

Table 3: List of used mouse lines.

2. Software and online tools

Name Software	Use/Producer
ImageLab V5	Western Blot analyses/ BioRad
Intas GDS	Agarose gel documentation/Intas Science Imaging
MicroWin 2010	Luciferase assays/ Berthold Technologies
StepOne	qPCR/ Applied Biosystems
ImageJ	Microscopy analyses/ Wayne Rasband
Cutadapt v1.18	NGS analyses/ TU Dortmund AG Rahmann
FastQC v0.11.7.	NGS analyses/ Simon Andrews
miRDeep2 v2.0.1.2	NGS analyses

Table 4: List of used software tools.

Name Online tool	URL
Target Scan	www.targetscan.org
NCBI	www.ncbi.nlm.nih.gov
Genome Browser	www.genome.ucsc.edu
Primer3	www.primer3.ut.ee
qPCR probefinder	www.qpcr.probefinder.com/organism.jsp
miRBase	www.mirbase.org
NEBuilder	www.nebuilder.neb.com

Table 5: List of used online tools.

3. Equipment

Name tool	Function	Producer
CO2 Incubator big	Cell culture incubation	Binder
CO2 Incubator small	Cell culture incubation	RS Biotech Nunc
PeqPower 300 V	Electrophorese electricity device	Peqlab Biotechnologies
Electrophorese chamber	Electrophorese device	Peqlab Biotechnologies
Gel iX20 Imager	Agarose gel documentation system	Intas Science Imaging
Agarose gel comb	Form pockets in agarose gel	Peqlab Biotechnologies
Certomat H	Incubator	Braun Biotech International
INCU-Line	Incubator	VWR
Certomat R	Incubator with shakers	Braun Biotech International
Fridge	Freezer (-20°C)	Liebherr Profiline
Revco ExF	Freezer (-80°C)	Binder
CentroXS LB 960	Luminometer	Berthold Technologies
Axiovert25	Microscope	Zeiss
EVOS XL	Microscope	Life Technologies
Neubauer chamber	Count cells (0,0025 mm2)	Brand
Accu-Jet Pro	Pipetboy	Brand
StepOnePlus Real Time PCR System	qPCR device	Applied Biosystems
Rollermixer SRT9D	Rollermixer	Stuart
Thriller	Heater with shakers	Peqlab Biotechnologies
Nano Drop One	Spektophotometer	Thermo Scientific
Hera Safe	Sterile workbench	Hera Safe
PeqStar 2x Thermocycler	Thermocycler	Peqlab Biotechnologies
Electroporator BTX BCM 830	Electroporator	Harvard Apparatus Inc
Leica CM3050S	Cryostat	Leica
DNA Engine Peltier Thermal Cycler	Thermocycler	MJ Research
VV3	Vortexer	VWR
ScoutPro 600g	scales	Ohaus
VWB 26	Waterbath	VWR
3-Speed Minicentrifuge	Centrifuge	NeoLab
Mikrocentrifuge	Centrifuge	NeoLab
Avanti J-26 XP	Centrifuge	Beckmann Coulter
Perfect Spin 24R	Centrifuge	Peqlab Biotechnologies
Heraeus Megafuge 16R	Centrifuge	Thermo Scientific
JLA 16.250	Centrifuge rotor	Beckmann Coulter
12 ml PP tube	tube	Greiner Bio One
12 well cell culture plate Cell star	12 well plate	Greiner Bio One
24 well cell culture plate Cell star	24 well plate	Greiner Bio One
5 ml Eppendorf tube	tube	Eppendorf
Cell culture plate Costar	6 well plate	Corning incorporated
96 PCR plate ABgene PCR	96 well PCR plate	Thermo Scientific

96 well cooling block	Cooling block	Eppendorf
Deposit bag		Roth
Safe-lock tube(1.5/2 ml)	reaction tube	Eppendorf
Falcon Racks		NeoRack
Falcon tube(15/50 ml)		Greiner Bio One
TipOne filter tips(10/20/200/1000 µl)	Pipette tips	TipOne
Parafilm	Laboratory film	Bernis
Latex gloves		VWR
Nitril gloves		StarGuard
PCR adhesive seal sheet		Thermo Scientific
PCR tubes(200 µl)		StarLab
PetriDish 96x16	Petri dish	Greiner Bio One
DiscoveryComfort Pipette(10/20/200/1000 µl)	Pipettes	Discovery Comfort
Rack for tubes(1.5/2 ml)		NeoLab
Sterile tubes(1.5 ml)		Sarstedt

Table 6: List of used machines and plastic ware.

4. Reagents and kits

Reagent/kit	**Producer**
EndoFree Maxi Plasmid Kit	Qiagen
HighPure RNA Isolation Kit	Roche
miRpremier miRNA Isolation Kit	Sigma Aldrich
Bio-X-act short DNA Polymerase Kit	Bioline
MinElute Gel Extraction Kit	Qiagen
Renilla Luciferase Assay System	Promega
TaqMan Advanced miRNA Assays	Applied Biosystems
TaqMan Fast Universal PCR Master Mix	Applied Biosystems
Takara SYBR PreMix Ex Taq II	Takara/Clontech
Revert Aid First Strand cDNA Synthesis Kit	Thermo Fisher
Lipofectamine 2000	Thermo Fisher
Lipofectamine 3000	Thermo Fisher
TransFectin	Bio Rad
Oligofectamine	Thermo Fisher
Tissue Tek	Sakura
100 bp DNA ladder	Fermentas
1 kB DNA ladder	Fermentas
6x Loading Dye	Thermo Scientific
2-Mercaptoethanol (99%)	Roth
Isopropanol	Roth
Agar-Agar	Roth
Agarose low EO	AppliChem
Ampicillin Sodium Salt	AppliChem
Calciumchloride	Roth
Disodiumhydrogenphosphate	Roth
dNTPs	Fermentas
DPBS 1x	Gibco Life Technologies

DMEM 1x high glucose	Gibco Life Technologies
Ethanol 99%, 1% MEK	AppliChem
Ethanol absolute	Sigma Aldrich
Etidiumbromide 1%	Roth
Fetal Bovine Serum	Gibco Life Technologies
H2O sterile	Braun
Yeast extract	Roth
Hepes –Pufferan	Roth
Luciferin	Sigma Aldrich
Penicillin Streptomycin (10,000 U/ml)	Gibco Life Technologies
Poly-L-Ornithine	Sigma Aldrich
Tryptone-Peptone	Roth
Sodiumchloride	Roth
Sodiumhydroxide	Roth
Renilla Luciferase	Promega
Click-iT™ EdU Cell Proliferation Kit for Imaging, Alexa Fluor™ 647 dye	Thermo Scientific

Table 7: List of used reagents and kits.

5. siRNAs

Name siRNA	**Supplier**
Synthetic oligonucleotide against mmu-miR-16-5p	Gene Copoeia
Synthetic oligonucleotide against mmu-miR15a-5p	Gene Copoeia
Synthetic oligonucleotide against mmu-miR15b-5p	Gene Copoeia
Synthetic oligonucleotide against SCR-si control (negative control)	Gene Copoeia

Table 8: List of used siRNAs.

6. Antibodies

Antibody	**Supplier**	**Catalog number**
mouse anti GFP (1:500)	Roche	11814460001
rabbit anti Satb2 (1:200)	Abcam	ab34735
rabbit anti Pax6 (1:100)	Biolegends	901301
rabbit anti Phospho Histone H3 (1:200)	Cell Signaling	9701S
chicken anti Tbr2 (1:200)	Millipore	AB15894
rabbit anti Ki67 (1:200)	Abcam	ab16667
rabbit anti Wee1 (1:500)	Abcam	ab137377
mouse anti Gapdh (1:1000)	Abcam	ab181602

Table 9: List of used antibodies.

Methods

1. MiRNA sequencing

1.1. MiRNA sequencing of neuronal progenitor cells (NPCs) and neurons

1.1.1. Isolation of NPCs and neurons from the murine cortex

In order to isolate primary cortical neurons from embryonic cortical tissue, time mated E14.5 pregnant NMRI mice were ordered from Janvier Labs (Saint Berthevin, France). The pregnant mice were sacrificed by cervical dislocation, the cortices of the embryos were dissected and collected in cooled DMEM high glucose media (Gibco Life Technologies). Under a sterile cell culture hood, a single cell suspension of these cortices was produced. For neuronal culture, 1.4x10^6 cells per well were seeded on Poly-L-ornithin and Laminin coated 6 well plates whereas for NPCs culture, 0.2x10^6 cells per well were seeded on Poly-L-ornithin and Laminin coated 6 well plates. The neurons were cultured in neurobasal medium containing 2% B27 supplement (Gibco Life Technologies) and 500 µM Glutamax (Gibco Life Technologies) whilst for culturing the NPCs, neurobasal medium containing 2% B27 -VitA supplement (Gibco Life Technologies), 500µM Glutamax (Gibco Life Technologies) and EGF (10ng/ml) and FGF (10ng/ml) was used.

1.1.2. RNA isolation

To isolate RNA from NPCs and neurons, the cells were scraped from their cell culture plates and centrifuged for 3 minutes at 200 g at RT to obtain a cell pellet. This pellet was dissolved in 100 µl RNA later reagent and was stored at -20°C until further use. For RNA isolation the miRNeasy Micro Kit (Qiagen) was used. This kit isolates total RNA including miRNAs from small input lysates. The frozen cell pellets were thawed at RT and lysed by adding 700 µl QIAzol Lysis reagent. The samples were vortexed for 1 min to disrupt the cells and create a homogenous solution. To start the dissociation of nucleoprotein complexes, the homogenate was incubated at RT for 5 min. Afterwards, 140 µl of chloroform were added to the lysates. The tubes were closed and shaked for 15 sec. After incubating at RT for 5 minutes the lysates were centrifuged at 12.000 g for 15 min at 4°C. During the centrifugation step the lysates are separated into 2 phases: the upper phase which contains RNA and the lower, organic phase. The upper phase was carefully collected from the tube by pipetting and transferred to a fresh 1.5 ml reaction tube. 1.5 volumes of 100 % EtOH were added and mixed with the sample by pipetting. The sample

was pipetted onto a RNeasy MinElute spin column and centrifuged at full speed for 15 sec at RT. The flow through was discarded and 700 µl RWT buffer were added to the column. Again, the column was centrifuged at full speed for 15 sec and the supernatant was discarded. 500 µl RPE buffer were added to the columns, the columns were centrifuged at full speed for 15 sec and the flow through was discarded. To finish the washing, 500 µl of 80% EtOH were added to the columns which then were centrifuged at full speed for 2 min. The flow through was discarded and the filter columns were placed into fresh 1.5 ml reaction tubes. To elute the RNA from the filter fleece, 14 µl of RNAse free H20 were pipetted directly on the filter and the spin columns were centrifuged at full speed for 1 min. The eluted RNA was quantified using a NanodropOne device (ThermoScientific) and stored at -80°C until further use.

1.1.3. Library preparation and miRNA sequencing

The miRNA sequencing libraries of the NPCs and Neurons were prepared using the Bioo Scientific NextFlex small RNA v3 Seq Kit (Bioo Scientific). 500 ng of total RNA (including miRNAs) were used as an input for the library preparation. The library preparation with the Bioo Scientific NextFlex Kit is divided into four steps: Ligation of an 3´-adenylated adapter to the insert RNA, ligation of an 5´-adapter, reverse transcription of the 5´- and 3´-adapter ligated RNA and PCR amplification of these cDNA constructs. For the first step, 500 ng of each RNA sample were mixed with RNAse free H_20 to get a total volume of 10.5 µl. The samples were heated to 70°C for 2 min and then incubated on ice for 3 min. The denatured RNA was supplied with 1 µl NextFlex 3´-4N adenylated adapter, 7 µl NextFlex 3´-ligation buffer and 1.5 µl NextFlex 3´-ligation enzyme. For adapter ligation the samples were then incubated for 2 hours at 25°C. In order to remove excess 3´-adapters, 25 µl NextFlex adapter depletion solution and 40 µl of NextFlex Cleanup beads were added to each sample. After mixing well by pipetting, 60 µl of isopropanol were added to the samples which then were incubated for 5 min at RT. Then, the samples were put on a magnetic stand for another 5 min until the solutions cleared. The supernatant was removed and discarded, 180 µl of 80% EtOH was added to each sample and samples were incubated for 30 sec. The complete supernatant was removed again and this washing step was repeated another time. After complete removal of the EtOH, the samples were removed from the magnetic stand and the bead pellets were dissolved in 22 µl of NextFlex Resuspension buffer. Following 2 min of incubation at RT, the

samples were put on the magnetic stand again and incubated there until the solutions appeared clear. 20 µl of the clear supernatant were transferred to a fresh reaction tube, supplemented with 25 µl NextFlex adapter depletion solution and 40 µl of NextFlex Cleanup beads and the whole cleanup process was repeated as described before. When the washing steps with the 80% EtOH were done the beads were eluted in 13 µl of RNAse free H_2O and put on the magnetic stand. When the solution appeared clear, 11.5 µl of the supernatant were transferred to a fresh tube. For the next step, the excess adapter inactivation, each of the 11.5 µl of purified 3´-adenylated adapter ligated RNA samples were supplied with 2 µl of NextFlex adapter inactivation buffer and 0.5 µl NextFlex adapter inactivation enzyme. The samples were mixed by pipetting and incubated at 12°C for 15 min, followed by an incubation at 50°C for 20 min. In the next step the 5´4N adapters were ligated to the 3´-adenylated adapter ligated RNA samples. For this, 1.5 µl of 5´4N adapter were heated to 70°C for 2 min and afterwards put on ice immediately. Next, 7.5 µl NextFlex 5´-ligation buffer, 2 µl NextFlex 5´- ligation enzyme and the prepared 1.5 µl of 5´4N adapter were added to the purified 3´-adenylated adapter ligated RNA samples which were then incubated at 20°C for 1 hour. For the reverse transcription, 13 µl of NextFlex RT buffer and 2 µl of M-MuLV reverse transcriptase were pipetted to each 5´- and 3´- adapter ligated sample. These reactions were then incubated at 42°C for 30 min followed by a 10 min incubation at 90°C. In order to remove RT reagents from the samples, another bead cleanup was performed. To each sample, 20 µl of NextFlex cleanup beads were added and mixed by pipetting. The mixtures were incubated at RT for 5 min and then placed on a magnetic rack. When the solution appeared clear, 70 µl of supernatant which contained the cDNA product were transferred to a fresh tube. 10 µl of adapter depletion solution and 20 µl of NextFlex Cleanup beads were added to the samples and mixed well by pipetting. Next, 68 µl of isopropanol was pipetted to the samples which were then incubated at RT for 5 min. The samples were magnetized afterwards and the supernatant was removed and discarded. Two washing steps with 180 µl of 80% EtOH followed as already described and in the end the bead pellet was dissolved in 20 µl RNAse free H_20. The samples were magnetized and 18 µl of supernatant were transferred to a fresh reaction tube. For the PCR amplification of the cleaned-up cDNA samples, 1 µl NextFlex Universal Primer, 1 µl NextFlex Barcoded primer and 5 µl NextFlex small RNA PCR Master Mix were added to

each purified cDNA sample. The reactions were cycled in a thermal cycler as described in table 10.

Cycling protocol		
95°C	2 min	1 cycle
95°C	20 sec	20 cycles
60°C	30 sec	20 cycles
72°C	15 sec	20 cycles
72°C	2 min	1 cycle

Table 10: Cycling protocol PCR Library preparation miRNA sequencing.

For the final cleanup, 32.5 µl NextFlex Cleanup beads were added to the amplified PCR product and incubated at RT for 5 min. Afterwards, the samples were magnetized until the solutions appeared clear and 52.5 µl of the supernatant containing the amplified PCR product were transferred to a fresh reaction tube. Another 30 µl of NextFlex Cleanup beads were added to the samples which again were incubated at RT for 5 min. Then, the samples were put on the magnetic stand, the supernatant was removed and discarded and 2 washing steps with 80% EtOH followed as described before. After washing, the beads were dissolved in 13.5 µl NextFlex resuspension buffer and incubated at RT for 2 min. To extract the final library from the cleanup beads, the samples were magnetized until the solutions appeared clear and 12 µl of the supernatant were transferred to a fresh reaction tube. The size distributions and concentrations of the prepared libraries were checked by Qubit dsDNA HS Assay (Life Technologies).

1.1.4. Bioinformatical analyses

To analyze the data of the sequencing run, the 3´adapter sequences had to be clipped and the first and the last 4 bases from the adapter clipped reads had to be trimmed using the tool cutadapt v1.18 and trimming instructions from Bioo Scientific. The quality check of the sequences was performed using the tool FastQC v0.11.7 and novel as well as known miRNAs with the tool miRDeep2 v2.0.1.2. All bioinformatic analyses were performed by the institutes bioinformatician, Dewi Hartwich.

1.2. MiRNA sequencing of the developing murine cortex (E14-P0)

1.2.1. Cortex preparation and miRNA isolation

To obtain RNA from murine cortices at different stages of development, time mated pregnant C57/Bl6 J mice were ordered from Janvier Labs (Saint Berthevin, France). For the time points E14 and E17 the pregnant mice were sacrificed by cervical translocation, the abdomen was opened and the uterus containing the embryos was removed from the mother's abdominal cavity. For the time point P0, the newborn mices' heads were cut off with a small surgical scissor. For later sex determination, the tail of each embryo/pup was cut off, put into a fresh 1.5 ml Eppendorf reaction tube and stored at -20°C until further use. The two cortical hemispheres of each embryo were dissected from the brains and the meninges were removed from them. The cortical hemispheres of each embryo/pup were each put into separate 1.5 ml Eppendorf reaction tubes (Eppendorf) with 100µl of RNA later solution (Sigma) to prevent the RNA from degradation by RNAses. To isolate total RNA (including miRNAs) from the embryonic cortices, the Trizol/Chloroform method was used. For this, 100 µl of Trizol reagent (Gibco Life Technologies) were added to each tube containing the 2 cortical hemispheres of one embryo. The tissue was homogenized using a pistil. After homogenization another 900 µl of Trizol reagent were added to the tissue and the reaction tubes were vortexed briefly. The homogenate was incubated for 5 minutes at RT and afterwards supplemented with 200 µl chloroform. Then, the mixture was shaken vigorously until it displayed a milky-pink color. After 2 minutes of incubation at RT, the homogenates were centrifuged at 12.000 g for 15 minutes at 4°C. After this centrifugation step, a clear separation of the two phases should be visible. The clear, uppermost phase war transferred to a fresh 1.5 ml Eppi containing 500 µl ice cold isopropanol. To mix the isopropanol with the clear phase, the tube was carefully inverted 2-3 times. After 10 minutes of incubation at RT the mixtures were again centrifuged at 12.000 g for 15 minutes at 4°C. Then, the supernatant was removed and the pellet was washed with 1 ml ice cold 70% EtOH. Next, the tubes were centrifuged at 12.000 g for 5 minutes at 4°C. This washing step was repeated once. After the washing steps, remaining EtOH was removed from the pellet using a pipette and the pellet was air dried. After 10 minutes the dried RNA pellet was dissolved in 30 µl of RNAse free H2O. To determine the

concentration of the isolated RNA a NanodropOne Spectrometer was used (ThermoScientific).

1.2.2. Sex determination of probes

In order to determine the sex of the embryos whose cortices were used for RNA isolation, the DNA had to be isolated from the dissected tissue fragments of each embryo. For this, 200 µl digestion buffer (table 11) and 25 µl Proteinase K were added to each tissue fragment.

Digestion buffer (30 ml)
3 ml Tris pH 8
400 µl 0.5 M EDTA
6 ml 1 M NaCl
60 µl 10% SDS
20.54 ml H2O

Table 11: Digestion buffer for DNA extraction of murine tissue.

To lyse the tissue, the tubes were incubated on a heated shaker at 57°C for at least 3 hours. Afterwards, the lysates were centrifuged at 13.500 rpm for 20 min. To dilute the DNA, 50 µl of the supernatant were mixed with 100 µl H_2O. For sex determination we used a primer pair of the gene *Sry* which is specifically expressed on the Y chromosome. As an autosomal control, the gene *Il2* was used. The primer sequences were adapted from a publication issued 2016 by Prantner et al (Prantner et al., 2016) (table 12).

Name	**Sequence 5´- 3´**
Il2_for	ctaggccacagaattgaaagatct
Il2_rev	gtaggtggaaattctagcatcatcc
Sry_for	ttgtctagagagcatggagggccatg
Sry_rev	ccactcctctgtgacactttagccct

Table 12: PCR primer sequences used for sex determination of mouse tissue.

For the PCR reaction, all reagents were pipetted into a 200 µl PCR tube according to table 13. The PCR reaction was run on a PeqLab thermal cycler with the cycling protocol shown in table 14.

PCR reaction (1 sample)	
10x PCR buffer with $MgCl_2$ (ThermoScientific)	2.5 µl
dNTPs	0.5 µl
Primer 1 (for + rev) 10 µM	1 µl
Primer 2 (for + rev) 10 µM	1 µl
Axon Taq Polymerase	0.2 µl
DNA	1 µl
H_2O	18.8 µl

Table 13: PCR reaction for sex determination PCR.

Cycling protocol		
95°C	3min	1 cycle
94°C	30 sec	35 cycles
62°C	30 sec	35 cycles
72°C	30 sec	35 cycles
72°C	10 min	1 cycle

Table 14: Cycling protocol for sex determination PCR.

To check for the amplified products' lengths, the PCR products were loaded on a 1.5 % agarose gel. Samples that showed two bands were determined to be male due to the successful amplification of both the autosomal control *Il2* and the Y chromosome specific gene *Sry*. Samples only showing the band for the gene *Il2* were determined to be of female origin as no expression of the male specific gene *Sry* could be observed.

1.2.3. Library preparation and miRNA sequencing

Library preparation for miRNA sequencing was performed according to the section 1.1.3.

1.2.4. Bioinformatical analyses

Bioinformatic analyses for miRNA sequencing was performed according to the section 1.1.4.

2. Validation of miRNA sequencing results with TaqMan Assays

To validate the results of the bioinformatical analyses of the miRNA sequencing, TaqMan Assays were performed with the same cortical miRNA samples that were used for the miRNA sequencing.

2.1. cDNA synthesis

The isolated miRNAs had to be transcribed into cDNA to carry out TaqMan assays. For this, the ThermoFisher TaqMan miRNA reverse transcription kit was used. For each sample, in addition to the 7 µl of RT reaction mix (0.15 µl 100mM dNTPs, 1 µl MultiScribe

Reverse Transcriptase, 1.5 µl 10x Reverse Transcription Buffer, 0.19 µl RNAse Inhibitor, 4.16 µl H_2O), 3 µl of 5x RT Primer and 10 ng of RNA dissolved in 5µl of RNAse free H_2O were pipetted into a fresh 200 µl reaction tube. The reverse transcription reactions were run on a thermal cycler using the protocol shown in table 15 and stored at -20°C until further use. A list of all miRNA assays used in this work is depicted in table 16.

Cycling protocol	
16°C	30 min
42°C	30 min
85°C	5 min
4°C	hold

Table 15: Cycling protocol for cDNA synthesis with TaqMan miRNA reverse transcription kit.

miRNA Assay	**Mature miRNA sequence 5´- 3´**
Mmu-miR-15b-5p	uagcagcacaucaugguuuaca
Mmu-miR-130b-3p	cagugcaaugaugaaagggcau
Mmu-miR-137-3p	uuauugcuuaagaauacgcguag
Mmi-miR-124-3p	uaaggcacgcggugaaugcc
Mmu-miR-128-3p	ucacagugaaccggucucuuu

Table 16: TaqMan miRNA Assays used in this work.

2.2. TaqMan Assays

To run the PCR on the real time qPCR cycler, a PCR reaction mix was prepared. For this, for each sample 10 µl Taq Man Universal Mastermix II without UNG (ThermoScientific), 1 µl 10x Taq Man miRNA Probe (ThermoScientific) and 7.67 µl of RNAse free H_2O were pipetted into one tube. The cDNA was diluted 1:10 with RNAse free H_2O and 1.33 µl of diluted cDNA was pipetted into each well of a 96-well reaction plate. Each cDNA sample was tested in triplets. 18.67 µl of the PCR reaction mix were added to each well of the plate, which was then sealed with adhesive film and centrifuged briefly. Afterwards the plate was put into a StepOnePlus qPCR cycler (ThermoScientific), and run with the protocol shown in table 17.

Cycling protocol		
50°C	2 min	1 cycle
95°C	10 min	1 cycle
95°C	15 sec	40 cycles
60°C	60 sec	40 cycles

Table 17: Cycling protocol for the TaqMan Assays.

3. Overexpression of miRNAs in the developing brain

To study the function of miR-16 and -15 in the developing mouse brain in vivo, in utero electroporation experiments were performed. This technique enables the experimenter to overexpress different DNA expression vectors in specific brain regions at distinct time points of embryonic brain development (Wang et al., 2013). As the time points of electroporation and analyses as well as the exact cortical areas in which the DNA constructs are about to be overexpressed can precisely be chosen by the experimenter, the in-utero electroporation technique is a powerful tool to study different aspects of neuronal development in vivo.

3.1. In utero electroporation of miRNAs 16 and 15

3.1.1. Cloning of constructs used for in utero electroporation

The coding sequences of the miRNAs miR-16 and miR-15 were cloned into the pCAGGs-IRES-GFP vector. This vector contains the Internal Ribosomal Entry Site (IRES), which enables the simultaneous expression of two proteins from the same RNA transcript (Jackson et al., 1990). Here, the IRES site was used to express the fluorescent protein GFP besides the target protein. Thus, successfully electroporated cells could easily be identified under the microscope. The insert DNA was cloned into the pCAGGs-IRES GFP vector with the use of the restriction enzymes XhoI and EcoRI. Table 18 shows the designed primers for the cloning of miR-16 and miR-15

Name	**Sequence 5´- 3´**
miR16_pCAGGsIRESGFP_for_**XHoI**	GATC**CTCGAG**ctgatcttctgaagagagtacc
miR16_pCAGGsIRESGFP_rev_**EcoRI**	GATC**GAATTC**tgagctgcattaccatccca
miR15a_pCAGGsIRESGFP_for_**XHoI**	GATC**CTCGAG**tgacttgcttttctcgtttcatg
miR15a_pCAGGsIRESGFP_rev_**EcoRI**	GATC**GAATTC**gccaaccttacttcagcagc

Table 18: Primer sequences for miRNA cloning.

The designed primers were ordered from SIGMA (Sigma Aldrich) in 100µM stocks, dissolved in H_2O. For amplification of the target sequences a PCR reaction with the ordered primers was performed on murine genomic DNA. The PCR reaction mix is shown in table 19. For PCR, the BIO-X-ACT™ Short DNA Polymerase-Kit was used (Bioline). The reaction was run in a thermal cycler using the protocol listed in table 20.

PCR reaction (1 reaction)	
Mouse DNA	1 µl
$MgCl_2$	1 µl
dNTPs	1 µl
Primer Mix (10 µM, for + rev)	1 µl
BIO-X-Act Polymerase	0.5 µl
BIO-X-Act Reaction buffer	1.5 µl
H_2O	18 µl

Table 19: PCR reaction of miRNA cloning PCR.

Cycling protocol		
95°C	3 min	1 cycle
95°C	30 sec	35 cycles
57°C	1 min	35 cycles
72°C	3 min	35 cycles
72°C	5 min	1 cycle

Table 20: Cycling protocol for miRNA cloning PCR.

After completion of the PCR, the reactions were loaded on a 1.5% agarose gel to check for the amplified product's correct size. Specific bands were cut from the gel and DNA was extracted using the Qiagen MinElute Gel Extraction Kit (Qiagen). For this, 3 volumes of the gel fragment´s weight of buffer QG were pipetted to the piece of agarose. This buffer helps the gel slice to solubilize properly and improves binding conditions for the DNA to the silica membrane of the MinElute columns. When the gel slice had been dissolved completely after an incubation time of 10 minutes at 50°C, 1 gel volume of isopropanol was added and the sample was mixed by inverting the tube. Next, the sample was pipetted on a MinElute column placed in a collection tube and was centrifuged at 13,500 rpm for 1 minute. The flow through was discarded and 500 µl of buffer QG were pipetted on to the MinElute column. After another minute of centrifugation at 13,500 rpm the supernatant was discarded again and 750 µl of ethanol containing buffer PE were added to the column. In this step the double stranded DNA binds to the silica membrane of the MinElute column whereas primers and other contaminants are being washed away. The column was centrifuged for 1 minute at 13,500 rpm and the flow through was discarded. To remove residual ethanol contained in buffer PE from the column it was again centrifuged for 1 minute at 13,500 rpm. After this step the MinElute column was placed into a fresh 1.5 ml Eppendorf tube. By adding 20 µl of buffer EB the DNA which by now was bound to the column was eluted. The

column was incubated for 1 minute at room temperature and then centrifuged for 1 minute at 13,500 rpm.

The total volume of extracted DNA was digested with the appropriate enzymes to create sticky ends. Additionally, to the insert DNA, the pCAGGs-IRES-GFP backbone vector was also digested by the according enzymes. For digestion, reactions (tables 21 and 22) were incubated at 37°C for 1 hour. The insert DNA reactions were then removed from the thermal cycler whereas the backbone vector reaction was supplied with 2 µl calf intestine alkaline phosphatase (CIP) and incubated for another hour at 37°C. The addition of CIP should prevent the re ligation of the digested vector with itself.

Digestion reaction of insert DNA	
Purified PCR product	20 µl
Enzyme I	1 µl
Enzyme II	1 µl
10x CutSmart buffer	3 µl
H_2O	5 µl

Table 21: Digestion reaction of insert DNA.

Digestion reaction of vector DNA	
Vector DNA	2 µl
Enzyme I	1 µl
Enzyme II	1 µl
10x CutSmart buffer	2 µl
H_2O	14 µl

Table 22: Digestion reaction of vector DNA.

Both the digested insert DNA as well as the digested backbone vector were loaded on a 1.5% agarose gel to check for successful digestion. The DNA bands were cut from the gel and extracted from the agarose using the Qiagen MinElute Gel Extraction Kit. The procedure is described above. Subsequently, the purified insert and vector DNA`s concentrations were measured using Nanodrop. For ligation, a vector: insert ratio of 1:3 was used. Ligation was conducted by using 1µl T4 DNA ligases and 2 µl T4 buffer for a 20 µl total reaction volume together with the calculated amounts of insert and vector DNA. The reactions were filled up to 20 µl with H_2O and incubated at 16°C over night in a thermal cycler. The ligation product was transformed into competent *Escherichia coli (E.coli)* bacteria. For this, the complete ligation product was mixed with 50 µl of defrosted, competent *E.coli* bacteria by pipetting and incubated on ice for 30 minutes. To make the bacteria absorb the cloned vectors, the *E.coli*-vector mix was put in a 42° C hot water bath

for 90 seconds. This so called “heat shock” is supposed to increase the amount of plasmids absorbed by the *E.colis* and therefore increases transformation efficiency. The heat shock was followed by another incubation on ice for 2 minutes after which 250 µl of LB media without ampicillin were given to the bacteria. The bacteria-media mixes were then shaked for 30 minutes in a 37° C warm incubator. During this time the *E.coli* bacteria start gene expression of the ampicillin resistance gene which was present in the 3’UTR containing vectors. After 30 minutes of shaking at 37° C the *E.colis* were plated on LB media plates containing ampicillin. Only bacteria that were successfully transformed with the ampicillin resistance gene containing constructs are able to grow on these plates. The plated *E.colis* were incubated at 37° C over night and grown colonies were picked the next day. To check whether the vectors contained the right insert bacteria were prepared for a plasmid preparation. For this colonies were picked from the plates and were transferred separately into 12 ml tubes each containing 3 ml of LB-amp media. These colonies were cultivated overnight shaking in a 37° C warm incubator. To isolate plasmid DNA from the cultured *E.coli* bacteria, 1 ml of each 3 ml culture were given into a 1.5 ml Eppendorf reaction tube. In order to remove the LB media, the bacteria were centrifuged for 5 minutes at 6,000 rpm. After having carefully removed the supernatant by using a piece of tissue the pellets were resuspended in 100 µl resuspension buffer P1 of the Qiagen EndoFree Plasmid Maxi-Kit. 100 µl lysis buffer P2 were added and the solution was incubated at room temperature for 5 minutes. After this time of incubation, the lysis reaction was stopped by adding another 100 µl of chilled buffer P3 which also enhances precipitation of the plasmid DNA. To ensure the complete precipitation of the DNA the reaction tubes were shortly vortexed before they were again incubated for 5 minutes at room temperature. To remove remaining cell fragments the tubes were then centrifuged for 10 minutes at 13,500 rpm. The supernatant containing the DNA was pipetted on 1 ml of 100% ethanol to precipitate the DNA. For this the tubes again were centrifuged for 10 minutes at 13,500 rpm. After this plasmid DNA was washed with 150 µl of 70 % ethanol and the tubes were centrifuged for 5 minutes at 13,500 rpm. The supernatant was removed, the plasmid DNA pellets were dried at 50 ° C and finally re-suspended in 50 µl of Millipore water.

To check the cloned sequence`s accuracy, the clones were Sanger sequenced using the primers listed in table 23.

Name	Sequence 5´- 3´
pCAGGs_seq_fw	CCATGTTCATGCCTTCTTCTTT
ß2_seq_fw	AAAGTTCTGGGGAGGGGTGAAT

Table 23: Sequencing primers for cloned constructs.

The miRNAs-15 and -16 were also cloned into the ß2 -vector. This vector contains a NeuroD promoter that drives neuronal expression in neurons. For this, the same procedure as described above was used. The PCR primers used can be found in table 24. For the cloning of the ß2 constructs the restriction enzymes BglII and HindIII were used.

Name	Sequence 5´- 3´
miR16_ß2_**BglII**_fw	GATC**AGATCT**aggagttttcaaaaccaaccct
miR16_ß2_**HindIII**_rv	GATC**AAGCTT**tgagctgcattaccatccca
miR15_ß2_**BglII**_fw	GATC**AAGCTT**tgacttgcttttctcgtttcatg
miR15_ß2_**HindIII**_rv	GATC**CTGCAG**gccaaccttacttcagcagc

Table 24: Cloning Primers for miR16 and mir15 into the ß2 vector.

3.1.2. In utero electroporation

To analyze the function of miR-15/-16 miRNAs during neuronal migration, the prepared DNA constructs were overexpressed in the embryonic mouse brain by in-utero electroporation. For this, timed mated, pregnant C57BL/6J mice were ordered from Janvier Labs (Saint Berthevin, France). For all experiments mice were electroporated at embryonic day 13 (E13) and analyzed at E15 or E18, depending of the experimental setup.

For analgesia, pregnant mice were treated with Buprenorphine (0.1 mg/kg bodyweight) which was injected subcutaneously. These treatments were performed 30 minutes before the surgery and in 4-hour intervals post-operatively. As the mice were kept in an animal care facility with light- and dark phases (simulation of day- and night times), during dark phases the Buprenorphine supply was guaranteed by adding 0.009 mg/ml Buprenorphine to the drinking water of the mice (Sauer et al. 2016). During surgery, the animals were anaesthetized using isoflurane. For this, the mouse was placed into a small chamber which was evaporated with isoflurane dissolved in oxygen. After 5 minutes, when the mouse had fell into the inaesthetic stadium of chirurgic tolerance, it was placed on a heated surgery platform to keep the body temperature at 36°C. To prevent the eyes from drying out, Bepanthen Eye and Nose Cream was applied to the animal's

eyes. During surgery, the mouse's legs were fixed to the surgery platform using Leukosilk. To open the abdominal cavity, a 1-2 cm long cut was made in the middle of the abdomen from the mammary glands upwards. Both the animal´s skin as well as the subjacent muscular layer were cut open. The area around the wound was covered with sterile surgery gauze which was soaked in 70% EtOH to disinfect the regions around the wound. During surgery, the inner organs of the pregnant mouse were continuously moistened with NaCl/benzylalcohol to prevent them from drying out. After opening the abdominal cavity, the two uterine horns were carefully dislocated from the abdomen and laid out on the sterile surgery gaze. Here, it is especially important to avoid lesions of the placental regions of each embryo as well as lesions of the blood vessels. Each embryo´s lateral ventricle was injected with 1 µl of 4 µg/µl concentrated DNA plasmid. The DNA plasmids were dyed with Fast Green to enable the experimenter to check the brain region where the plasmid DNA was injected. Each DNA construct was cotransfected to the neuronal cells with a pCAGGs-GFP plasmid (0.5 µg/µl), carrying a green fluorescent protein expression sequence in it for later identification of successfully electroporated cells. The pCAGGs-GFP construct was co-electroporated to enhance the GFP expression of the electroporated constructs. To transfect the cells lining the ventricle, electric current was applied to the embryonic brains using a pair of platin electrodes. The plus pole of the electrode was placed on the region of the motor cortex and the minus pole was placed on the opposite side of the embryo´s head. By applying an electric current to the electrodes, the negatively loaded plasmid DNA was transferred to the area where the plus pole of the electrodes was placed. Like this, the plasmid DNA can be directed to all possible brain regions and is transfected into the neuronal cells growing there. After electroporation, the uterus horns were carefully placed back into the abdominal cavity and the muscle as well as the skin layer of the pregnant mouse were sewed with PERMA Hand Seide (Ethicon). The suture was disinfected with NaCl/benzyl alcohol and the mouse was placed back into its home cage. To prevent the animal from cooling down it was rolled into paper tissue and supplied with some additional nesting material.

3.1.3. Analyses of electroporated brains

To analyze the brains of the electroporated embryos, the pregnant mother was sacrificed by cervical dislocation at E15 or E18 and the embryos were removed from the

abdominal cavity. The heads of the embryos were cut off with a surgical scissor and placed into a 10 cm dish covered with PBS. To select successfully electroporated embryos, the heads were illuminated under a fluorescent flashlight. Brains which were successfully electroporated with the plasmid DNA displayed a green signal in the area of the motor cortex. The brains of the GFP positive embryos were dissected and stored in 4% paraformaldehyde (PFA) at 4°C over-night for fixing.

To prepare the dissected brains for cryo-conservation, the PFA was removed from the brains and they were transferred to a fresh falcon with 15% sucrose solution in PBS. After 24 hours at 4°C, the 15% sucrose solution was replaced by 30% sucrose solution in PBS. The brains were again incubated for 24 hours at 4°C. Incubation in sucrose solutions extracts water from the cells via osmosis and therefore prevents them from being damaged during the freezing process. When the brains were completely saturated with sucrose, they were transferred to a falcon with 30% sucrose solution in PBS with 50% TissueTek (Sakura). During the incubation time of 10 min at RT, the cryomolds were prepared for embedding the brains. Each brain was placed into a single cryomold, covered with TissueTek and shock frozen with an ethanol – dry ice mixture providing temperatures about -72°C. The frozen brains were stored in a -80°C freezer until further use. For further analyses, the brains were cut into 20 µm thick sections using a Leica cryostat. The sections were put on SuperFrost Plus adhesion slides (Thermo Scientific) and stored at -20°C until further use.

3.2. Immunohistochemical staining of electroporated brains

For immunohistochemical stainings, the slides were shortly incubated in PBS + 0.2% Triton to rehydrate them after storage in the freezer. Subsequently the slides were incubated in 10mM sodium citrate + 0.05% Tween20 for 25 minutes at 85°C for antibody retrieval. Afterwards, the slides were washed again in PBS + 0.2% Triton and blocked for 1 hour in PBS + 0.2% Triton with 2% sheep serum. After blocking, the primary antibodies were prepared in blocking solution and carefully pipetted on the slides. The primary antibodies were incubated on the slides over night at 4°C. Table 25 shows the concentrations used for the different antibodies. The next day, the slides were washed 3 times 15 minutes with PBS + 0.2% Triton. Next, the secondary antibodies were diluted in blocking solution, pipetted on the slides, and incubated in the dark at RT.

Subsequently, the slides were washed 3 times 15 minutes with PBS + 0.2% Triton and embedded using Fluoromount with DAPI.

Antibody	Supplier	Catalog number
mouse anti GFP (1:500)	Roche	11814460001
rabbit anti Satb2 (1:200)	Abcam	ab34735
rabbit anti Pax6 (1:100)	Biolegends	901301
rabbit anti Phospho Histone H3 (1:200)	Cell Signaling	9701S
chicken anti Tbr2 (1:200)	Millipore	AB15894
rabbit anti Ki67 (1:200)	Abcam	ab16667

Table 25: Antibodies used for immunohistochemical stainings.

4. Expression analyses of miRNA 16 target genes

To identify possible target genes of miR-16, mRNA sequencing was performed. For this, murine cortical cells which were in utero electroporated with miR-16 were used.

4.1. Fluorescent activated cell sorting (FACS)

To prepare the brain lysates for FACS sorting, the electroporated brains had to be collected and dissected as already described in chapter 3.1.3. For FACS sorting the brains were dissected at E14, 24 hours after in utero electroporation. The cortices were dissected from the GFP positive brains and the meninges were removed from them. All cortices electroporated with the same construct were pooled and collected in a 50 ml falcon with DMEM media (Gibco) on ice. To produce single cell suspensions from these pooled cortices, the DMEM media was carefully removed from them and 2 ml of trypsin (Gibco) was pipetted on the tissue. The falcons were incubated at 37°C for 6 minutes. This incubation time enables the proteatic activity of tryspin to digest extracellular proteins of the isolated tissue in order to obtain a single cell solution. After incubation at 37°C, 6 ml of DMEM media supplemented with 20% FBS were added to the falcons containing the digested tissue. This step stops the proteatic activity of trypsin and preserves the cells contained in the digested tissue from being destroyed. The falcons were centrifuged for 3 minutes at 300g and the supernatant was carefully removed and discarded. The pellets were washed with 10 ml PBS (Gibco) and centrifuged for 3 minutes at 300g. This step was repeated twice. To produce a single cell suspension, the cell pellet was dissolved in 1 ml of PBS (Gibco). The cells were carefully pipetted up and down around 30 times and finally run through a 100 µM filter mesh for further separation. The resulting single cell suspension was stored on ice until FACS sorting.

In order to separate the electroporated, GFP positive cells from the non-transfected, GFP negative cells, the prepared single cell solutions were subjected to FACS. During this procedure, GFP positive cells are detected with a laser and sorted into a separate reaction tube for later analyses. FACS sorting was conducted by the TRON FACS Core Facility in Mainz. The GFP positive cells were sorted into the RLT buffer of the RNeasy Micro Kit (Qiagen) supplied 1:100 with ß-Mercaptoethanol.

4.2. RNA isolation

To isolate RNA from the sorted, GFP positive cells, the RNeasy Micro Kit (Qiagen) was used. This kit is especially suitable to isolate RNA from very small amounts of cells. With the FACS, 10.000 to 50.000 GFP positive cells were isolated. The sorted cells were vortexed for 1 minute for homogenization. Then, 100 µl of 70% EtOH was added to the lysate and mixed well by pipetting. The sample was transferred to a RNeasy MinElute spin column and centrifuged for 15 seconds at 8000 g. The flow through was discarded and 350 µl buffer RW1 was added to the spin column. Again, the column was centrifuged for 15 seconds at 8000 g and the flow through was discarded. For the on-column DNAse digestion, 10 µl of DNAse I and 70 µl of buffer RDD were pipetted on the spin column. After incubation time of 15 minutes at RT, 350 µl of buffer RW1 were pipetted on the column which was then centrifuged for another 15 seconds at 8000 g. The Flow through was discarded and the column was washed with 500 µl of buffer RPE. The flow through was again discarded and 500 µl of 80% EtOH were pipetted on the spin column. The column was centrifuged for 2 minutes at 8000 g, the flow through was discarded and the empty column was centrifuged for 5 minutes at full speed to remove residual EtOH from the filter membrane. For elution of the RNA, 14 µl of RNase water was pipetted on the spin column which then was centrifuged at full speed for 1 minute. The isolated RNA was quantified using the Qubit RNA High Sensitivity Assay kit (Thermo Scientific) and stored at -80°C until further use.

4.3. mRNA sequencing of FACS sorted cells

The mRNA sequencing of the miR-16 overexpressing RNA samples was performed by StarSeq Mainz.

4.4. Bioinformatical analyses

The bioinformatical analyses of the sequencing data was performed as described in chapter 1.1.4.

5. Validation of miRNA 16 target genes

The bioinformatical analyses of the RNA sequencing data identified 415 differentially expressed genes (DEGs) between miR-16 overexpressed samples and the control cells. Among these, 221 DEGs were downregulated after miR-16 overexpression. To validate this finding, RT-qPCR and Luciferase Assays were performed.

5.1. Validation with RT-qPCR

5.1.1. Overexpression of miRNA 16 in N2A cells

For the validation of the RNA sequencing data, miR-16 was overexpressed in N2A cells. For this, one day prior transfection, N2A cells were seeded into 12 well cell culture plates, 75.000 cells per well. 14 hours later, 3 wells each were transfected with either 10 nM of miR-16 miRNA mimic or negative control (Qiagen) using Lipofectamine3000 (Thermo Scientific). Forty-eight hours after transfection, the cells were harvested using a cell scraper and the pellets were solved in 80 µl RNA later reagent (Sigma). The pellets were stored at -20 °C until further use.

5.1.2. RNA isolation

RNA was isolated from the cell pellets using the Roche High Pure RNA isolation kit. First, the pellets were thawed and resuspended in 120 µl PBS. Then, 400 µl Lysis/binding buffer was added and the samples were vortexed for 15 seconds. The samples were transferred to a High Pure filter tube and centrifuged for 15 seconds at 8000 g. The flow through was discarded and 10 µl of DNAse I solution was pipetted on the spin columns together with 90 µl of DNAse I incubation buffer. The tubes were incubated for 15 minutes at RT. After this incubation time, 500 µl wash buffer I was added to the spin columns and they were centrifuged for 15 seconds at 8000 g. The flow through was discarded and 500 µl of wash buffer II was added to the spin columns. The columns were centrifuged for 2 minutes at maximum speed and the flow through was discarded. To elute the RNA, 50 µl elution buffer was pipetted on the spin column, which was then centrifuged for 1 minute at maximum speed. The RNA was quantified using the Nanodrop One (Thermo Scientific) and stored at -80°C until further use.

5.1.3. cDNA synthesis

The isolated RNA had to be reverse transcribed into cDNA for further analyses with qPCR. For this, the RevertAid Reverse Transcription Kit (Thermo Scientific) was used. 500 ng of each RNA sample were diluted in 10 µl of H_2O. Then, each 1 µl of Oligo dT and Random Hexamer primer were pipetted to the diluted RNA. 4 µl of 5x Reaction buffer, 1 µl of RiboLock RNAse Inhibitor (20 U/µl), 2 µl of 10 mM dNTP mix and 1 µl of RevertAid M-MuLV RT (200 U/µL) were added to the reaction. The tubes were incubated for 5 minutes at 25°C followed by 60 minutes at 42°C in a thermal cycler. The reaction was terminated by an incubation at 70°C for 5 minutes. The cDNA samples were stored at -20°C until further use.

5.1.4. RT-qPCR

For real time quantitative PCR (RT-qPCR), the cDNA was diluted to a final concentration of 5 ng/µl. 2 µl of cDNA were pipetted in each tested well of a 96 well plate together with 8 µl of qPCR Master Mix (0.4 µl Primer Mix fw+rv 10µM, 5.2 µl 2x Takara SYBR green reagent (Takara), 2.4 µl H_2O). The plate was sealed with an adhesive foil, centrifuged briefly and put into the qPCR cycler (PeqLab, OneStep). Quantification of the obtained cT values was performed using the delta-delta-cT method.

5.2. Validation with Luciferase Assays

Through our RNA sequencing analyses, miR-16 was identified to be an interactor of different target genes in the developing embryonic brain. To validate the predicted effect of miR16 on these candidate genes, luciferase assays were performed in HEK293 cells.

5.2.1. Cloning of Luciferase Assay constructs

For the luciferase assays, the 3' UTRs of the newly identified miR16 targets Wee1 were cloned downstream of the *renilla* luciferase into the psiCheck2 vector (Promega). For this, the GeneArt Gibson Assembly Master Mix EX (Thermo Scientific) was used. The Primer sequences can be seen in table 26.

Name	**Sequence**
Wee1_fw	cagtaattctaggcgatcgcactgctcacattccccag
Wee1_rv	gatattttattgcggccagcttaaggtaagcacggaatgac

Table 26: Primers for cloning of luciferase assay constructs.

First, the 3’ UTR sequences were PCR amplified from genomic mouse DNA. For this, the Q5 High Fidelity polymerase (NEB) was used. The tables 27 and 28 display the PCR reaction setup and cycling parameters.

Reagent	**Volume**
5x Q5 Reaction buffer	10 µl
10 mM dNTPs	1 µl
10 µM Primer Mix (fw+rv)	5 µl
Template DNA	500 ng
Q5 High Fidelity DNA Polymerase	0.5 µl
H_2O	to 50 µl

Table 27: PCR reaction for cloning of luciferase assay constructs.

Temperature	**Cycles**	**Time**
98°C	1x	3 min
98°C	35x	10 sec
66°C	35x	30 sec
72°C	35x	30 sec
72°C	1x	2 min
4°C		hold

Table 28: Cycling protocol for cloning of luciferase assay constructs.

To check for correct size of the amplified DNA, the PCR products were loaded on a 1.5 % agarose gel. The bands were cut from the gel and the DNA was eluted using the High Pure PCR Product Purification Kit (Roche). The purified DNA was quantified using a NanoDrop One and stored at -20°C until further use.

To ligate the amplified 3’ UTR sequences into the psiCheck2 vector, the GeneArt Gibson Assembly Master Mix EX (Thermo Scientific) was used. For this, the psiCheck2 vector was digested with the same 2 enzymes (NotI, XHoI) that were also used for the 3’ UTR primer design to facilitate a side directed ligation of the 3’ UTR sequences into the backbone vector. For the Gibson Assembly, 0.04 pico moles of each insert and backbone vector were mixed with 5 µl of Gibson Master Mix A and filled up to a total volume of 10 µl with H_2O. The reactions were incubated in a thermal cycler using the cycling protocol shown in table 29.

Temperature	Time
37°C	5 min
75°C	20 min
Cool to 60°C 0.1°C/sec	
60°C	30 min
Cool to 4°C 0.1°C/sec	

Table 29: Incubation protocol Gibson Assembly.

Afterwards, 10 µl of Gibson Master Mix B was pipetted on each reaction and the tubes were incubated at 45°C for 15 minutes.

After this incubation the ligates were diluted 1:3 and transformed into competent *escherichia coli* bacteria. The bacteria were plated onto LB-Ampicillin plates and incubated over night at 37°C. The next day, colonies were picked, mini-plasmid preparation was conducted and the DNA of the clones was sent to StarSeq for sanger sequencing to check for the correct insert size and sequence. Table 30 shows the sequencing primers used for the psiCheck2-vector.

Name	Sequence
psiCheck2_fw	CAGGAGGACGCTCCAGATGAAATG
psiCheck2_rv	GTCAGACAAACCCTAACCACCG

Table 30: Sequencing primers for psiCheck2 vector.

After successful validation of the correct insert size and sequence, the according clone was used for maxi-plasmid preparation. For this, the Qiagen Plasmid Maxi Kit was used, according to the manufacturer's protocol.

5.2.2. Transfection of Luciferase constructs into HEK293 cells

To transfect the cloned luciferase assay constructs into HEK293 cells, Lipofectamine2000 was used (ThermoScientific). Besides the cloned 3'UTR of the target genes, a miR-16 miRNA mimic was co-transfected into the cells to test the effect of this miRNA on the target gene Wee1. The miR-16 miRNA mimic was bought from Qiagen. One day prior

transfection, 7,5 x 10^4 HEK293 cells were seeded in each well of a 12 well plate. For transfection one day later, one tube was prepared containing 80 µl OptiMEM (Gibco) plus 600 ng miRNA mimic and 200 ng of the cloned 3' UTR construct of Wee1 and another tube containing 80 µl OptiMEM (Gibco) plus 4 µl Lipofectamine2000 transfection reagent (Thermo Scientific). The contents of the two tubes were mixed and incubated at RT for 5 minutes. Then the complete sample was pipetted drop wise on one well of the pre plated cells and incubated on them at 37°C for 48h.

5.2.3. Lysate preparation and Luciferase Assay

48h after transfection, the cells were washed once with PBS. Then, 200 µl of 1x Lysis buffer (Promega) was pipetted on each well. The plates were incubated at RT on a shaker for 15 min. After incubation, each lysate was pipetted in a separate tube. The lysates were either stored at 4°C until further use or directly used for Luciferase Assays.

To measure the relative luciferase activity of the prepared cell lysates, 20 µl of each sample were pipetted into separate wells of a 96-well plate. Each sample was tested in triplicates. The plate was loaded onto a CentroXS3 LB 960 Luminometer (Berthold Technologies) and the Firefly- and Renilla- luciferase activity of the samples was measured. The Luminometer was set to add 100 µl of Firefly or Renilla buffer to each scanned well. To quantify the relative luciferase activity of the samples, the Renilla values were divided by the firefly values (normalization).

5.3. Validation with western blot analyses

To check for the effect of miR-16 on the protein level of the target genes Wee1 and Fbxw7, western blot analyses were performed. For this, N2A cells were transfected with miR-16 miRNA mimics as described in chapter 5.2.2. 48h after transfection, the cells were washed once with PBS, scraped from the surface of the plates with a sterile cell scraper and transferred to a 15 ml falcon. Then, the cells were centrifuged at 300 g for 3 min and the supernatant was removed carefully. The cell pellet was dissolved in 50 µl of Magic Mix (table 31) and the whole volume was pipetted on a QIAShredder column (Qiagen)and centrifuged for 2 min at 8000rpm. The flow through was transferred to a fresh 1.5 ml Eppi and quantified on a NanodropOne.

Ingredient	Volume
Urea-nitrate	4.8 g
1 M Tris pH 7.5	150 µl
Glycerin	870 µl
SDS	100 mg
Protease Inhibitor	1 tablet (for 10 ml)

Table 31: Magic mix (10 ml) for western blot lysates.

During the western blot, the protein mix loaded to the SDS gel is first separated by size, then the proteins are transferred to a solid membrane and lastly the proteins of interest are marked using specific primary and secondary antibodies. First, the SDS gel was made (10% separating- and 10% stacking gel), following the protocol described in tables 32 and 33.

Ingredient	Volume
H_2O	1,4 ml
0,5M Tris pH6,8	250 µl
30% Acrylamide	330 µl
10% SDS	20 µl
10% APS	20 µl
TEMED	2 µl

Table 32: 10% Stacking gel for western blot.

Ingredient	Volume
H_2O	1,9 ml
1,5M Tris pH8,8	1,3 ml
30% Acrylamide	1,7 ml
10% SDS	50 µl
10% APS	50 µl
TEMED	2 µl

Table 33: 10% Separating gel for western blot.

The gels were poured into a SDS gel running apparatus and incubated for 30 minutes at RT until they were solid. 60 µg of each protein lysate plus 5 µl of Magic Mix with 1% beta-Mercaptoethanol and bromophenol blue were cooked for 5 min at 95 °C and loaded to the SDS gel. The SDS gel was connected to a power supply, the running

chamber was filled with running buffer (for 1 liter: 3g Tris, 14.4g Glycine, 1g SDS) and was run at 200 V for 45 minutes. Afterwards, the SDS gel was transferred to the membrane of a Trans-Blot Turbo Transfer Sandwich (BIO RAD) and blotted in the Trans-Blot turbo transfer system for 11 minutes at 25 V. Afterwards, the membrane with the transferred proteins was blocked in 5% milk (for 50 ml: 2.5 g milk powder plus 50 ml H_2O) at RT for 1h. The primary antibodies were incubated in 3ml blocking solution and a concentration of 1:200 on the membranes at 4°C over-night. The next day, the membranes were washed 3 times for 10 min with PBS-Tween (for 1 liter: 1 liter PBS plus 1 ml Tween) before incubation with the secondary antibody. The secondary antibody (1:6000) was incubated on the protein membranes in 3 ml blocking solution. The membranes were put on a roller mixer at RT for 1h and afterwards washed again 3 times with PBS-T for 10 minutes each. To quantify the protein, the washed membrane was provided with 300 µl ECL mix and placed under a BIO RAD Chemidoc where the proteins were detected using chemiluminescence. The BIO RAD tool Image Lab V5 was used for quantification of the proteins on the membrane.

6. Rescue of miRNA 16 induced phenotype in vivo

To evaluate if the phenotype induced by miR-16 overexpression in the developing brain can be rescued, the miR-16 target gene Wee1 was overexpressed together with miR-16 via in utero electroporation in murine embryonic brains.

6.1. Cloning of rescue constructs

To clone the coding sequence of Wee1 into the pCAGGs-IRES-GFP vector, the Gibson Assembly Cloning Method was used. This method is described in chapter 5.2.1. For this cloning, primers were designed using the NEBuilder online tool (New England Biolabs; https://nebuilder.neb.com/). The primers carried sequences of the restriction enzymes XmaI and EcoRI to insert the Wee1 cDNA into the plasmid in a directed manner. The primer sequences can be seen in table 34.

Name	Sequence
Wee1_pCAGGs_fw	gatctcgagctcaagcttcgATGAGCTTCCTGAGCCGAC
Wee1_pCAGs_rev	gggagggagaggggcggatcTCAGTATATAGTAAGGCTGACAGAG

Table 34: Cloning primers Wee1.

For sequencing of the resulting constructs, the primers of table 35 were used.

Name	Sequence
pCAGGs_seq_fw	CCATGTTCATGCCTTCTTCTTT
M13_seq_rv	CAGGAAACAGCTATGACC

Table 35: Sequencing primers for Wee1 cloning.

6.2. In utero electroporation of Wee1 construct

The description of the method of in utero electroporation can be found in chapter 3.1.2. The brains were electroporated at E13, analyzed at E15 and processed according to the protocol described in chapter 3.1.3. The brains were cut transversally at a Leica Cyrotome. Table 36 lists the plasmid concentrations for the different samples.

	pCAGGs-IRES-GFP	**pGAGGs-GFP**	**pCAGGs-miR16-IRES-GFP**	**pCAGGs-Wee1-IRES-GFP**
control	3 µg/µl	0.5 µg/µl	/	/
miR-16+control	1.5 µg/µl	0.5 µg/µl	1.5 µg/µl	/
miR-16+Wee1	/	0.5 µg/µl	1.5 µg/µl	1.5 µg/µl

Table 36: Plasmid concentrations for the Wee1 in utero electroporation.

Results

1. MiRNA expression in the developing brain

Over the last years it has become more and more evident, that miRNAs play important roles in gene regulation in the developing brain (Rajman et al., 2017). Yet, little is known about miRNA expression patterns during different stages of embryonic development. To shed a light on this, we carried out miRNA sequencing of cultured cortical NPCs and neurons as well as cerebral cortex tissue at embryonic stages E14 (embryonic day 14), E17 (embryonic day 17) and P0 (day of birth). These time points were picked according to the fact, that embryonic neurogenesis is active at E14 and E17 and ends at around E18 (Liscovich et al., 2013). The aim of this experiment was not only to obtain an overall impression of miRNA expression during brain development, but also to achieve more insights into the expression profile of the miR-15 miRNA family. As described in the introduction, the miR-15 miRNA family has been shown to be involved in NPC proliferation and neuronal differentiation in the developing murine cortex and therefore was of special interest for us (Lv et al., 2014).

1.1. MiRNA expression in NPCs and neurons

To obtain an overview of miRNA expression profiles in the different cell types of the developing mouse brain, we performed small RNA sequencing with RNA isolated from cultured cortical NPCs and neurons. The bioinformatical analyses was performed by the Institute's bioinformatician, Dewi Hartwich.

The Principal Component Analysis (PCA) clearly separates NPCs and neurons into different clusters according to their miRNA expression profiles (figure 8).

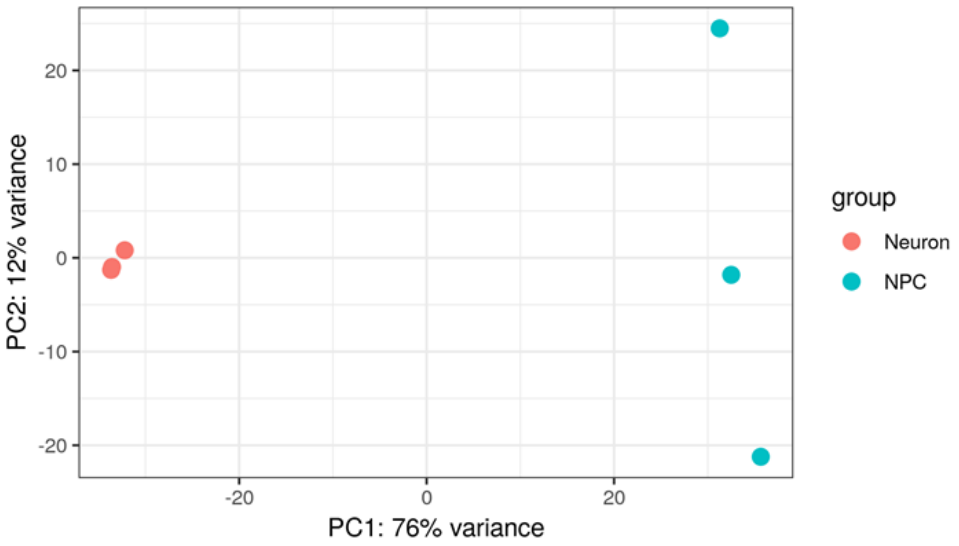

Figure 8: Principal Component Analysis (PCA plot) of miRNA sequencing data in NPCs and neurons. 3 biological replicates of neurons and NPCs were sequenced. NPCs are depicted as blue dots, neurons as red dots.

Table 37 gives an overview of miRNA results in NPCs and neurons. In total, 241 miRNAs were differentially expressed between NPCs and neurons. While expression of 114 of these miRNAs increased in neurons compared to NPCs, expression of 127 of these miRNAs decreased.

No. of upregulated miRNAs in neurons vs. NPCs	**No. of upregulated miRNAs in NPCs vs. neurons**	**Total No. of differentially expressed miRNAs between NPCs and neurons**
114	127	241

Table 37: Differentially expressed miRNAs in NPCs vs neurons.

1.2. MiRNA expression in the developing murine cortex (E14-P0)

To evaluate the expression profiles of different miRNAs in the developing cerebral cortex across different time points of development, miRNA sequencing was performed with RNA isolated from cerebral cortex tissue of E14, E17 and P0 NMRI mice. This experiment was performed, to complete the data we already obtained by miRNA sequencing in NPCs and neurons and to gain more insights into miRNA expression across brain development. As expected, the PCA separates E14, E17 and P0 into different clusters by their small RNA expression profiles (figure 9).

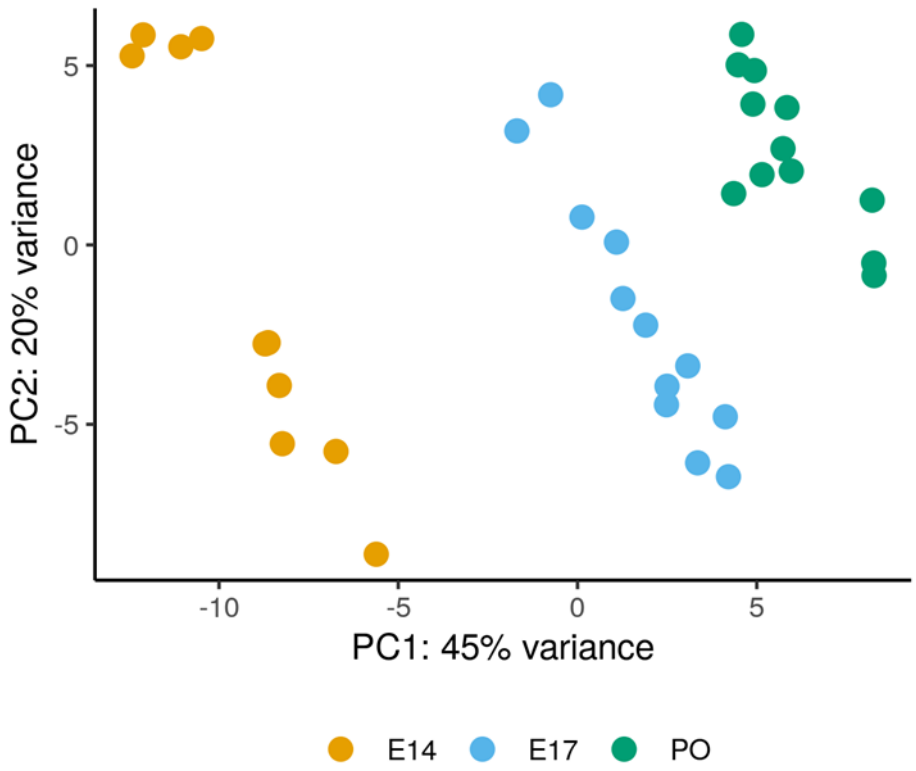

Figure 9: Principal Component Analysis (PCA plot) miRNA sequencing in cortical tissue of E14, E17 and P0 mice. 12 biological replicates were used for miRNA sequencing. E14 samples are depicted as orange dots, E17 samples as blue dots and P0 samples as green dots.

Table 38 gives an overview of the sequencing results of the miRNA sequencing of E14, E17 and P0 mouse cortex. In total, 277 differentially expressed miRNAs could be identified when E14 and E17 lysates were compared. 335 miRNAs were differentially expressed between E14 and P0 and 175 miRNAs between the time points E17 and P0.

	No. of upregulated miRNAs	**No. of downregulated miRNAs**	**Total No. of differentially expressed miRNAs**
E14 vs. E17	133	144	277
E14 vs. P0	163	172	335
E17 vs. P0	82	93	175

Table 38: Differentially expressed miRNAs in E14, E17 and P0 cortical lysates.

The Top 10 up- and downregulated miRNAs for the time points E14 vs. E17, E14 vs. P0 and E17 vs. P0 are listed in heat maps in figures 10-12. Many of these miRNAs have already been shown to have important functions during embryonic brain development and neurogenesis. MiR-124, for example, which we found to be upregulated at P0

compared to E14, is evolutionally highly conserved and has been described to be highly expressed in the developing brain where it is involved in neuronal differentiation and maturation (Kozuka et al., 2019). Two other miRNAs which appeared in our Top 10 up- and downregulated miRNAs at the different stages of development were miR-137 and miR-153. In the past, these miRNAs have been shown to be important regulators of neuronal differentiation and dendritic spine morphology. MiR-137 has been shown to target the gene *NeuroD1*, which is an important transcription factor driving neurogenesis whereas miR-153 targets *Fmr1*, an important translational regulator involved in the fragile X syndrome (Cherone et al., 2019).

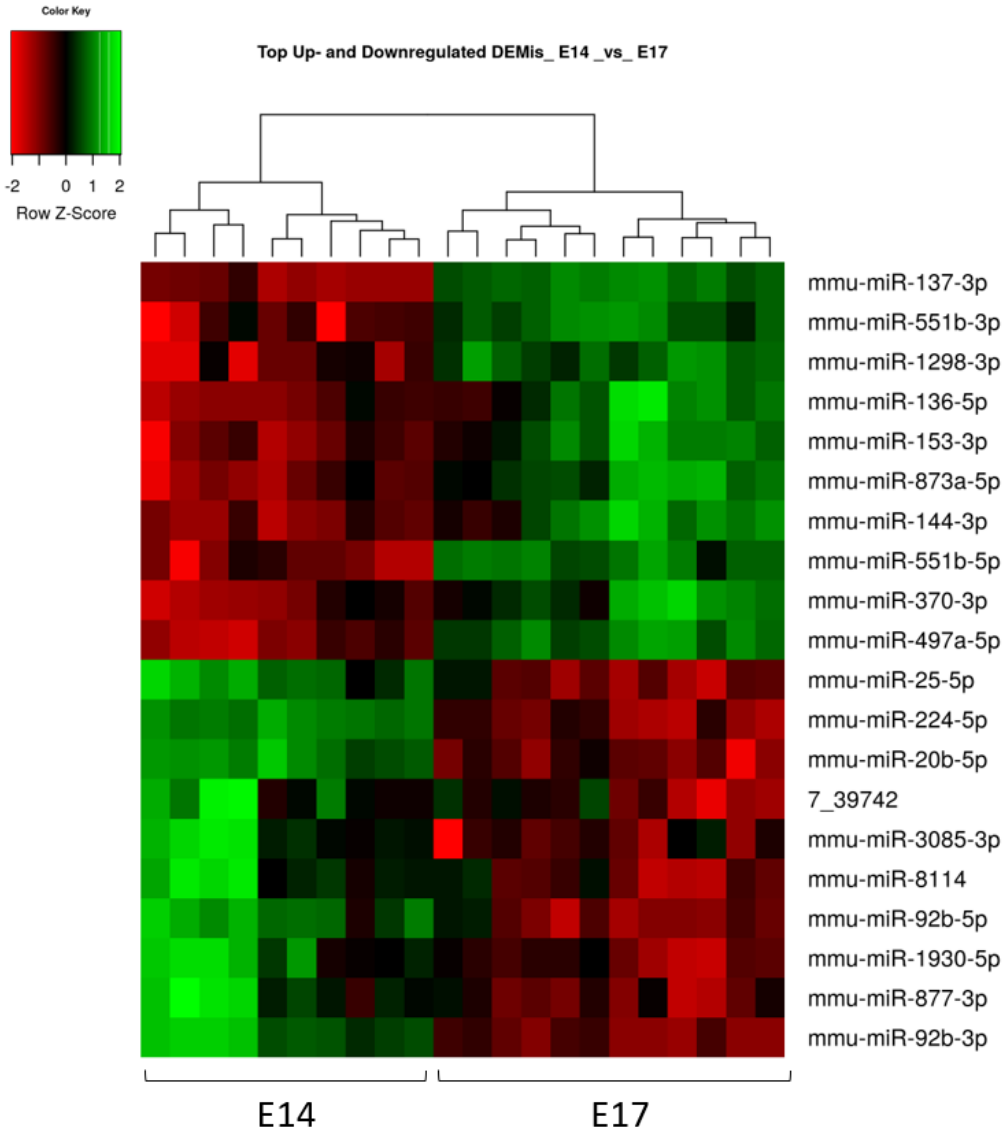

Figure 10: Top up- and downregulated miRNAs between stages E14 and E17. For E14, 10 biological replicates are listed and for E17, 12 biological replicates are listed.

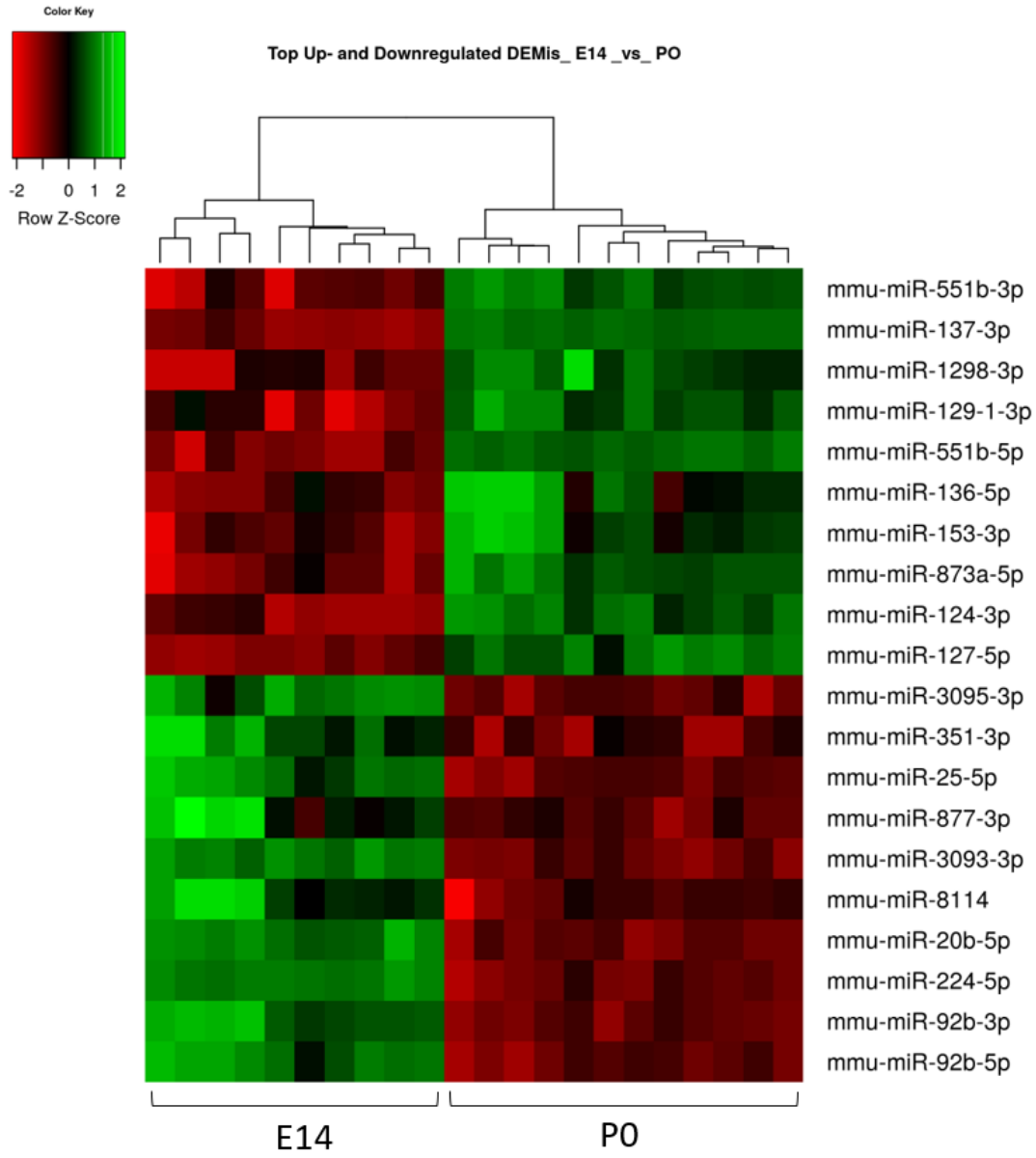

Figure 11: Top up- and downregulated miRNAs between stages E14 and P0. For E14, 10 biological replicates are listed and for P0, 12 biological replicates are listed.

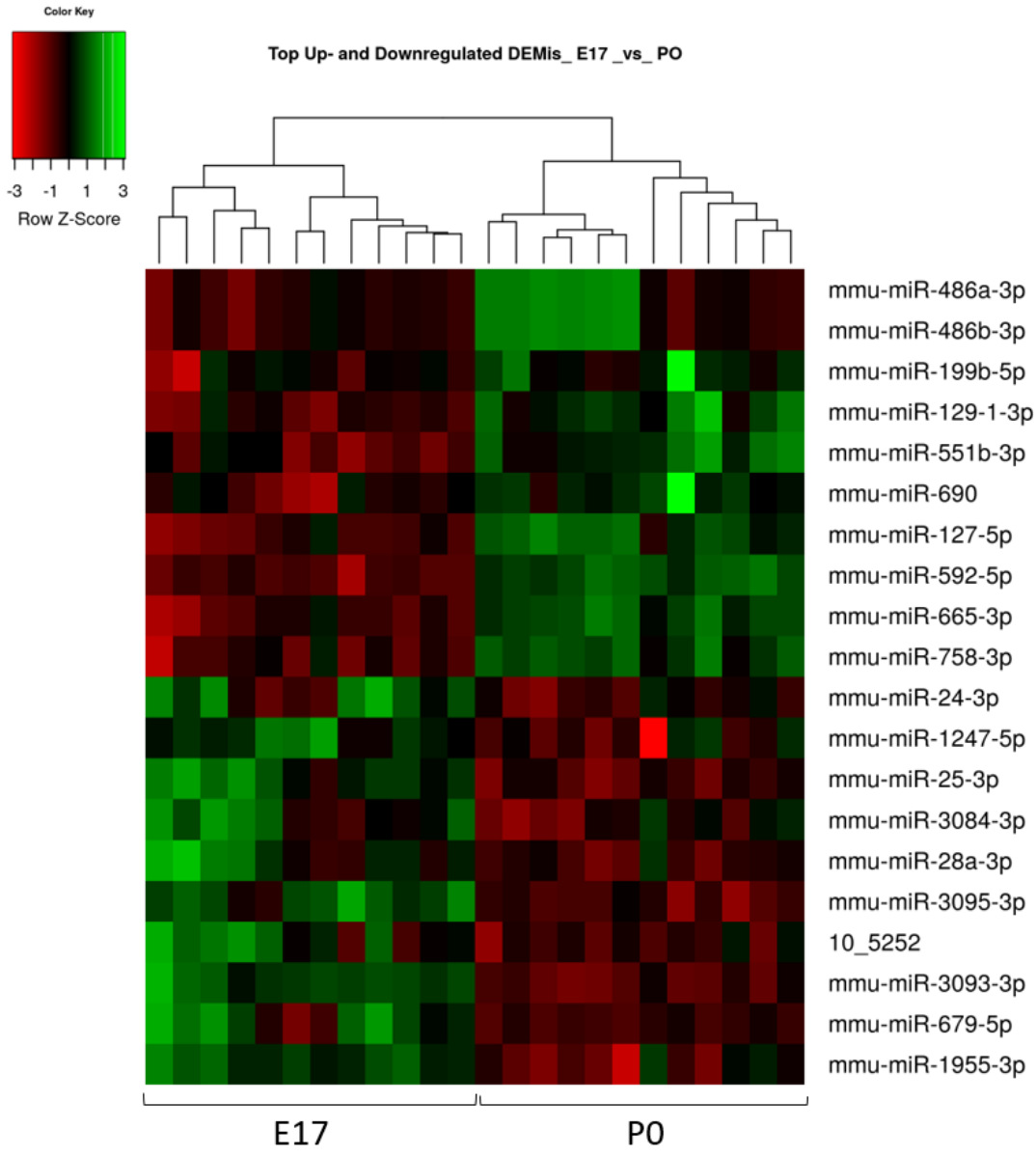

Figure 12: Top up- and downregulated miRNAs between stages E17 and P0. For E17 and P0, 12 biological replicates are listed.

During embryonic brain development, the number of NPCs in the brain slowly decreases as they give rise to an increasing number of neurons by neuronal differentiation. Due to this transition, we also expected an overlap of differentially expressed miRNAs between the later time points of development, as for example P0 and the sequenced neurons as well as an overlap of differentially expressed miRNAs of the E14 cortical lysates and the sequenced NPCs.

To check if a common set of miRNAs is differentially expressed between NPCs and neurons and between the different cortical stages, the data of these experiments were compared with each other. The Venn diagram in figure 13 shows an overlap of 74 miRNAs that are upregulated in NPCs compared to neurons and in the E14 cerebral cortex compared to later stages of cortical development. Similarly, another set of 74 miRNAs are upregulated in both neurons and P0 cerebral cortex when compared to NPCs and P14 cortex, respectively (figure 14).

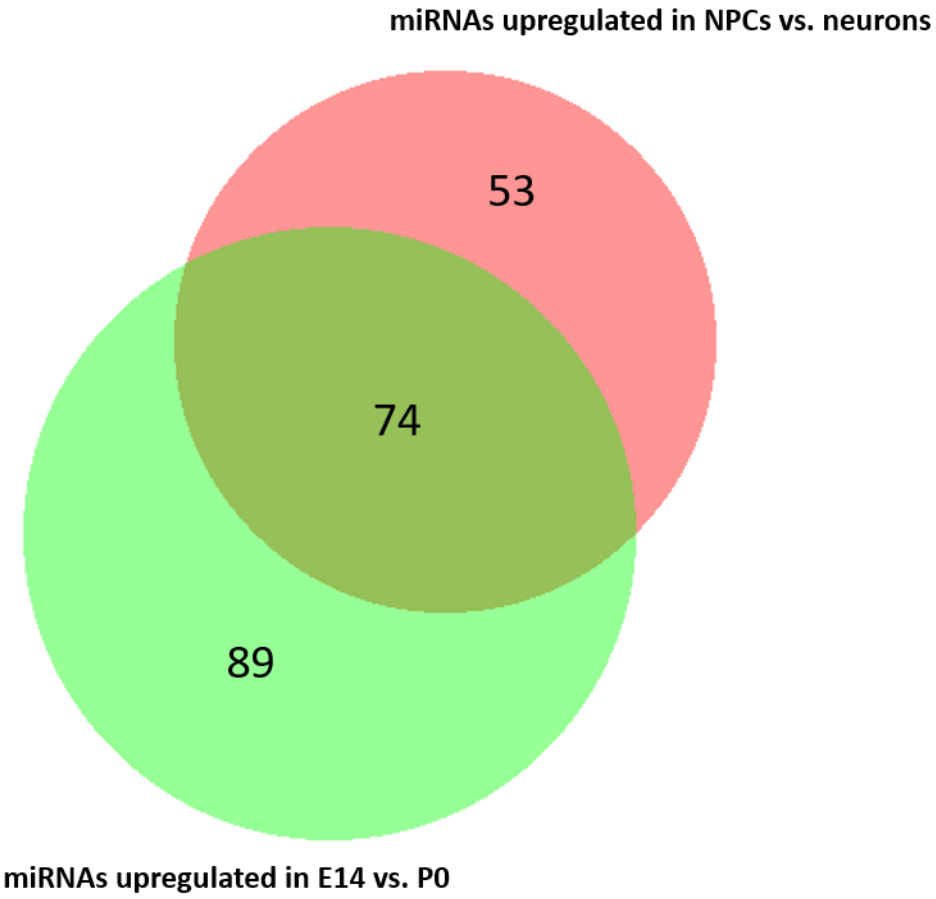

Figure 13: Venn diagram of miRNAs upregulated in NPCs vs. neurons and miRNAs upregulated in E14 vs. P0 cerebral cortex. 89 miRNAs are upregulated in E14 cerebral cortex but not in NPCs and 53 miRNAs are upregulated in NPCs but not in E14 cerebral cortex. 74 miRNAs are upregulated in both E14 cerebral cortex and NPCs.

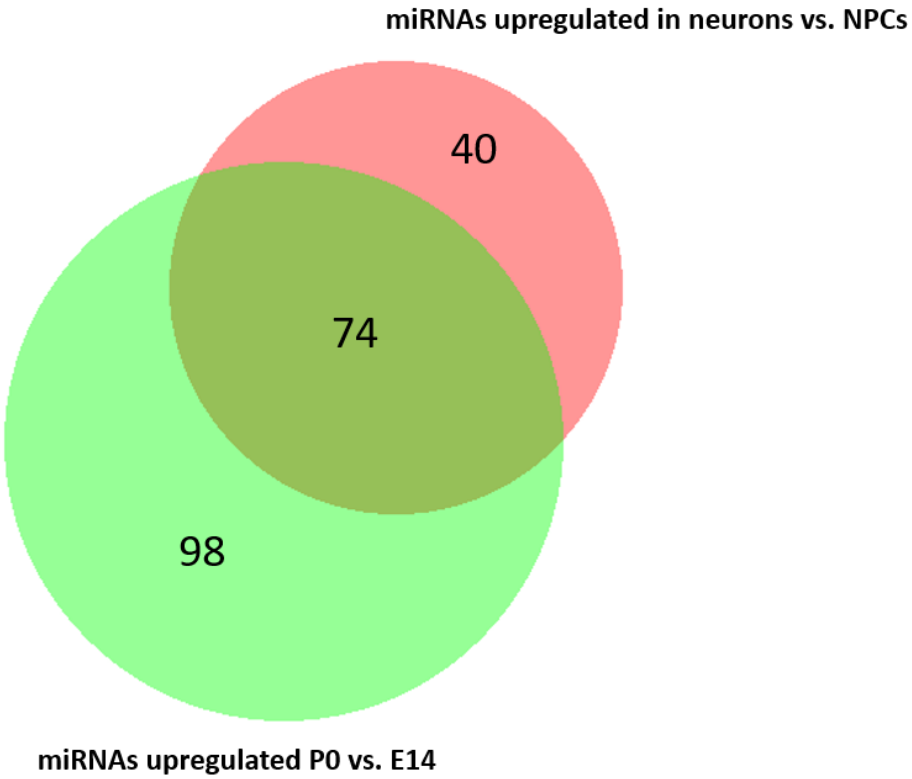

Figure 14: Venn diagram of miRNAs upregulated in neurons vs. NPCs and miRNAs upregulated in P0 vs. E14 cortical lysates. 98 miRNAs are upregulated in P0 cerebral cortex but not in neurons and 40 miRNAs are upregulated in neurons but not in P0 cerebral cortex. 74 miRNAs are upregulated in both P0 cerebral cortex and neurons.

To validate the results of the small RNA sequencing, TaqMan Assays were used as second method. Five miRNAs for which differential expression between E14, E17 and P0 was identified in the small RNA-Seq were chosen for validation: Figure 15 shows that miRNAs -137-3p, -124-3p as well as -128-3p increase their levels of expression in the sampled cortical tissue from early time points of brain development (E14) to early post-natal stages (P0). These results of the miRNA sequencing data could also be validated with miRNA expression analyses in cortical tissue via TaqMan Assays (figures 16 -18) A One-Way ANOVA with post-hoc Tukey demonstrates that all expression differences for miRNAs-137-3p, -124-3p and -128-3p between the stages E14, E17 and P0 are significant.

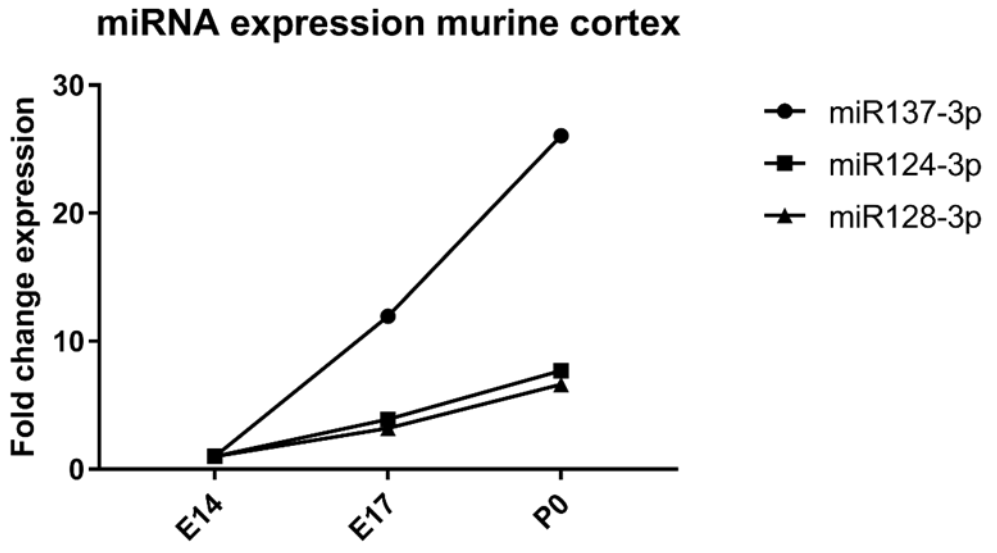

Figure 15: Fold change expression of miR-137-3p, miR-124-3p and miR-128-3p in E14, E17 and P0 cortical tissue. All 3 candidate miRNAs show increasing levels of expression from E14-P0.

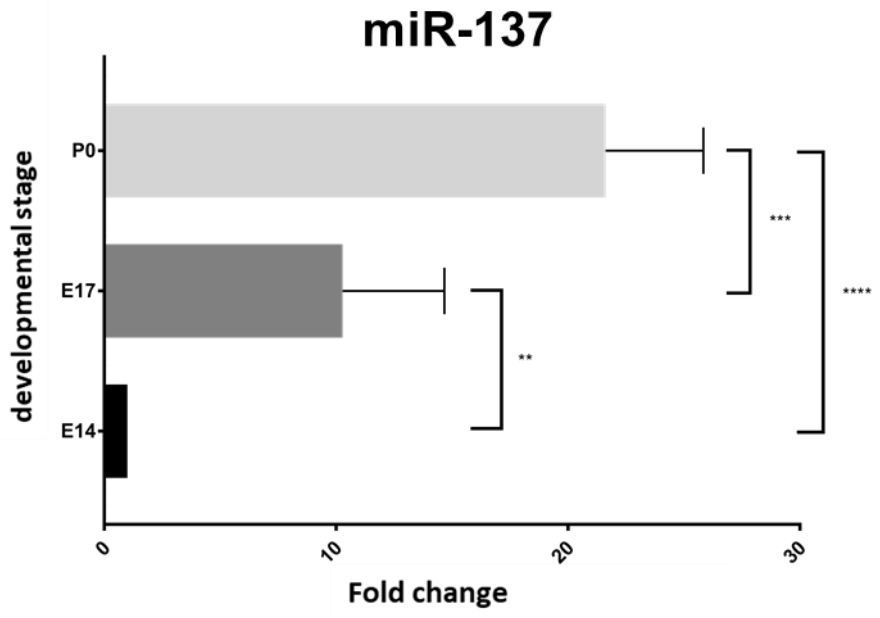

Figure 16: Expression of miR-137-3p increases during embryonic development of the cerebral cortex. Relative expression of miR-137-3p in cortical tissue at E14, E17 and P0 was measured by TaqMan Assays. Shown is the mean of three biological replicates. For the statistical analyses the One-Way ANOVA test with post-hoc Tukey was used. Expression E14 vs. E17 p=0.0011(**); E17 vs. P0 p=0.0002(***); E14 vs. P0 p<0.0001(****).

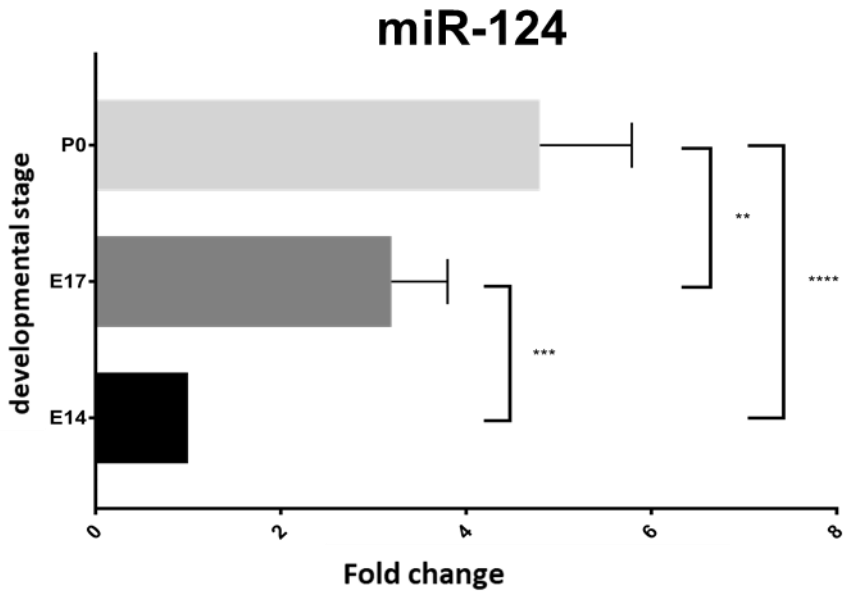

Figure 17: Expression of miR-124-3p increases during embryonic development of the cerebral cortex. Relative expression of miR-124-3p in cortical tissue at E14, E17 and P0 was measured by TaqMan Assays. Shown is the mean of three biological replicates. For the statistical analyses the One-Way ANOVA test with post-hoc Tukey was used. Expression E14 vs. E17 p=0.0001(***); E17 vs. P0 p=0.0027(**); E14 vs. P0 p<0.0001(****).

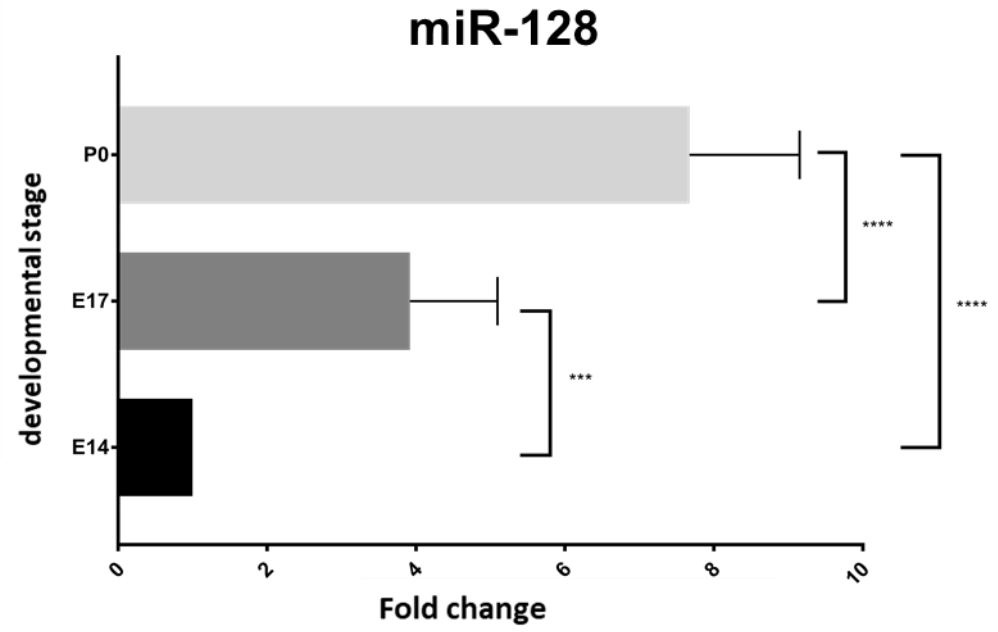

Figure 18: Expression of miR-128-3p increases during embryonic development of the cerebral cortex. Relative expression of miR-128-3p in cortical tissue at E14, E17 and P0 was measured by TaqMan Assays. Shown is the mean of three biological replicates. For the statistical analyses the One-Way ANOVA test with post-hoc Tukey was used. Expression E14 vs. E17 p=0.0010(***); E17 vs. P0 p<0.0001(****); E14 vs. P0 p<0.0001(****).

The small RNA-Seq data indicate that expression levels of miR-15b-5p and miR-130b-3p decrease from E14 to P0 (figure 19). Also, these expression changes could be validated by TaqMan Assays (figures 20 and 21). MiR-15b-5p as well as miR130b-3p both show significantly decreased expression from E14 to P0.

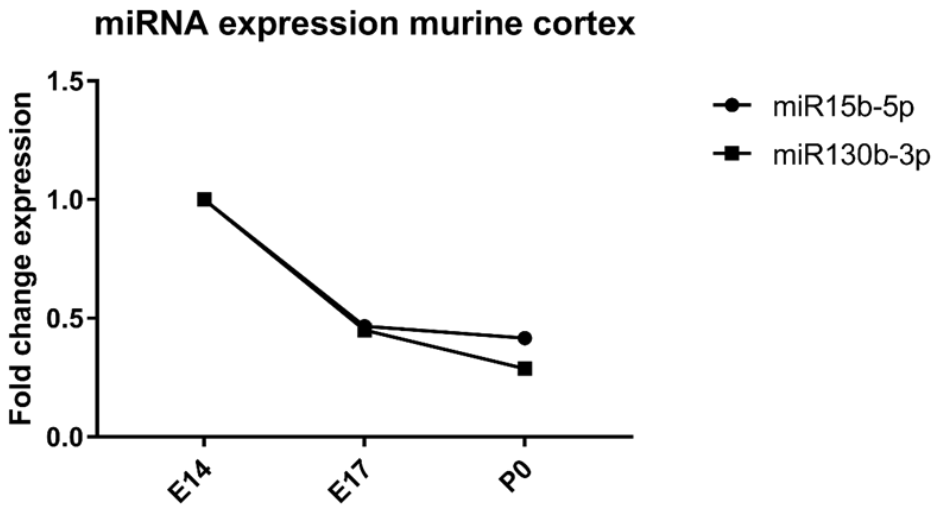

Figure 19: Fold change expression of miR-15b-5p and miR-130b-3p in E14, E17 and P0 cortical tissue. Expression of all three candidate miRNAs decreases during cerebral cortex development.

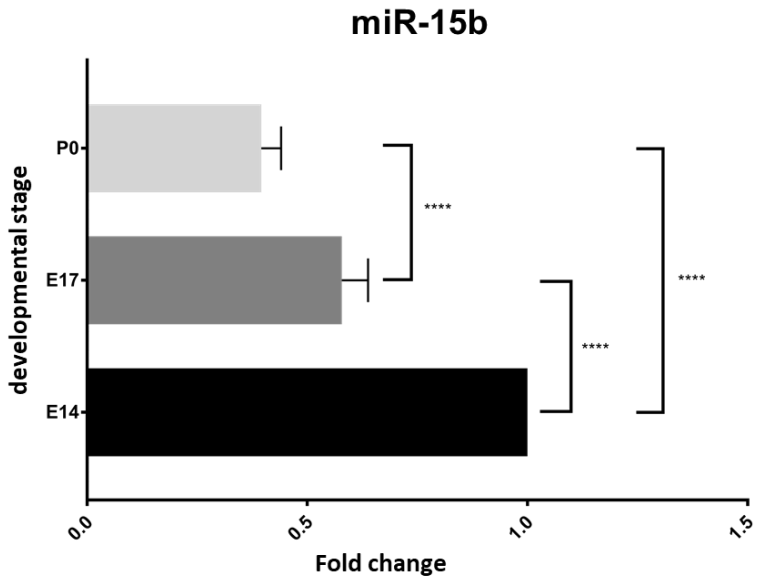

Figure 20: Expression of miR-15b-5p decreases during embryonic development of the cerebral cortex. Relative expression of miR-15b-5p in cortical tissue at E14, E17 and P0 was measured by TaqMan Assays. Shown is the mean of three biological replicates. For the statistical analyses the One-Way ANOVA test with post-hoc Tukey was used. Expression E14 vs. E17 $p<0.0001$(****); E17 vs. P0 $p<0.0001$(****); E14 vs. P0 $p<0.0001$(****).

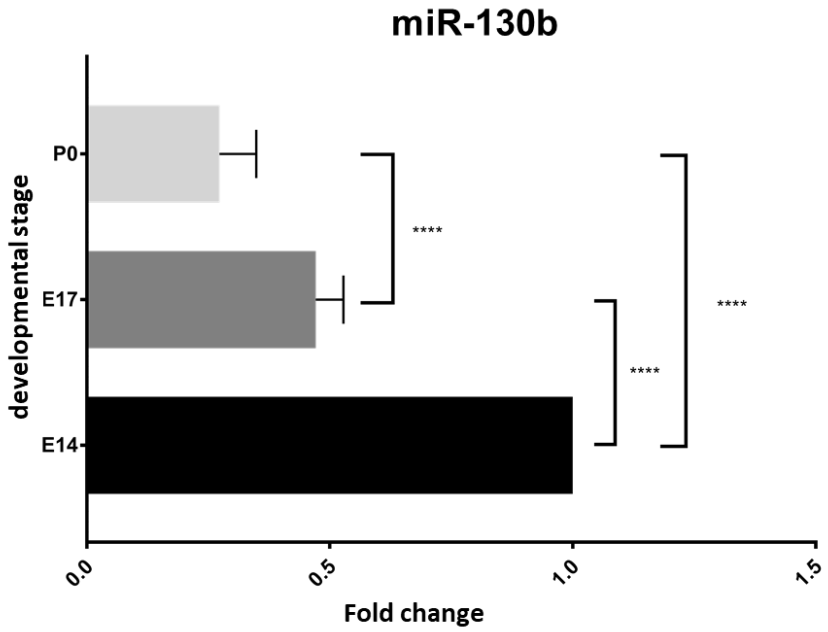

Figure 21: Expression of miR-130b-3p decreases during embryonic development of the cerebral cortex. Relative expression of miR-130b-3p in cortical tissue at E14, E17 and P0 was measured by TaqMan Assays. Shown is the mean of three biological replicates. For the statistical analyses the One-Way ANOVA test with post-hoc Tukey was used. Expression E14 vs. E17 p<0.0001(****); E17 vs. P0 p<0.0001(****); E14 vs. P0 p<0.0001(****).

2. MiR-16 regulates neurogenesis in the embryonic neocortex

2.1. MiR-16 is strongly expressed in the developing brain

While there is no doubt that miRNAs in general fulfil important functions during neural development the specific functions of only a few miRNAs have been studied so far. In my work I decided to focus on the miRNA miR-16 for the following reasons: (i) miR-16 is a member of the miR-15 miRNA family and another member of this family (miR-15b) was already shown to regulate neural differentiation in vivo (Lv et al., 2014) and (ii) miR-16 regulates proliferation and apoptosis in non-neuronal cells and in cultured NPCs (He et al., 2016). I therefore hypothesized that miR-16 is an important regulator of cerebral cortex development.

To get more insights into the expression profile of miR-16 in NPCs/neurons and the developing cerebral cortex, I analyzed the miRNA sequencing data and performed TaqMan Assays.

The sequencing data indicates that miR-16 is highly expressed during embryonic development of the cerebral cortex. Whereas a known driver of neurogenesis, miR-124-3p, was strongly upregulated in neurons compared to NPCs (130-fold), miR-16-5p only showed a trend of upregulation in neurons which was not significant (1.3-fold; p-value=0.22; figure 22). This trend was also validated with TaqMan Assays (figure 23). Due to the high standard deviations, this effect was, however, not significant.

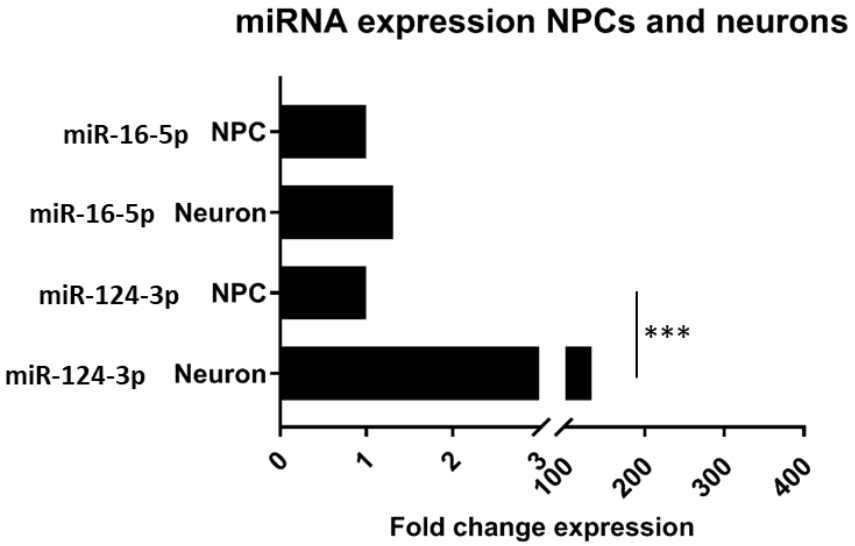

Figure 22: Fold change expression of miR-16-5p and miR-124-3p in NPCs and neurons. Three biological replicates each of neurons and NPCs were sequenced. P-value miR-16-5p =0.22 and p-value miR-124-3p<0.005. The shown data was obtained from miRNA sequencing.

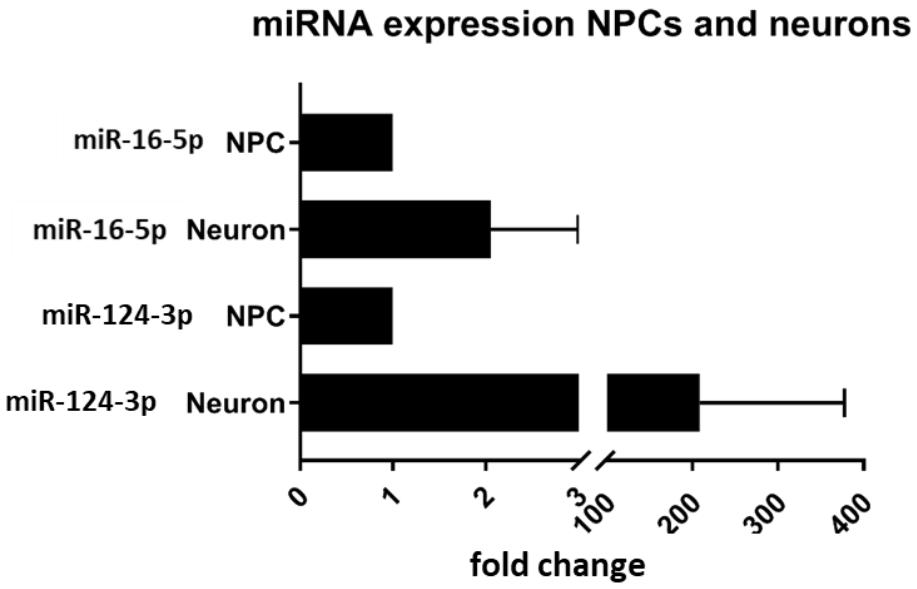

Figure 23: Expression of miR-16-5p and miR-124-3p in NPCs and neurons. Three biological replicates were used for TaqMan Assays. P-value miR-16-5p =0.09 and p-value miR-124-3p=0.08.

2.2. MiR-16 overexpression in the developing neocortex

To check, if a certain level of miR-16 expression in the developing neocortex is crucial for proper development and function, we decided to overexpress this miRNA in the mouse brain in vivo. For this, miR-16 and for comparison the closely related miR-15 were cloned into a pCAGGs-IRES-GFP expression vector and overexpressed in the embryonic mouse neocortex by in utero electroporation. Because the IRES-GFP generated only a weak green fluorescent signal, a pCAGGs-GFP expression vector was co-electroporated to distinguish between electroporated and non-electroporated cells.

2.2.1. Validation of successful miR-15/-16 overexpression

To test for miR-15/-16 expression levels after overexpression by in utero electroporation, the electroporated, GFP positive cells were FACS sorted and collected. Subsequently, RNA was isolated from these cells and expression levels of miR-16 and miR-15 were measured by TaqMan Assays. Figure 24 shows, that in the overexpression samples expression levels of both miR-16 and miR-15 are higher compared to the control. Because in these experiments, the primary miRNA transcripts (pri-miRNAs) were expressed from the vector and further processed into precursor miRNAs (pre-miRNAs) that contained the 5'- and the 3'-arm, both the mature 5p- and 3p-miRNAs, were processed and expressed in the electroporated cells. The TaqMan Assays revealed a 2.9-fold increase in miR-16-5p expression, a 7-fold increase in miR-16-3p expression, a 3.8-fold increase in miR-15-5p expression and a 4-fold increase in miR-15-3p expression.

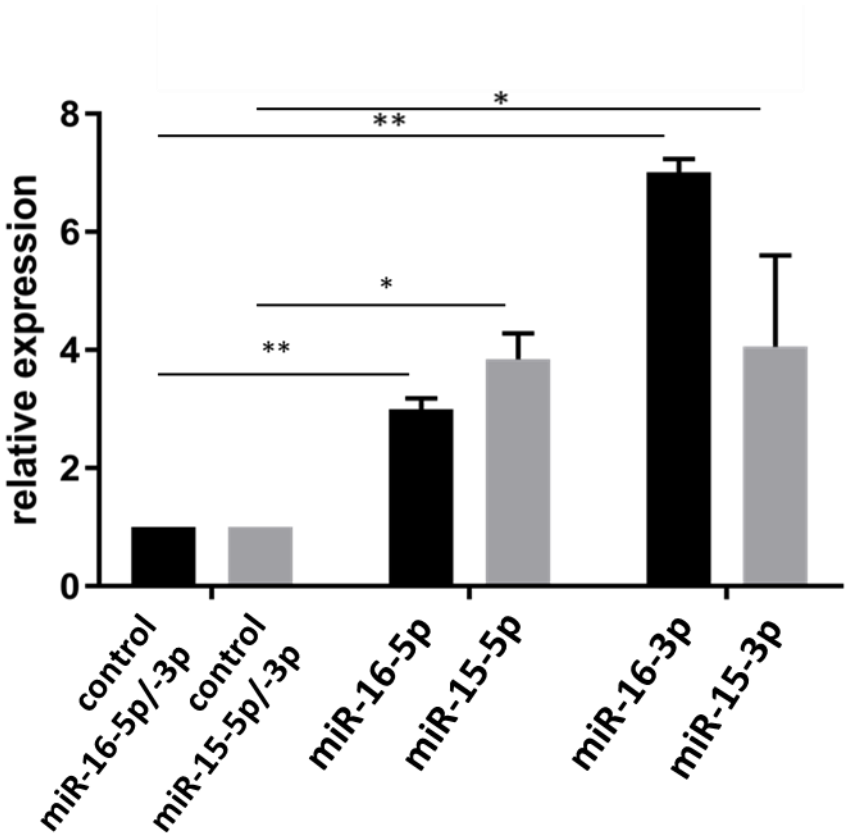

Figure 24: Fold increase in expression of the mature miRNAs miR-16-5p/-3p and miR-15-5p/-3p in the embryonic neocortex after in utero electroporation of miRNA overexpression constructs. Three biological replicates were pooled for this analysis. For the statistical analyses the students t-test was used. Expression miR16-5p vs. miR-16 control $p<0.01$(**); miR-15-5p vs. miR-15 control $p<0.05$(*); miR-16-3p vs. miR-16 control $p<0.01$(**); miR-15-3p vs. miR-15 control $p<0.05$(*).

2.2.2. MiR-16 overexpression causes phenotype in the developing brain

To study the function of miR-16 during neurogenesis, the pCAGGs-miR-16-IRES-GFP construct was electroporated into the motor cortex of mouse embryos at E13. The brains were analyzed two days later, at stage E15. Because of its similarity in seed sequence and binding targets to miR-16 and to check if these two miRNAs induce different phenotypes in the developing neocortex, miR-15 was also included in this study.

As depicted in figure 25, overexpression of miR-16 as well as miR-15 resulted in a significant increase in GFP positive cells in the intermediate zone and a decrease in GFP positive cells in the cortical plate. Whereas in the control, 10% of GFP positive cells had entered the cortical plate by E15, in miR-16 and miR-15 overexpressing cells, 0% and 2%

of GFP positive cells, respectively, were located in the cortical plate. Instead, in the miR-16 and miR-15 overexpressing brains GFP positive cells accumulated in the intermediate zone. Hence, after miR-16 overexpression 98% and after miR-15 overexpression 95% of the electroporated cells were located in the intermediate zone. In the empty control only 81% of the electroporated, GFP positive cells were located in the intermediate zone of the developing cortex. Furthermore, although not significant, a trend of fewer GFP positive cells in the ventricular zone of miR-15/-16 overexpressing brains in comparison to the control brains could be observed (p-value miR-16 vs. control = 0.06; p-value miR-15 vs. control= 0.07).

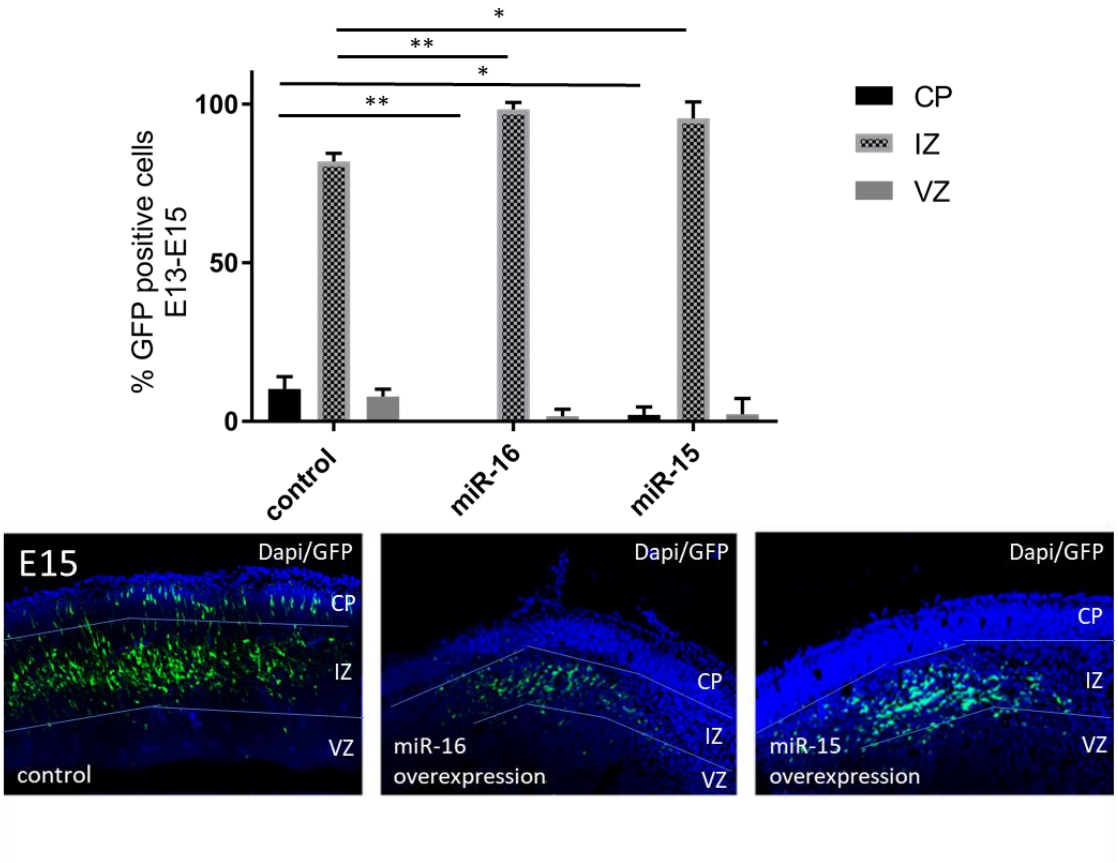

Figure 25: Distribution of miR-16 and miR-15 overexpressing GFP positive cells in the different layers of the developing neocortex. Constructs were electroporated into the neocortex at E13. Brains were analyzed at E15. Three biological replicates were pooled for this analysis. The brains were cut transversally. Depicted area: motor cortex. For statistical analyses the One-Way ANOVA test with post-hoc Tukey was used. CP: cortical plate, IZ: intermediate zone, VZ: ventricular zone. GFP pos. cells CP control vs. CP miR-16 p=0.0070(**); CP control vs. CP miR-15 p=0.0462; IZ control vs. miR-16 p=0.0020(**); IZ control vs. miR-15 p=0.0179(*); VZ control vs. miR-16 p=0.06; VZ control vs. miR-15 p=0.07.

To determine if the phenotype observed after miR-16 and miR-15 overexpression is still present in the developing neocortex at later developmental stages, both miR-16 and miR-15 were overexpressed in utero at E13, and brains were analyzed at E18. This is the last prenatal day of development as C57BL/6 mice usually give birth at E19. Figure 26 shows, that at E18 miR-16 and miR-15 overexpressing cells are strongly impaired from entering the cortical plate. Whereas in the control brains, a very low number of GFP positive cells were located in the intermediate zone (9% of all electroporated, GFP positive cells), miR-16 and miR-15 overexpressing brains accumulated GFP positive cells in this zone. Fifty-one % of all GFP positive, electroporated cells were located in the intermediate zone after miR-16 overexpression and 50% after miR-15 overexpression. In comparison to the control in which 90% of all electroporated, GFP positive cells were located in the cortical plate, this cell number was significantly decreased in miR-16 (48%) and miR-15 (49%) overexpressing neocortex.

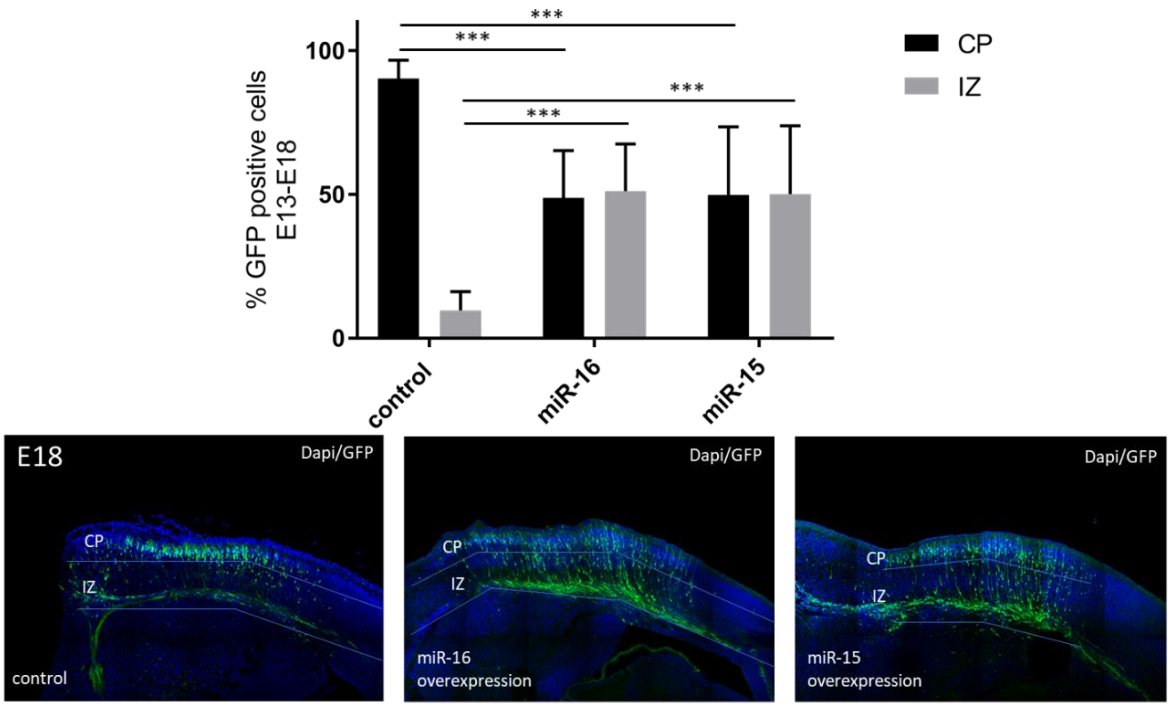

Figure 26: Distribution of miR-16 and miR-15 overexpressing cells in the different layers of the developing neocortex at E18. Constructs were electroporated into the neocortex at E13. Brains were analyzed at E18. Three biological replicates were pooled for this analysis. Depicted area: motor cortex. For statistical analyses the One-Way ANOVA test with post-hoc Tukey was used. CP: cortical plate, IZ: intermediate zone. GFP pos. cells CP control vs. CP miR16 p=0.0004(***); CP control vs. miR-15 p=0.0009(***); IZ control vs. IZ miR-16 p=0.0004(***); IZ control vs. IZ miR-16 p=0.0009(***).

2.2.3. Restricting miR-16/-15 overexpression to newborn neurons abolishes the phenotype

Having shown that the overexpression of miR-16 and miR-15 causes a delay in cells entering the cortical plate, I wanted to investigate the cellular origin of this defect. The pCAGGS IRES GFP vector that was used for overexpressing the miRNAs in the previous experiments contains the chicken beta actin promoter which is active in all different cell types of the developing neocortex. The observed phenotype could therefore be due to a stem cell or neuron defect. To restrict the miRNA overexpression to newborn neurons miR-16 and miR-15 genes were cloned into the ß2 expression vector containing the NeuroD promoter which is exclusively active in neurons. Figure 27 shows, that when overexpressed exclusively in neurons, miR-16 and miR-15 overexpression does not cause a phenotype. The amount of GFP positive cells between the cortical plate or intermediate zone of control and miRNA overexpressing cells did not differ significantly from each other.

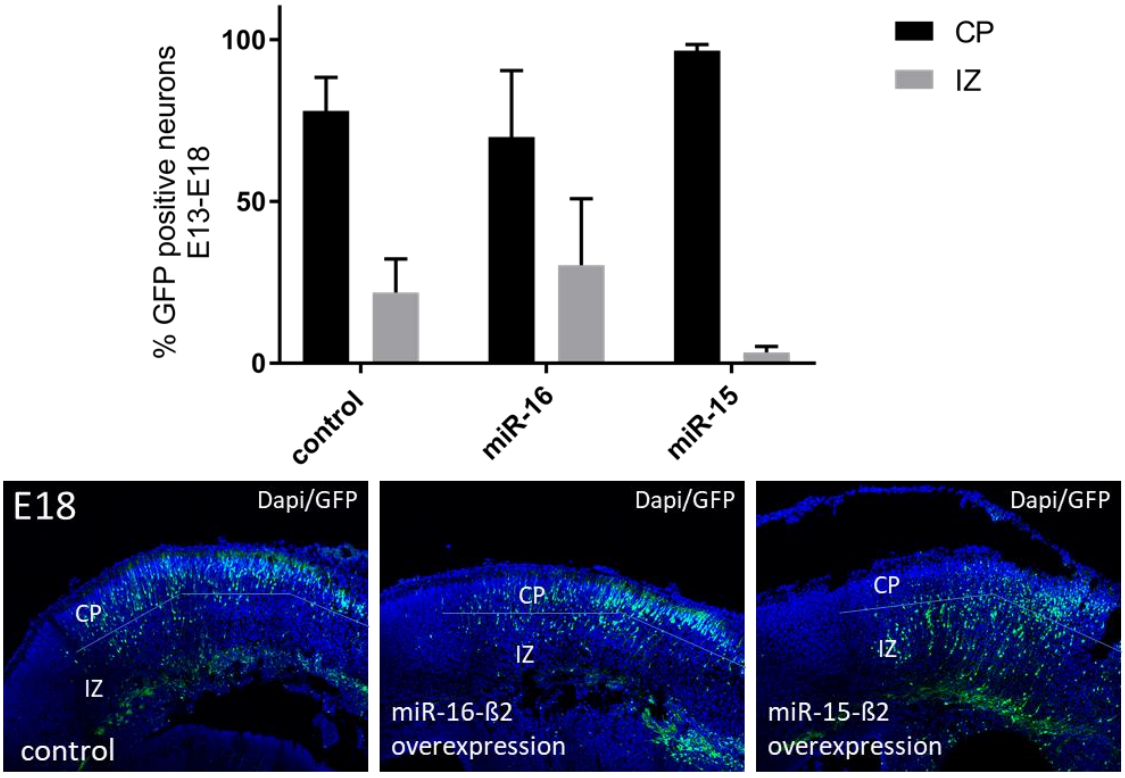

Figure 27: Distribution of miR-16 and miR-15 overexpressing cells under the NeuroD promoter in the different layers of the developing neocortex at E18. Constructs were electroporated into the neocortex at E13. Brains were analyzed at E18. Three biological replicates were pooled for this analysis. Depicted area: motor cortex. For statistical analyses the One-Way ANOVA test with post-hoc Tukey was used. CP: cortical plate, IZ: intermediate zone. All p-values > 0.05.

3. The effect of miR-16 overexpression on cell cycle and proliferation

In order to examine the phenotype induced by miR-16 in the developing neocortex in further detail and to investigate the effect of miR-16 overexpression on the cell cycle and proliferation, miR-16 overexpressing brain slices (cut from E15 brains electroporated with pCAGGs-miR-16-IRES-GFP + pCAGGs-GFP plasmids at E13) were immunostained with a selection of cellular markers. Figures 28 and 30 depict the stainings and quantification of miR-16 overexpressed brains with the radial glial marker Pax6. The upper panel in figure 28 represents the control brain, and the lower panel the miR-16 overexpression. The phenotype already described in the previous chapters which displays a significant decrease in GFP positive, electroporated cells in the cortical plate in miR-16 overexpressing neocortex, compared to the control could also be observed in these experiments.

The overall amount of Pax6 expressing, GFP positive cells did not differ significantly between control brains and the miR-16 overexpressed brains (figure 29).

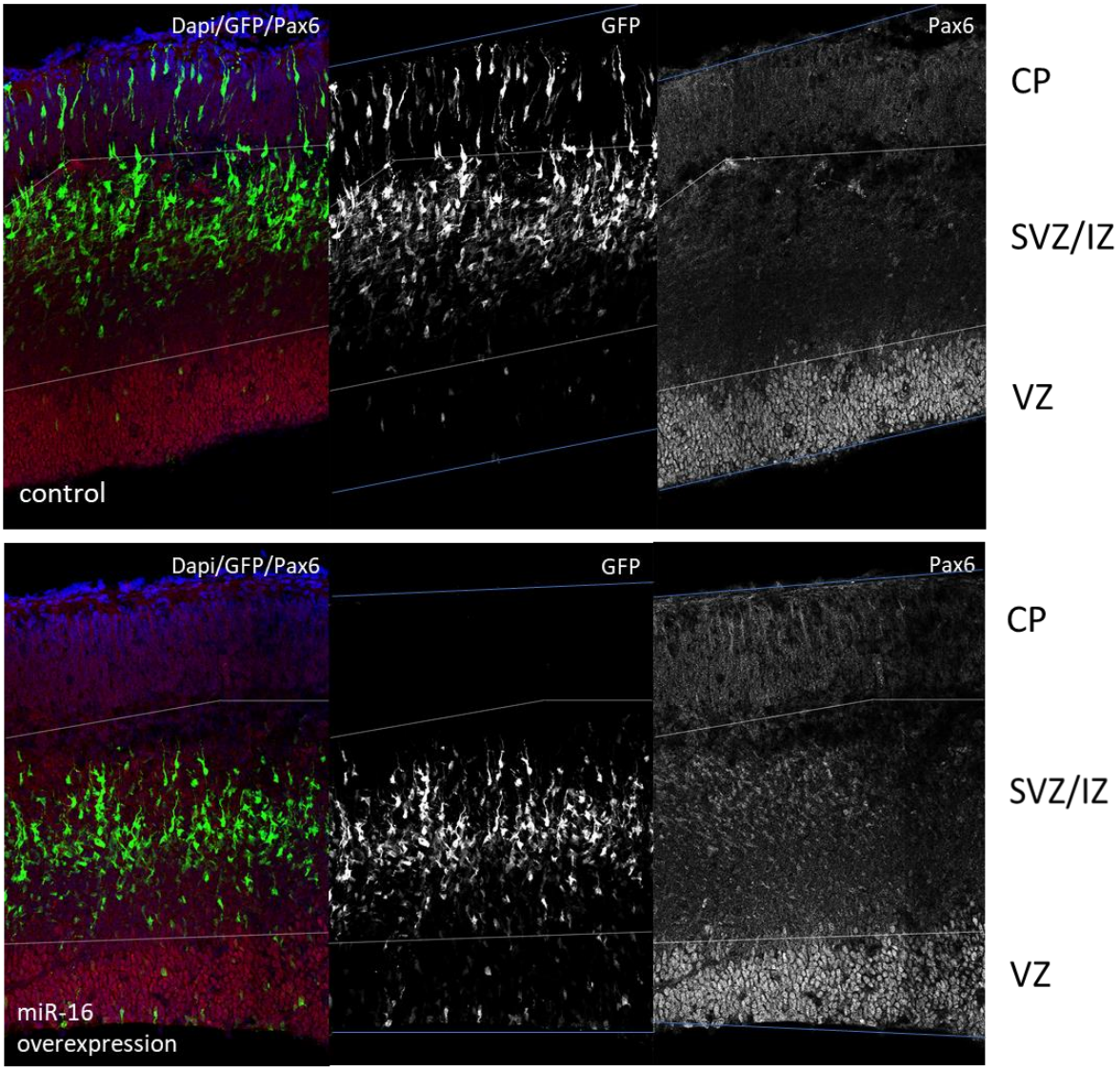

Figure 28: Pax6 staining of miR-16 overexpressing and control brains. The brains were electroporated at E13 and analyzed at E15. Depicted area: motor cortex, CP: cortical plate, IZ: intermediate zone, SVZ: subventricular zone, VZ: ventricular zone.

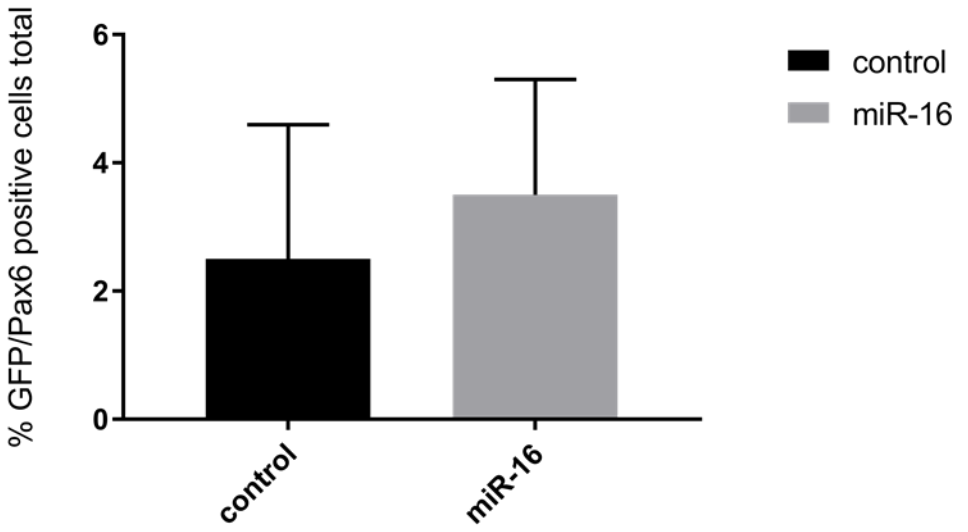

Figure 29: Quantification of Pax6/GFP positive cells after miR-16 or control overexpression. Three biological replicates were analyzed. For statistical analyses the unpaired students t-test was used. P-value >0.05.

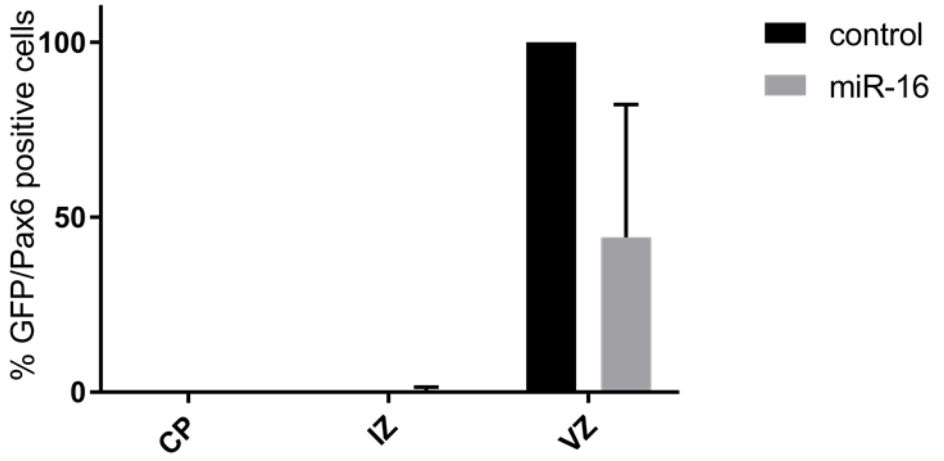

Figure 30: Percentage of GFP/Pax6 positive cells after miR-16 or control overexpression in the different layers of the developing neocortex. Three biological replicates were used for this analysis. For the statistical analyses the unpaired students t-test was used. CP: cortical plate, IZ: intermediate zone, VZ: ventricular zone. P-value >0.05.

During development Pax6 positive radial glial cells divide asymmetrically to give rise to one new radial glial cell and one intermediate progenitor. Intermediate progenitors divide usually only once to give rise to two newborn neurons. To test for changes in neural differentiation upon miR-16 overexpression, slices of the electroporated brains were immunostained with antibodies against the intermediate progenitor marker Tbr2 and the neuron marker Satb2. Figures 31 and 33 show the stainings and quantification of miR-16 overexpressing brains with the intermediate progenitor marker Tbr2. The upper panel of pictures in figure 31 represents the control brain, the lower panel the miR-16 overexpression. The percentage of Tbr2/GFP positive cells differed significantly between control and miR-16 overexpressing neocortex. After miR-16 overexpression, significantly more GFP positive cells were also Tbr2 positive than in the control (figure 32). This effect could be observed in both the ventricular as well as the subventricular/intermediate zone (miR-16 overexpression: 9% of GFP positive cells in the subventricular/intermediate zone and 42% of GFP positive cells in the ventricular zone were also Tbr2 positive; control: 0.5% of GFP positive cells in the intermediate zone and 0% of the ventricular zone were Tbr2 positive) (figure 33).

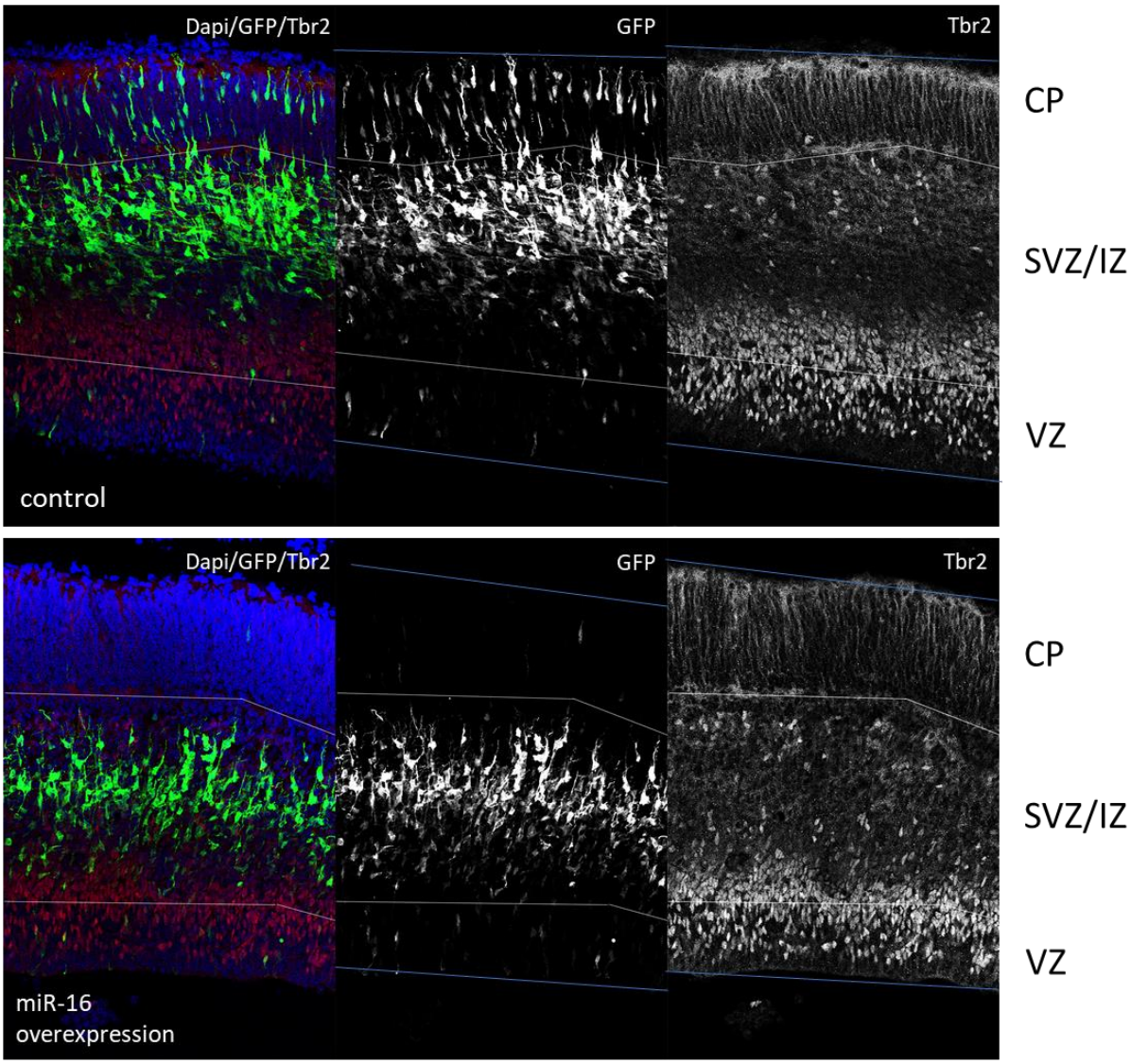

Figure 31: Tbr2 staining of miR-16 overexpressing and control brains. The brains were electroporated at E13 and analyzed at E15. Depicted area: motor cortex, CP: cortical plate, IZ: intermediate zone, SVZ: subventricular zone, VZ: ventricular zone.

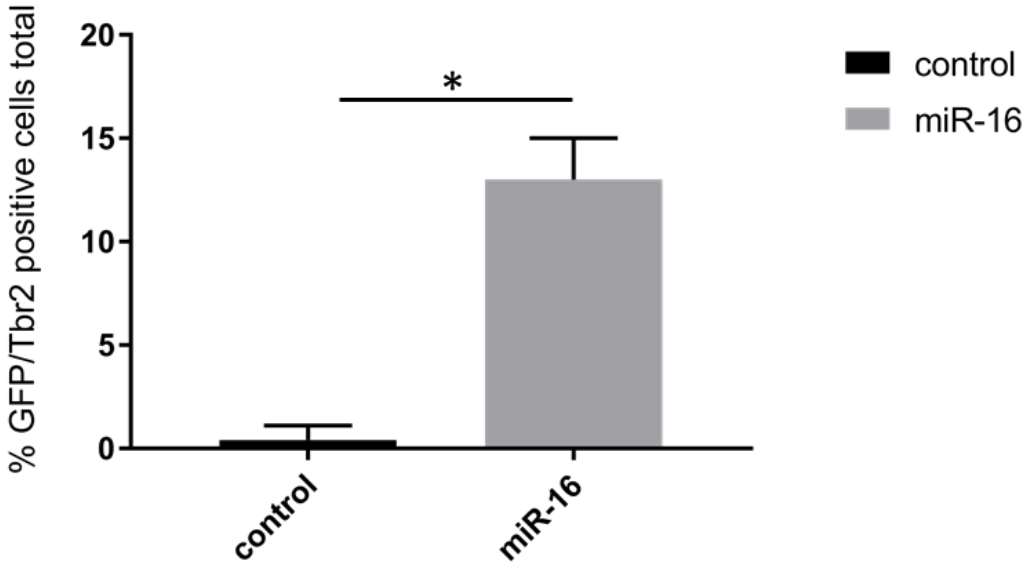

Figure 32: Quantification of Tbr2/GFP positive cells after miR-16 or control overexpression. Three biological replicates were analyzed. For the statistical analyses the unpaired students t-test was used. Control vs. miR-16 p=0.04(*).

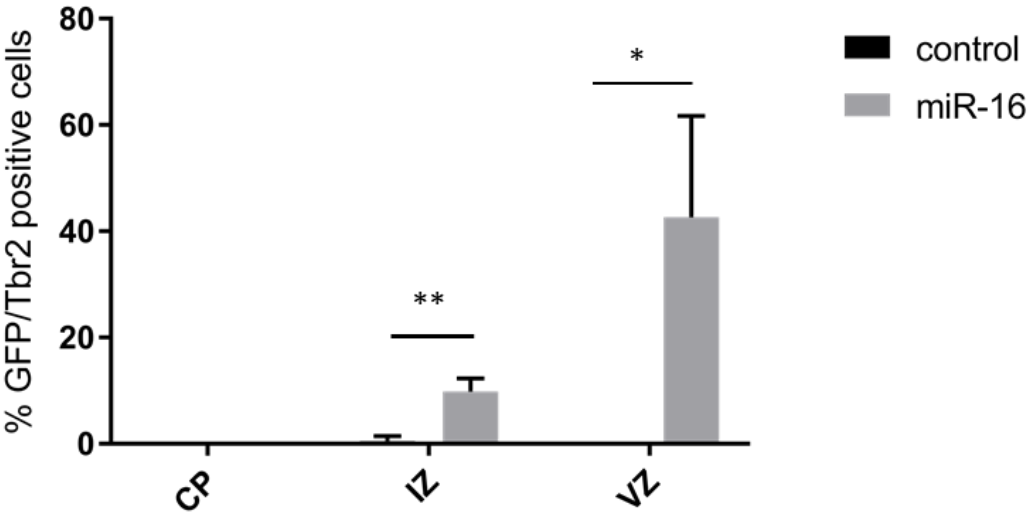

Figure 33: Percentage of GFP/Tbr2 positive cells after miR-16 or control overexpression in the different layers of the developing neocortex. Three biological replicates were analyzed. CP: cortical plate, IZ: intermediate zone, VZ: ventricular zone. For the statistical analyses the unpaired students t-test was used. IZ control vs. IZ miR-16 p=0.009(**); VZ control vs. VZ miR-16 p=0.03(*).

Figures 34 and 36 show the Satb2 stainings and the quantification. The upper panel of pictures in figure 34 represents the control brain, and the lower panel miR-16 overexpression. The quantification of these stainings revealed a significant decrease in GFP/Satb2 positive cells in the cortical plate of miR-16 overexpressing brains in comparison to the control. In the miR-16 overexpressing neocortex, no GFP/Satb2 positive cells could be detected in the cortical plate, whereas the ratio of GFP/Satb2 positive cells in the cortical plate of control brains was significantly higher (92% of GFP positive cells in the cortical plate were also Satb2 positive). This significant difference in Satb2 expression between miR-16 overexpressing and control brains was also visible in the intermediate zone (miR-16 overexpression: 28% of GFP positive cells in the intermediate zone were Satb2 positive; control: 67% of GFP positive cells in the intermediate zone were Satb2 positive) (figure 34). The percentage of Satb2 expressing, GFP positive cells was significantly higher in the control neocortex in comparison to the miR-16 overexpressing neocortex (figure 35).

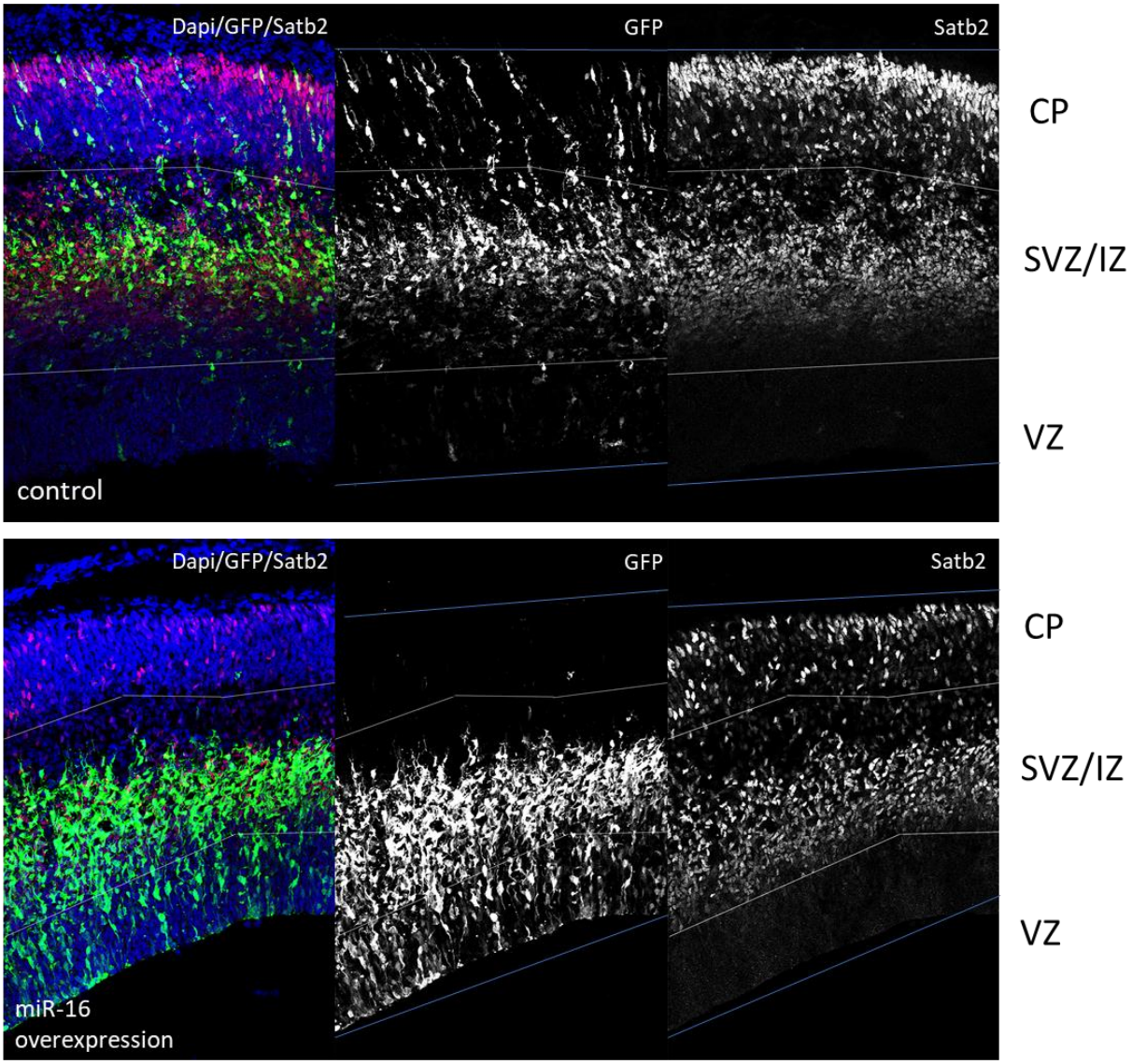

Figure 34: Satb2 staining of miR-16 overexpressing and control brains. The brains were electroporated at E13 and analyzed at E15. Depicted area: motor cortex, CP: cortical plate, IZ: intermediate zone, SVZ: subventricular zone, VZ: ventricular zone.

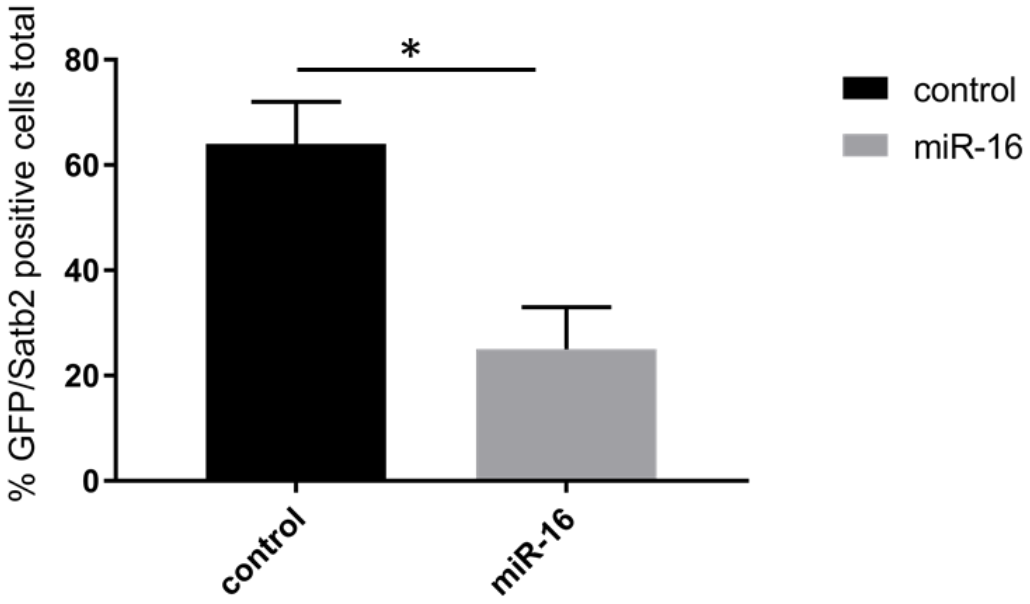

Figure 35: Quantification of Satb2/GFP positive cells after miR-16 or control overexpression. Three biological replicates were analyzed. For the statistical analyses the unpaired students t-test was used. Control vs. miR-16 p=0.02(*).

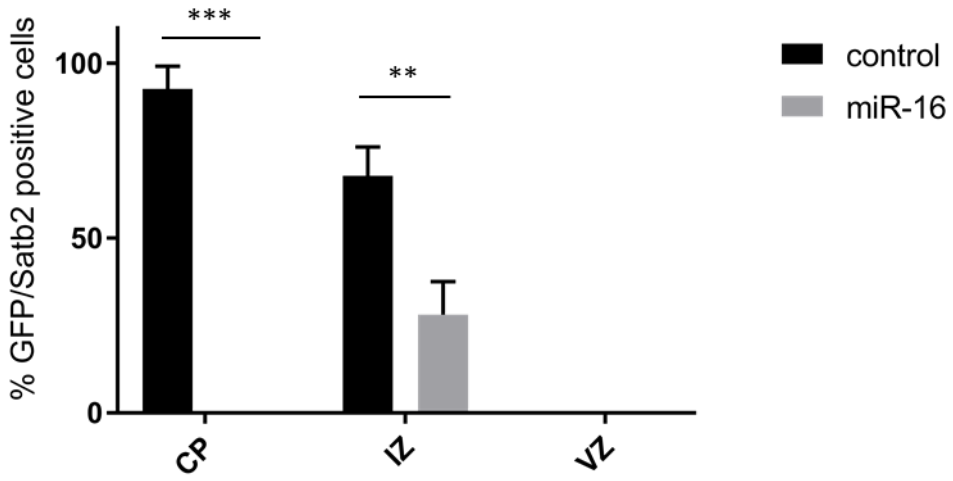

Figure 36: Percentage of GFP/Satb2 positive cells after miR-16 or control overexpression in the different layers of the developing neocortex. Three biological replicates were analyzed. CP: cortical plate, IZ: intermediate zone, VZ: ventricular zone. For the statistical analyses the unpaired students t-test was used. CP control vs. CP miR-16 p=0.0008(***); IZ control vs. IZ miR-16 p=0.007(**)

The decrease in GFP/Satb2 positive postmitotic neurons and the increase in GFP/Tbr2 positive intermediate progenitors in the miR-16 overexpressing cortices suggest defects in differentiation and/or proliferation due to miR-16 overexpression in the developing neocortex.

To study the rate of proliferation in the neocortex electroporated with the miR-16 or control constructs, the proliferation marker Ki67 was stained. Figures 37 and 38 show the Ki67 stainings and quantification. The upper panel of pictures in figure 37 represents the control brain, the lower panel miR-16 overexpression.

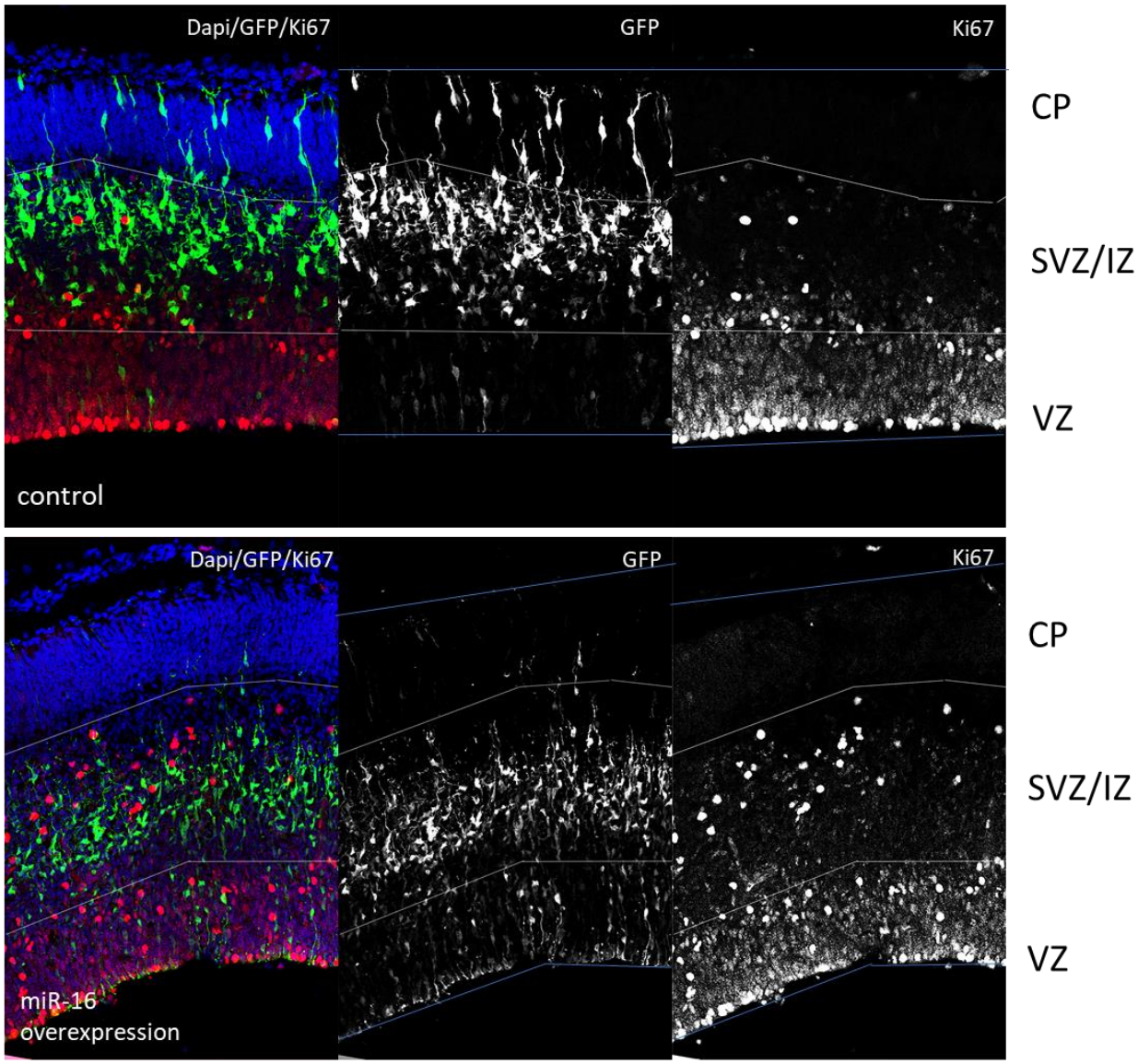

Figure 37: Ki67 staining of miR-16 overexpressing and control brains. The brains were electroporated at E13 and analyzed at E15. Depicted area: motor cortex, CP: cortical plate, IZ: intermediate zone, SVZ: subventricular zone, VZ: ventricular zone.

The percentage of Ki67 expressing, GFP positive cells, did not differ significantly between control and miR-16 overexpressing brains (figure 38).

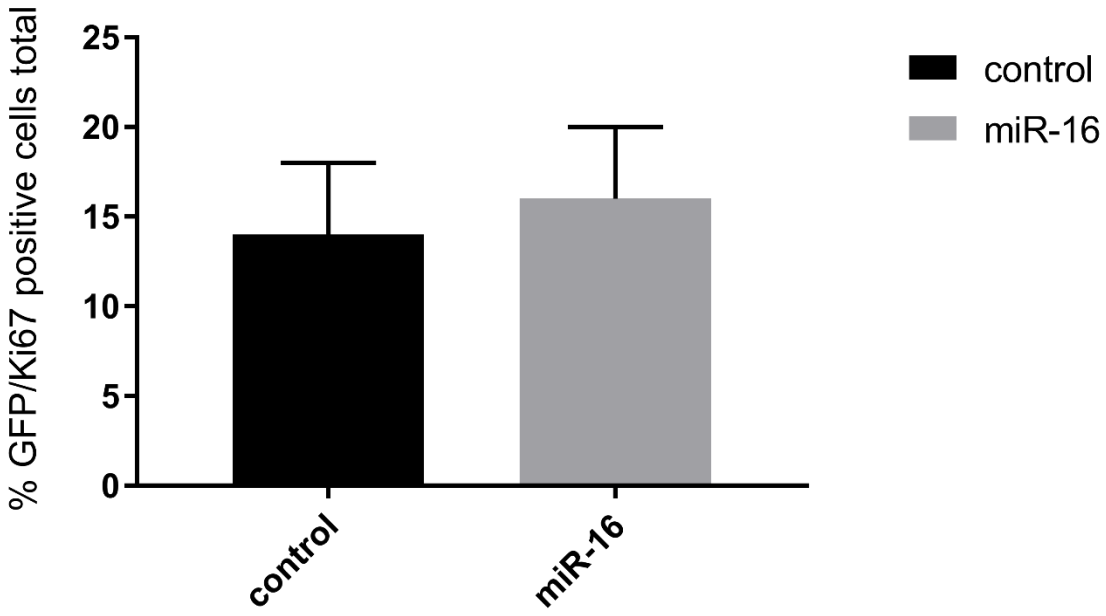

Figure 38: Quantification of Ki67/GFP positive cells after miR-16 or control overexpression. Three biological replicates were analyzed. For the statistical analyses the unpaired students t-test was used. P-value >0.05.

Besides proliferation miR-16 could also influence progenitor mitosis. To analyze possible changes in the rate of mitosis, stainings with antibodies against Phospho-Histone-H3 (PhH3) were performed. Whereas Ki67 is expressed by both inter- and mitotic phase cells, PhH3 is exclusively expressed by cells that are in mitosis. Figures 39 and 41 show the stainings and quantification of miR-16 overexpressing neocortex with antibodies against PhH3. The upper panel of pictures in figure 39 represents the control neocortex, the lower miR-16 overexpression. No significant differences could be observed between the percentages of GFP/PhH3 positive cells in the miR-16 overexpressing and control neocortex (figure 40).

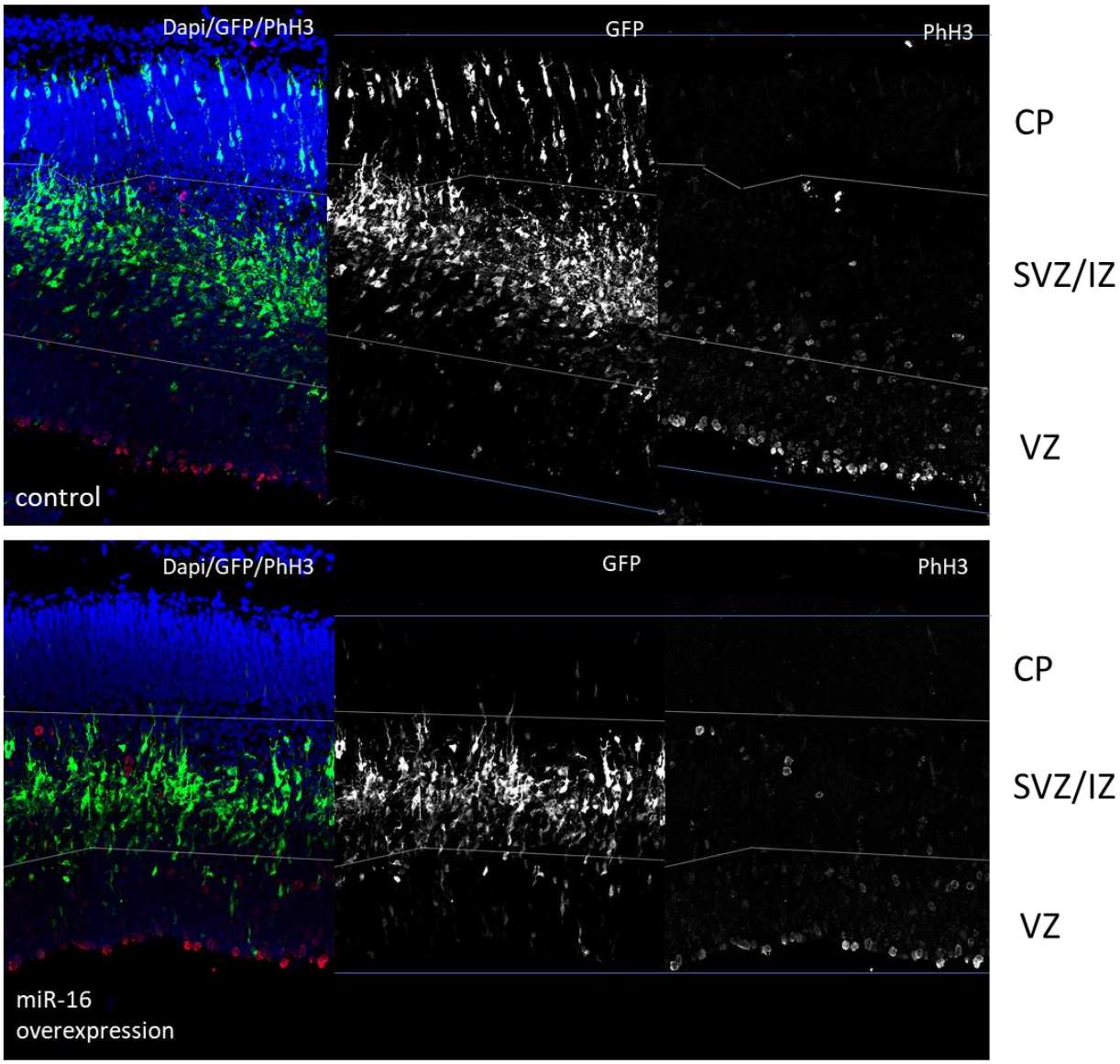

Figure 39: PhH3 staining of miR-16 overexpressing and control neocortex. The brains were electroporated at E13 and analyzed at E15. Depicted area: motor cortex, CP: cortical plate, IZ: intermediate zone, SVZ: subventricular zone, VZ: ventricular zone.

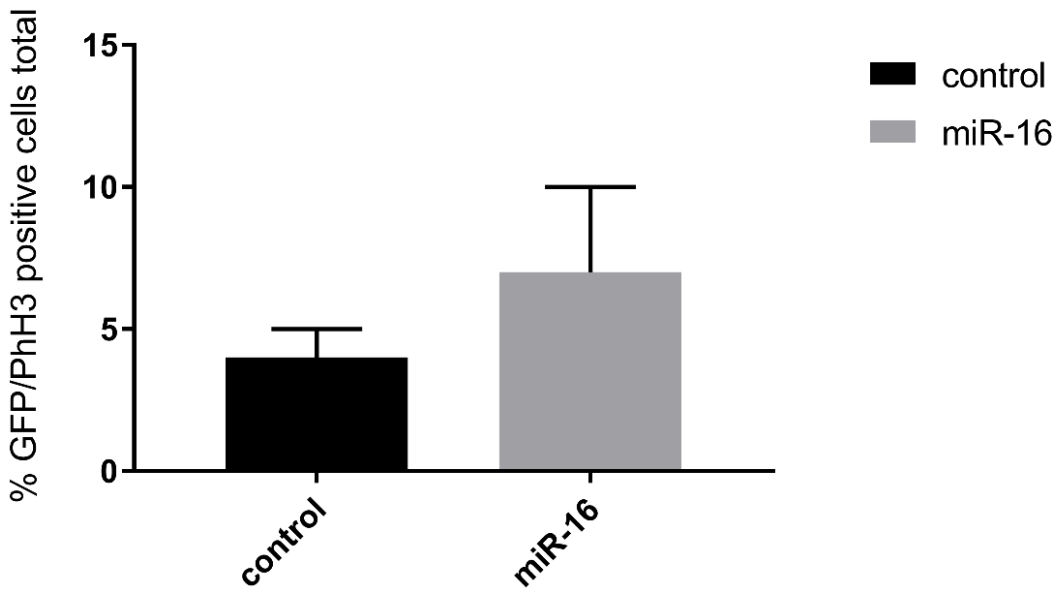

Figure 40: Quantification of PhH3/GFP positive cells after miR-16 or control overexpression in the developing neocortex. Three biological replicates were analyzed. For statistical analyses the unpaired students t-test was used. P-value >0.05.

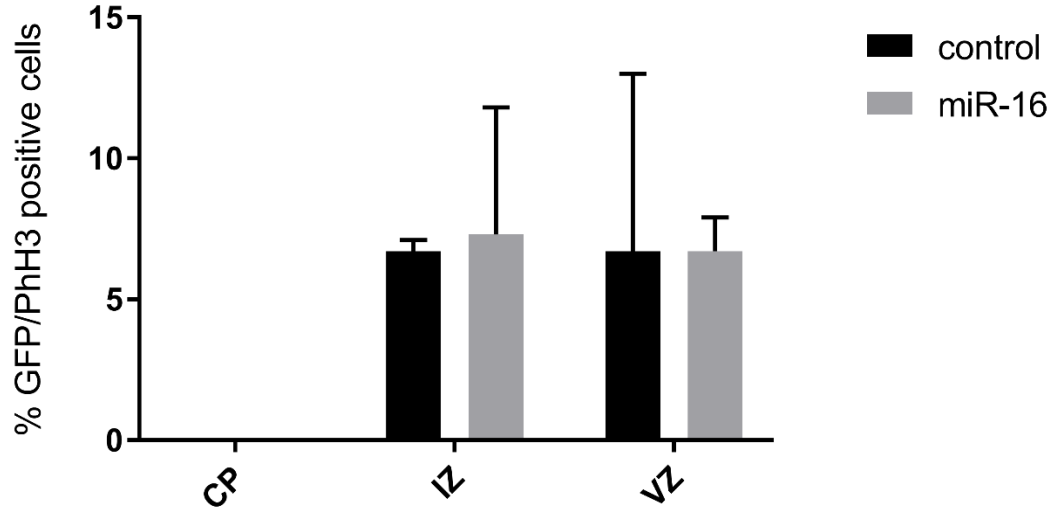

Figure 41: Percentage of GFP/PhH3 positive cells after miR-16 or control overexpression in the different layers of the developing neocortex. Three biological replicates were analyzed. CP: cortical plate, IZ: intermediate zone, VZ: ventricular zone. For the statistical analyses the unpaired students t-test was used. P-values >0.05.

Finally, to assess the number of apoptotic cells in the miR-16 overexpressing brains in comparison to the control, cleaved Caspase-3 (Cas3) stainings were performed. Cas3 is a marker for apoptotic cells. Figures 42 and 44 show the stainings and quantification of

miR-16 overexpressing neocortex with antibodies detecting Cas3. The upper panel of pictures in figure 42 represents the control brain, the lower panel miR-16 overexpression. The quantification shows, that there is no significant difference in GFP/Cas3 positive cells between the miR-16 overexpressing cortices and the control (figure 43). Almost no GFP positive cells were also positive for the apoptotic marker Cas3.

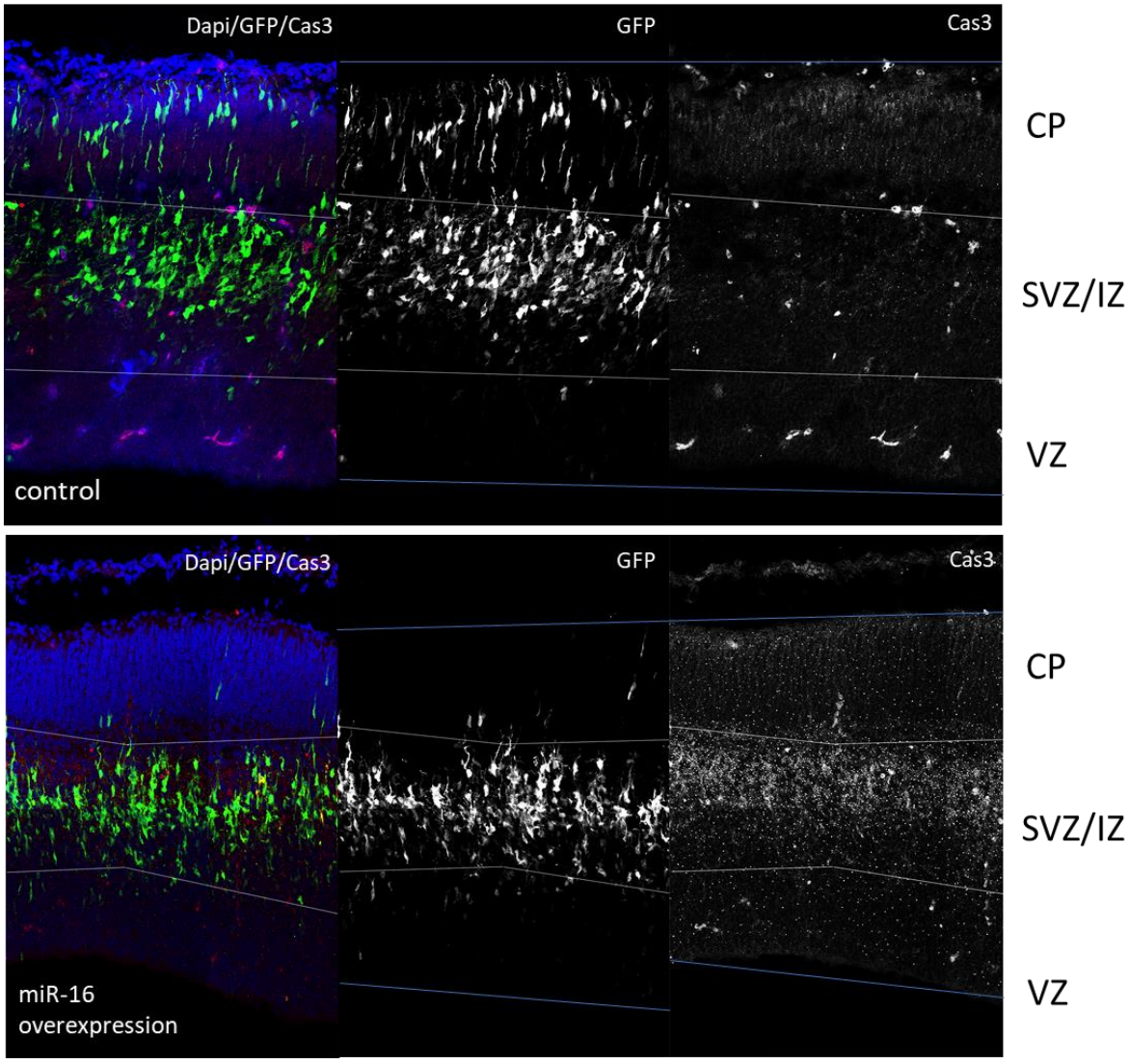

Figure 42: Cas3 staining of miR-16 overexpressing and control neocortex. Neocortices were electroporated at E13 and analyzed at E15. Depicted area: motor cortex, CP: cortical plate, IZ: intermediate zone, SVZ: subventricular zone, VZ: ventricular zone.

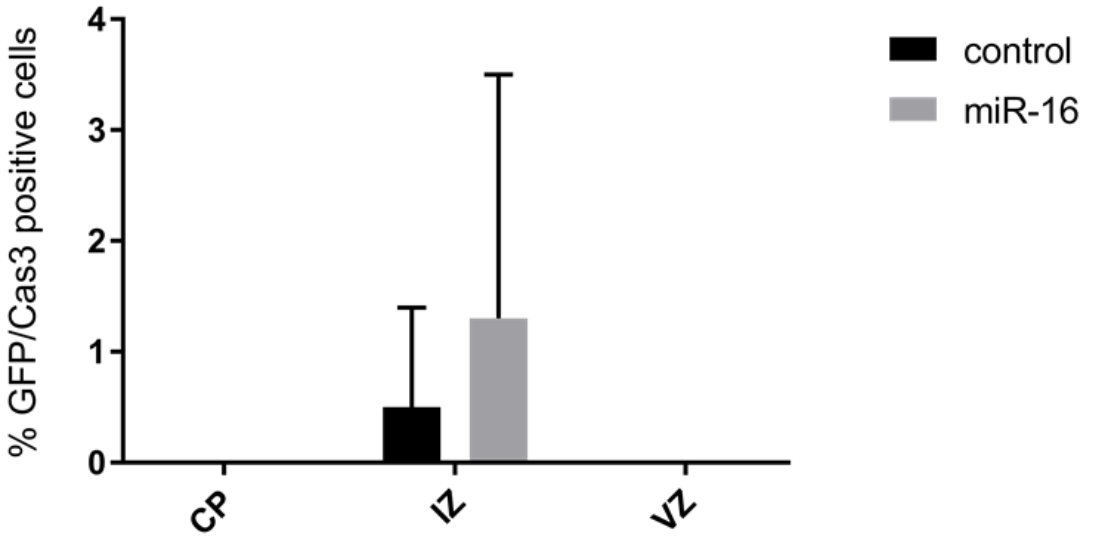

Figure 43: Percentage of GFP/Cas3 positive cells after miR-16 or control overexpression in the different layers of the developing neocortex. Three biological replicates were analyzed. CP: cortical plate, IZ: intermediate zone, VZ: ventricular zone. For the statistical analyses the unpaired students t-test was used. P-values >0.05.

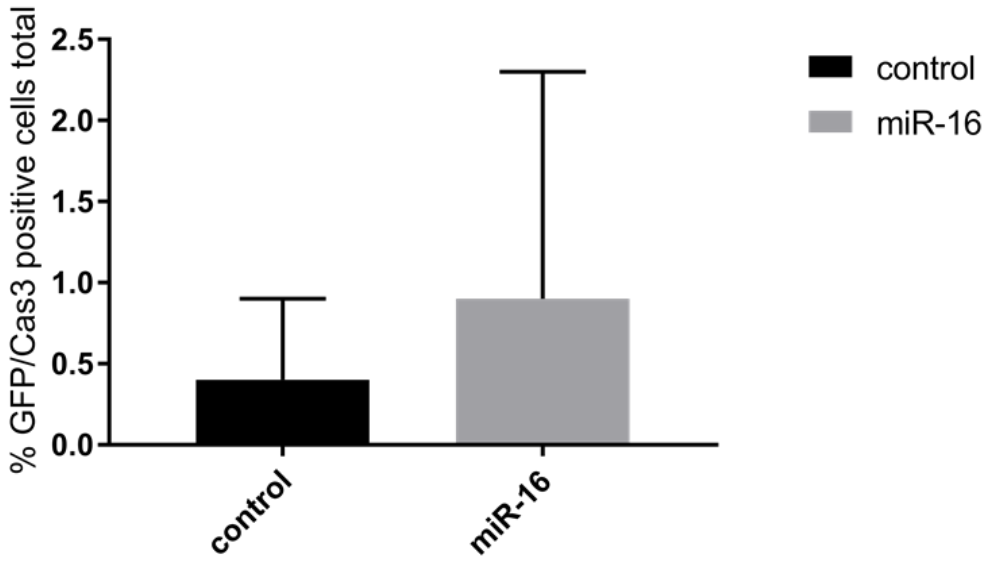

Figure 44: Percentage of Cas3/GFP positive cells after miR-16 or control overexpression. Three biological replicates were analyzed. For statistical analyses the unpaired students t-test was used. P-value >0.05.

4. MiR-16 targets are involved in cell cycle regulation and proliferation

After having established and described the phenotype miR-16 overexpression evokes in the developing embryonic neocortex, miR-16 targets were identified and studied in a next step. For this, RNA sequencing and a range of downstream analyses in miR-16 overexpressing neuronal cells was performed.

4.1. RNA sequencing in miR-16 overexpressing neuronal cells

To identify direct targets of miR-16 in the developing mouse neocortex, the pCAGGs-IRES-GFP miR-16 construct was electroporated in utero into E13 mouse cortices to overexpress miR-16. A pCAGGs-GFP vector was co-electroporated to enhance the GFP expression in electroporated cells. At E15 the brains were dissected, GFP positive cells were isolated via FACS sorting, RNA was isolated from them and was sent to StarSeq (Mainz) for RNA sequencing. The bioinformatical analyses of the sequencing data was conducted by the bioinformatician of the Institute, Dewi Hartwich. Figure 45 shows the plot of the principal component analyses (PCA). miR-16 and control overexpressing samples cluster in different groups.

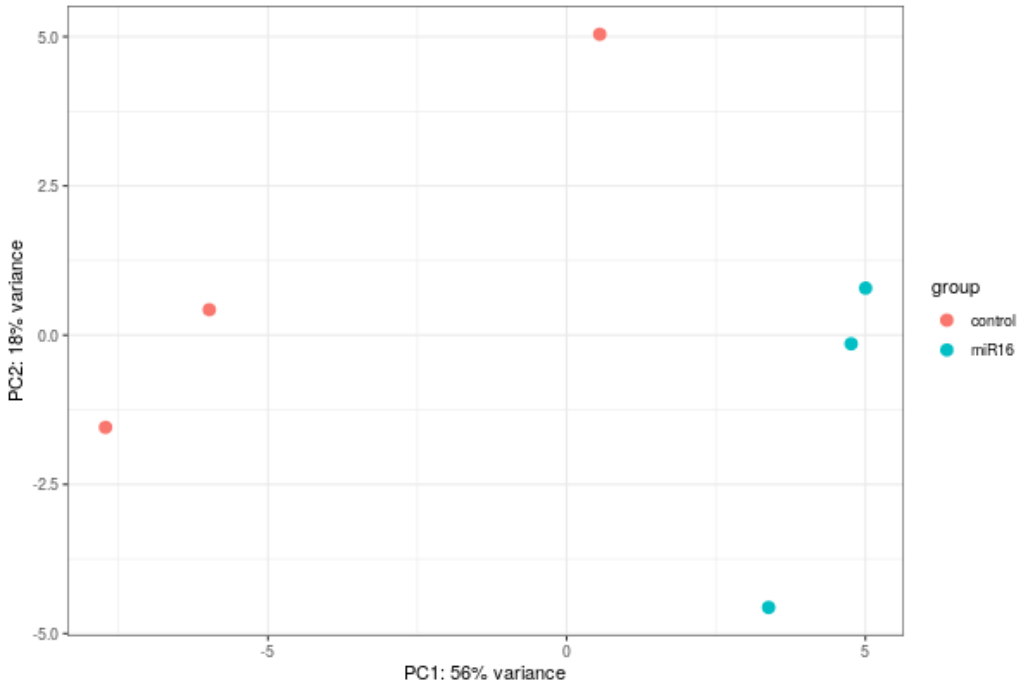

Figure 45: Principal Component Analysis (PCA) of the RNA sequencing data in neocortical tissue after miR-16 or control overexpression. Each group is represented by 3 biological replicates. The control samples are depicted as red dots, the miR-16 samples as blue dots.

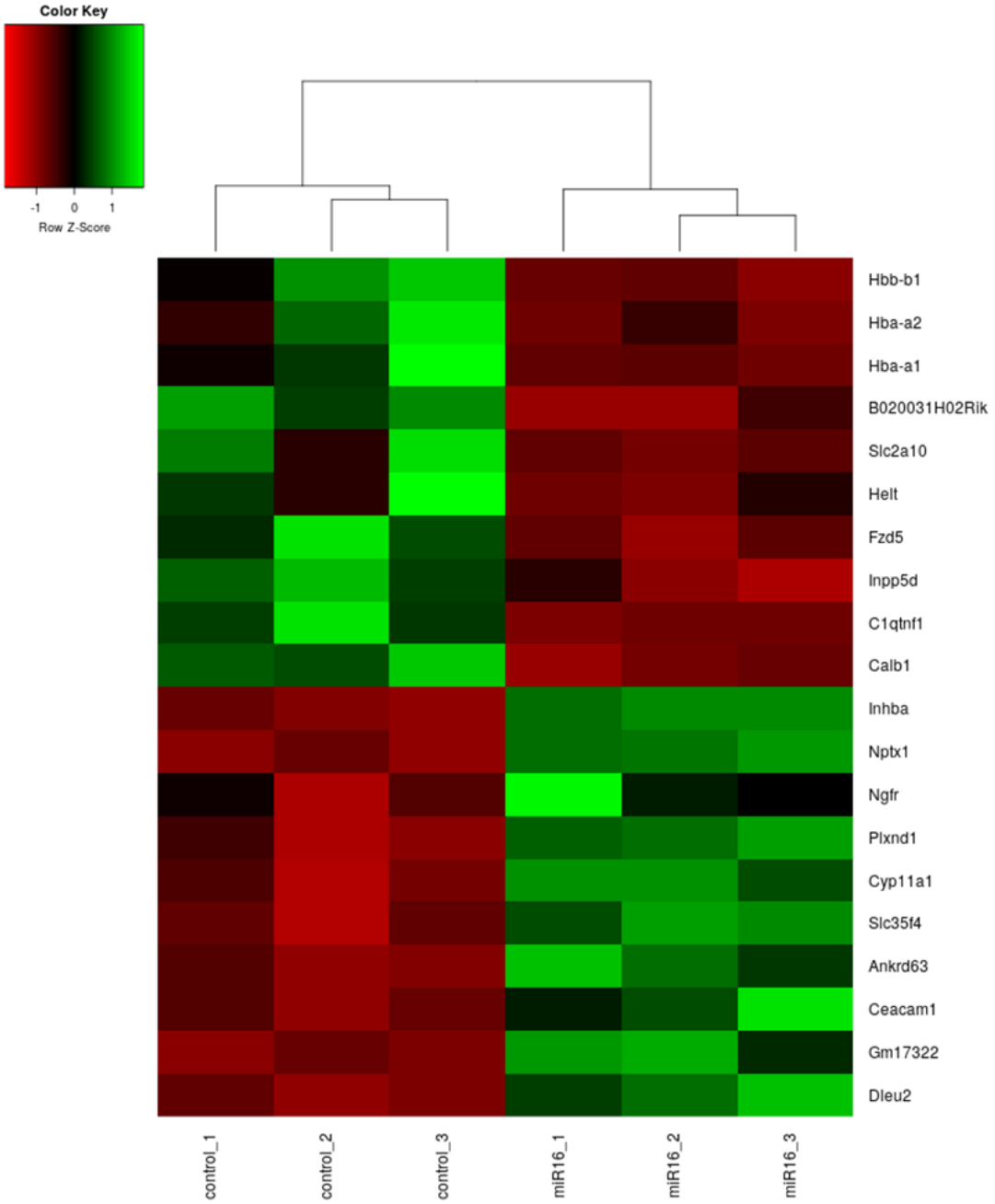

Figure 46: Top 10 up- and downregulated DEGs after miR-16 or control overexpression.

Figure 46 shows a heatmap of the top 10 up- and downregulated DEGs for miR-16 overexpressing samples and the control. In total, 451 DEGs were identified between the miR-16 overexpressed samples and the control. 221 of these DEGs were downregulated after miR-16 overexpression. Furthermore, table 40 (see attachment) shows a list of genes, that display decreased expression levels after miR-16 overexpression and at the same time have predicted miR-16 binding sites in their 3' UTRs (TargetScan analysis).

The downregulated DEGs were of special interest for our study, as we were looking for mis regulated genes which could explain the earlier observed miR-16 overexpression phenotype in the developing neocortex. The gene ontology analyses of the mRNA sequencing revealed, that most of the identified genes that are downregulated after miR-16 overexpression in the brain are connected to keywords such as “DNA replication” and “cell division”, suggesting miR-16 to be a key regulator of cell proliferation, cell differentiation and mitosis (figure 47).

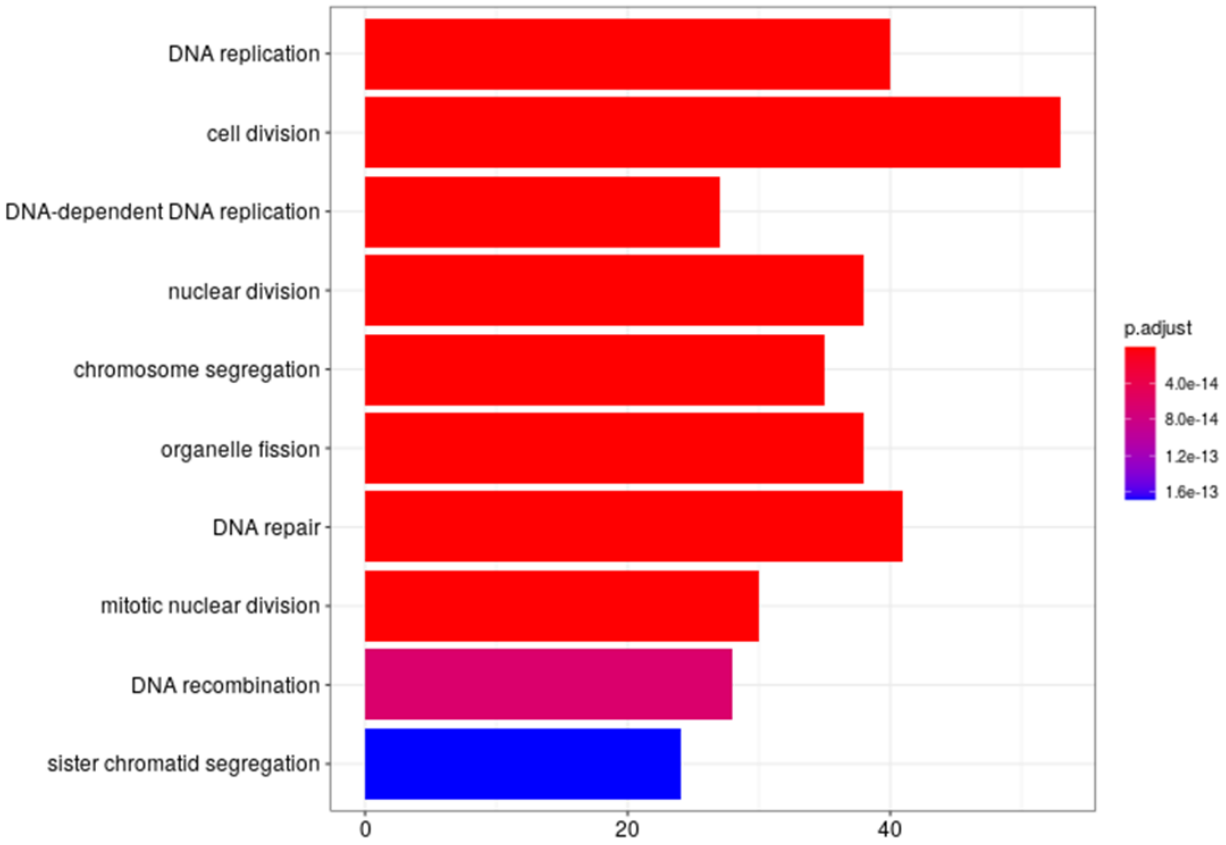

Figure 47: Gene ontology analyses of downregulated genes after miR-16 overexpression.

4.2. Validation of downregulated genes

The RNA sequencing analyses resulted in a list of genes that were downregulated after miR-16 overexpression in the developing neocortex. Table 39 shows a selection of five downregulated DEGs that have also been predicted to be miR-16 targets by the free online tool TargetScan and play important roles in cell proliferation and/or differentiation.

Gene	Function
Fbxw7	Tumor suppressor, E3 ligase
Taf15	Binds RNA/DNA, cell proliferation
Wee1	Cell cycle progression, inhibits Cdk1
Cdk1	Cell cycle progression
Chek1	DNA damage response, cell cycle checkpoint

Table 39: Predicted miR-16 target genes that were downregulated after miR-16 overexpression.

To validate the result of the RNA sequencing, miR-16 or a scrambled control were overexpressed in Neuro 2A cells (N2A cells), a murine neuroblastoma cell line. RNA was isolated from these cells and qPCR was performed to evaluate the expression level of the 5 candidate miR-16 targets. Figure 48 shows the fold reduction (normalized to Gapdh) of the 5 candidate targets *Fbxw7, Taf15, Wee1, Cdk1* and *Chek1* in N2A cells after miR-16 overexpression when compared to a scrambled control miRNA. The predicted downregulation after miR-16 overexpression was validated for all 5 candidate DEGs. The significance was tested with a student's t-test ($p<0.05$).

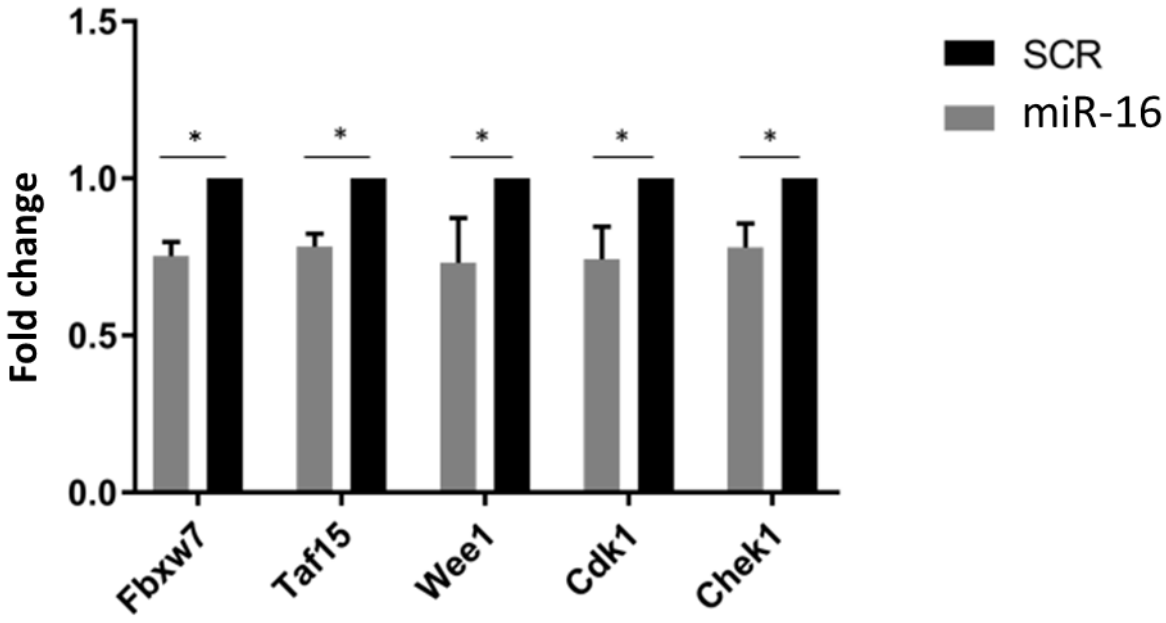

Figure 48: Fold reduction of *Fbxw7, Taf15, Wee1, Cdk1* and *Chek1* in N2A cells after overexpression of miR-16 or a scrambled control (SCR). Data is normalized to Gapdh. Three biological replicates were analyzed. For statistical analyses the unpaired student's t-test was used. P-value for all target genes <0.05(*).

4.3. Wee1 is regulated by miR-16

In order to study the connection between miR-16 and its targets in further detail, I decided to concentrate on one target of particular interest. The nuclear kinase *Wee1* is known to be a critical regulator of cell cycle and mitosis as it controls the cell's transition from G2 to M-phase (Moiseeva et al., 2019). The RNA sequencing of miR-16 overexpressing cells revealed a downregulation of *Wee1* in comparison to the control (table 39). This effect was validated by qPCR in N2A cells (figure 48). To confirm that Wee1 is a direct miR-16 target, luciferase assays were performed. For this, the 3'UTR of Wee1 was cloned into a psiCHECK-2 luciferase expression vector, downstream of the Renilla luciferase. The Firefly luciferase, which is also expressed in the psiCHECK-2 vector, was used to normalize the Renilla values. HEK293 cells were transfected with the 3'UTR construct and miR-16. Figure 49 shows, that the relative luciferase activity of the cells transfected with Wee1 together with miR-16 is significantly decreased in comparison to the samples in which Wee1 was transfected together with an empty control plasmid into HEK293 cells.

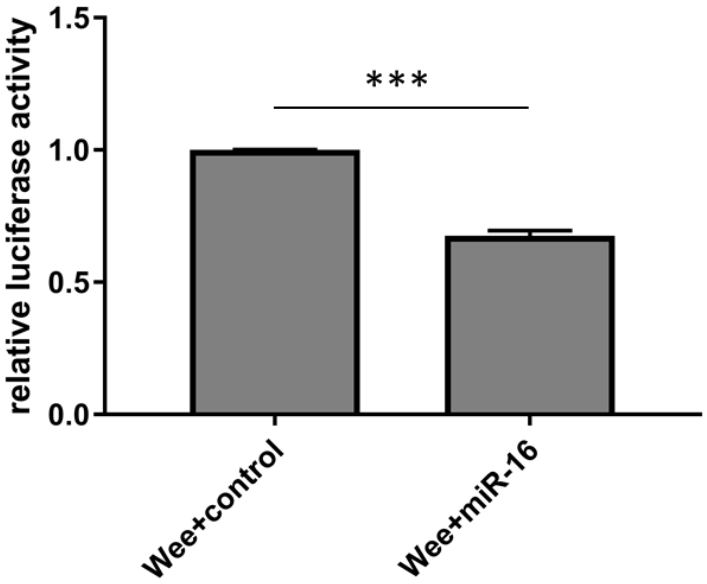

Figure 49: Relative luciferase activity of Wee1 after co-transfection with miR-16 or control in HEK293 cells. Data is normalized to Firefly luciferase values. Three biological replicates were analyzed. For statistical analyses the unpaired student's t-test was used. $p<0.005$(***).

To study the effect of miR-16 on *Wee1* protein expression, Western Blot analyses were performed. Both N2A and HEK293 cells were transfected with either miR-16 miRNA mimics or a scrambled control. Forty-eight hours after transfection, cells were harvested, protein lysates were prepared and Western Blot analysis was performed. Figures 50, 51 and 51 show, that both N2A and HEK293 cells display a significant decrease in the *Wee1* protein level after miR-16 overexpression.

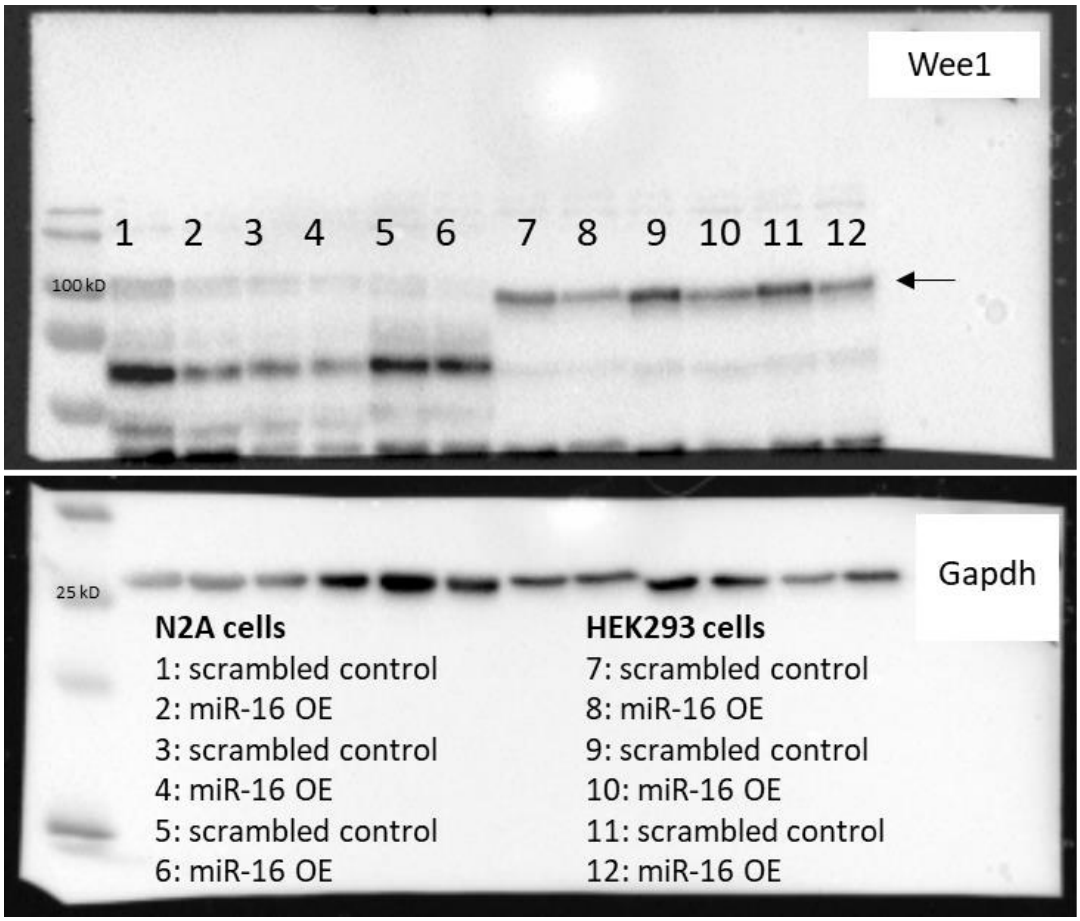

Figure 50: Western blot analysis to detect Wee1 protein expression in N2A and HEK293 cells after miR-16 or control overexpression. Lanes 1-6: N2A cells; Lanes 7-12: HEK293 cells. Upper blot: Wee1; Lower blot: Gapdh. Correct band size of Wee1 is indicated with arrow.

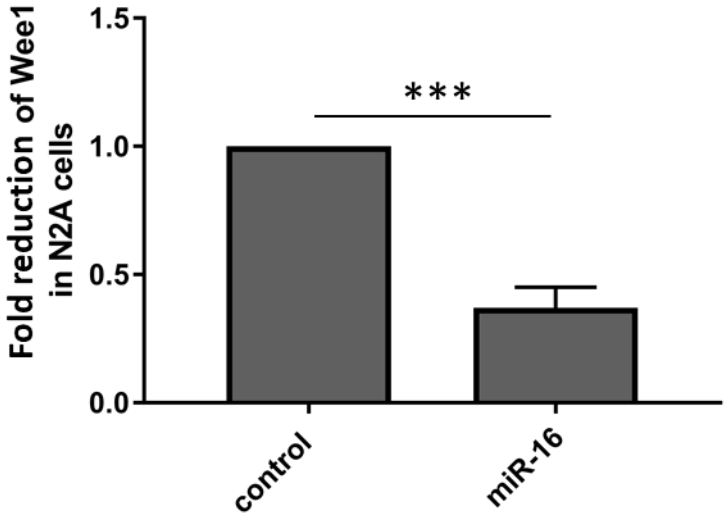

Figure 51: Fold reduction of Wee1 in N2A cells after miR-16 overexpression. Data is normalized to Gapdh. For the statistical analyses the unpaired student's t-test was used. $p<0.005$(***).

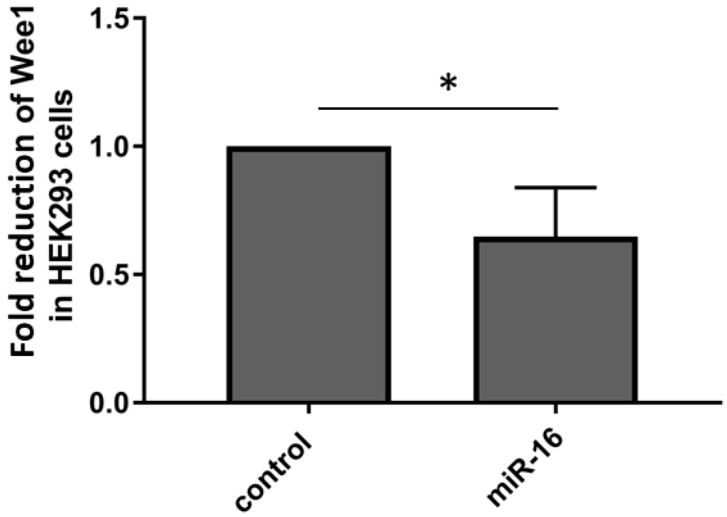

Figure 52: Fold reduction of Wee1 in HEK293 cells after miR-16 overexpression. Data is normalized to Gapdh. For the statistical analyses the student's t-test was used. $p<0.05$(*).

After having validated that miR-16 downregulated Wee1 expression at RNA and protein level and that Wee1 is a direct miR-16 target, in a next step, it was tested whether inhibiting miR-16 and its family members miR-15a and miR-15b in the developing neocortex causes an upregulation of Wee1 expression. For this, miArrest miRNA inhibitors (siRNAs) were purchased from Genecopoeia (Maryland, USA) and co-electroporated with GFP into the motor cortices of E13 mice. The electroporated cells

were FACS sorted at E15, total RNA including miRNAs was isolated and TaqMan Assays were performed to test for knockdown efficiency. Figure 53 shows, that all tested miRNAs (miR-16, miR-15a, miR-15b) were significantly and strongly (>70%) downregulated after electroporating the miArrest miRNA inhibitors into the developing mouse neocortex.

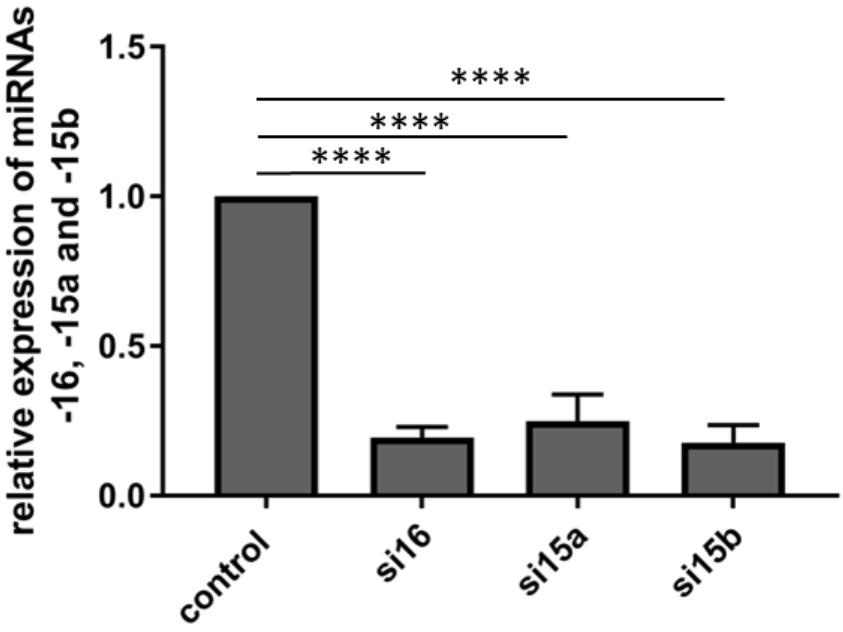

Figure 53: Fold reduction of miRNAs -16, -15a and -15b after electroporation of the particular miRNA inhibitors into the developing mouse neocortex. Data is normalized to U6. Three biological replicates were analyzed. For statistical analyses the One-Way ANOVA test with post-hoc Tukey was used. $p<0.001$(****).

To check if the knockdown of miR-16 and its seed-sequence identic family members miR-15a and miR-15b has an effect on *Wee1* expression, RNA from the FACS sorted cells was used for qPCR with *Wee1* primers. *Wee1* expression was significantly increased after knockdown of all three miRNAs in comparison to the control ($p<0.01$). However, a knockdown of miR-16 alone did not cause a significant upregulation of *Wee1* compared to the control ($p>0.05$). Knocking down all three miRNAs simultaneously resulted in significantly increased *Wee1* levels, compared to the single knockdown of miR-16 ($p<0.05$) alone and the control ($p<0.01$) (figure 54).

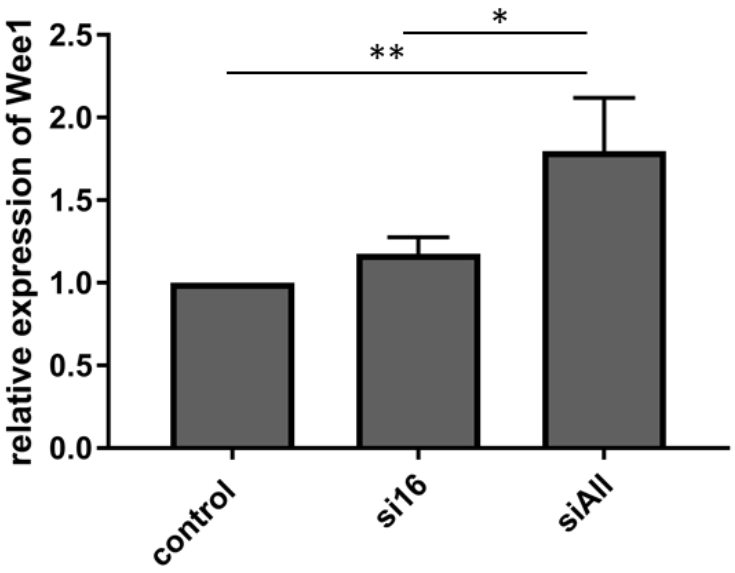

Figure 54: Fold increase of Wee1 after knockdown of miR-16 alone or miRNAs -16, -15a and -15b simultaneously in the developing mouse neocortex. Data is normalized to Gapdh. Three biological replicates were analyzed. For statistical analyses the One-Way ANOVA test with post-hoc Tukey was used. Control vs. siAll (miR-16 + miR-15a + miR-15b knockdown) $p<0.01$ (**); si16 vs. siAll $p<0.05$ (*).

4.4. Co-expression of Wee1 together with miR-16 does not rescue the miR-16 overexpression phenotype

As described in sections 2 and 3, overexpression of miR-16 in the embryonic mouse neocortex caused a specific phenotype and an increase in Tbr2 positive progenitors and a decrease in Satb2 positive neurons. To test whether this phenotype was caused by the downregulation of Wee1, miR-16 was overexpressed together with miR-16 resistant *Wee1* in the developing neocortex. Figure 55 shows representative pictures of E15 neocortex electroporated with either a control (pCAGGs IRES GFP), miR-16 (pCAGGs-miR-16-GFP) or both miR-16 and a pCAGGs-Wee1-GFP construct. The quantification of this experiment revealed a significant decrease of GFP positive cells in the cortical plate of the miR-16 + *Wee1* electroporated brains (0% of electroporated cells in the cortical plate) in comparison to both the control (17% of electroporated cells in the cortical plate) and the miR-16 electroporated brains (9% of electroporated cells in the cortical plate) (figure 56). In addition to this, the Satb2 staining of these brains showed a decrease of Satb2/GFP positive cells in the cortical plate of miR-16 (36% of GFP positive

cells were Satb2 positive in the cortical plate) and miR-16 + *Wee1* (0% of GFP positive cells were Satb2 positive in the cortical plate) overexpressing neocortices in comparison to the control (91% of GFP positive cells were Satb2 positive in the cortical plate) (figure 57). This decrease of Satb2/GFP positive cells also applied to the intermediate zone, where significantly less GFP/Satb2 positive cells could be found after miR-16 (33% of GFP positive cells were Satb2 positive in the intermediate zone) and miR-16 + *Wee1* (31% of GFP positive cells were Satb2 positive in the intermediate zone) overexpression compared to the control (75% of GFP positive cells were Satb2 positive in the intermediate zone). The expected rescue of the miR-16 induced phenotype in the developing neocortex could not be observed after overexpression of miR-16 together with *Wee1*. Overexpression of *Wee1* in the developing brain seems to induce its own phenotype and thus does not cause as an immediate rescue of the effects induced by miR-16.

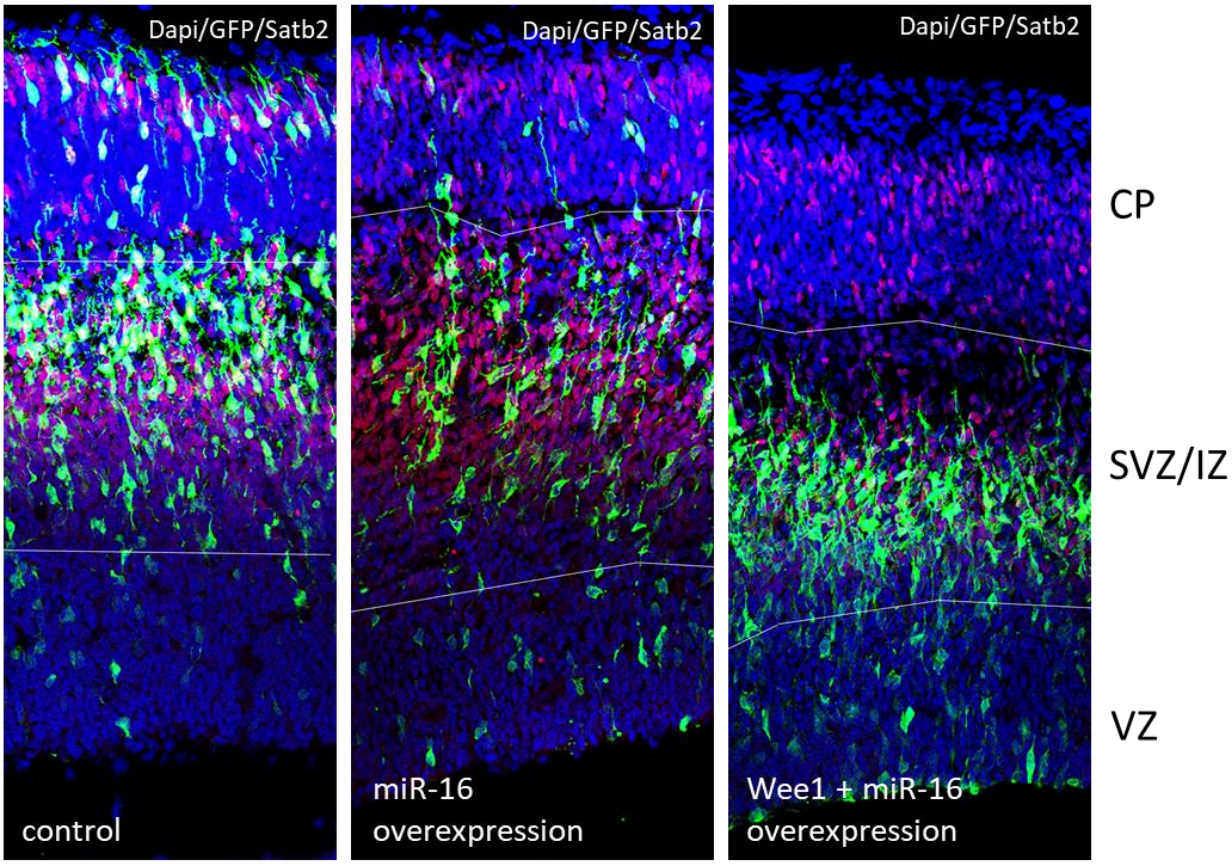

Figure 55: Satb2 staining of control, miR-16 and miR-16 + Wee1 overexpressing neocortex. Neocortices were electroporated at E13 and analyzed at E15. Depicted area: motor cortex, CP: cortical plate, IZ: intermediate zone, SVZ: subventricular zone, VZ: ventricular zone.

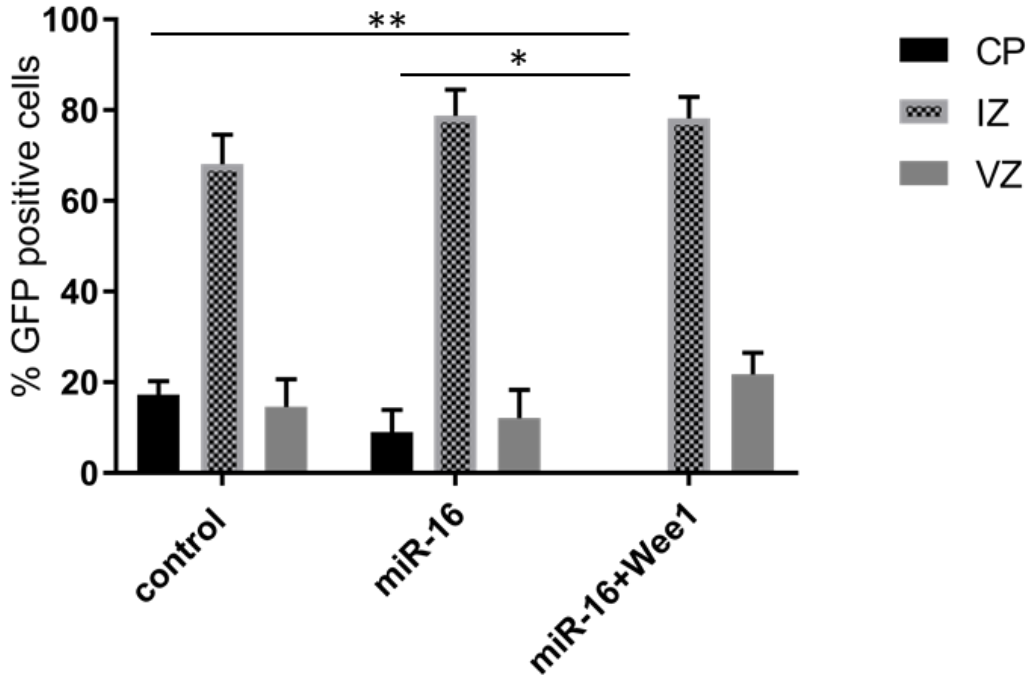

Figure 56: Percentage of GFP positive cells after control, miR-16 or miR-16 + Wee1 overexpression in the different layers of the developing neocortex. Three biological replicates were analyzed. Depicted area: motor cortex, CP: cortical plate, IZ: intermediate zone, SVZ: subventricular zone, VZ: ventricular zone. For the statistical analyses the One-Way ANOVA test with post-hoc Tukey was used. GFP pos. cells CP control vs. CP miR-16 + Wee1 $p<0.01$(**); CP miR-16 vs. CP miR-16 + Wee1 $p<0.05$(*).

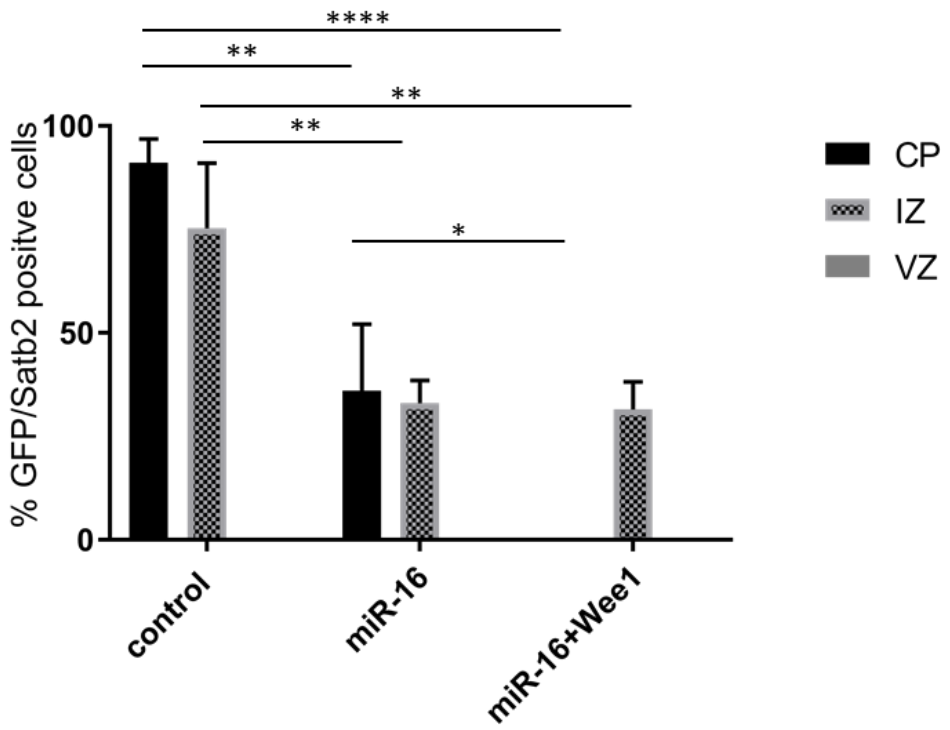

Figure 57: Percentage of GFP/Satb2 positive cells after control, miR-16 or miR-16 + Wee1 overexpression. Three biological replicates were analyzed. CP: cortical plate, IZ: intermediate zone, VZ: ventricular zone. For the statistical analyses the One-Way ANOVA test with post-hoc Tukey was used. CP control vs. CP miR-16 $p<0.01$(**); CP control vs. CP miR-16 + Wee1 $p<0.001$(****); CP miR-16 vs. CP miR-16 + Wee1 $p<0.05$(*); IZ control vs. IZ miR-16 $p<0.01$(**); IZ control vs. IZ miR-16 + Wee1 $p<0.01$(**).

Discussion

1. MiRNA expression in the developing brain

Since the discovery of miRNAs in higher eukaryotes, these small non-coding RNAs have been identified as regulators of a huge variety of processes, both during development and in disease states as for example cancer (Friedman & Jones, 2009). miRNAs are important negative posttranscriptional regulators of mRNA expression. More than 2600 miRNAs are encoded in the human genome alone, predicted to target more than 50% of all 3'UTRs of protein coding genes (Agarwal et al., 2015; Plotnikova et al., 2019). Several studies have also pointed out the importance of miRNAs for neuronal development. As the complex process of embryonic brain development has to be precisely orchestrated, miRNA-mediated regulation complements other gene regulatory mechanisms as for example alternative splicing (Stefani & Slack, 2008). Knockouts of the miRNA processing endoribonuclease Dicer in mice and zebrafish proved the importance of miRNAs for neurodevelopment when Dicer absent animals displayed a skewed neurodevelopmental phenotype (Radhakrishnan & Alwin Prem Anand, 2016). Other studies underlined the significance of miRNAs for neurogenesis and brain development, cell proliferation and differentiation (Lang & Shi, 2012; Gao, 2010; Shi et al., 2010).

In order to achieve an overview of miRNA expression in the developing mouse brain, in this work the miRNA transcriptome was profiled in NPCs, neurons and cortical lysates of different neurodevelopmental stages (E14, E17, P0).

The miRNA sequencing in NPCs and neurons revealed, that in total, 241 miRNAs are differentially expressed between these two cell types. In NPCs, 127 miRNAs were upregulated compared to neurons whereas in neurons, 114 miRNAs showed increased expression compared to NPCs. This pattern of differential expression of miRNAs in NPCs and neurons suggests, that a different set of miRNAs is important in NPCs than in neurons to regulate neurodevelopmental processes. These differentially expressed miRNAs could be promising candidates for further studies evaluating the role of miRNA regulation in NPCs and neurons.

In order to gain an overview of expression levels of different miRNAs across different time points of brain development, the miRNA sequencing experiment performed in

NPCs and neurons was extended to miRNA sequencing of cortical lysates of the developmental stages E14, E17 and P0 in mouse brains.

Just as for NPCs and neurons, we also identified a range of miRNAs that are differentially expressed between the developmental stages E14, E17 and P0. Between E14 and E17, 277 differentially expressed miRNAs were identified. 133 of these miRNAs showed higher expression in NPCs and 144 displayed decreased expression in E14, compared to E17. The top up- and downregulated miRNAs between E14 and E17 are listed in the heatmap, shown in figure 10. Here, for example, miR-137 shows an increased expression at E17 compared to E14. This miRNA is known to be an important key player in neuronal development and proliferation (Mahmoudi & Cairns, 2017). In general, many of the miRNAs we found to be differentially expressed between E14 and E17, are described to be involved in a variety of diseases and developmental malfunctions (Sárközy et al., 2018; Zhu et al., 2016; Lee et al., 2019).

Between E14 and P0, 335 miRNAs showed differential expression. 163 of them were upregulated at E14, compared to P0 and 172 were downregulated at E14, compared to P0. Some of the differentially expressed miRNAs between E14 and E17 also show differential expression between E14 and P0. For example, the earlier described miR-137 shows an increase of expression not only from E14 to E17 but also from E14 to P0. As miR-137 is known to be involved in a range of neurodevelopmental processes, the increased expression of this miRNA during brain development is not surprising.

175 miRNAs in total were differentially expressed between the time points E17 and P0 of embryonic development. Here, 82 miRNAs were upregulated at E17 compared to P0 and 93 miRNAs were downregulated at E17 compared to P0. MiR-25 for example, which was already downregulated in E17 and P0 cortices compared to E14, also showed a decreased expression in P0 cortices compared to E17. In the literature, this miRNA has been identified as important regulator of many aspects of neurogenesis like cellular proliferation and neuronal migration and has been shown to be involved in a wide range of diseases and malfunctions (Sárközy et al., 2018).

The comparison of miRNAs upregulated between NPCs and neurons and the developmental stages E14 and P0 revealed, that they share 74 differentially expressed, upregulated miRNAs. This overlap can be explained by the higher number of NPCs in E14

cortical samples than in P0 and the increased number of neurons in P0 samples compared to E14 samples. We also identified 74 miRNAs that showed less expression in E14 compared to P0 as well as in NPCs compared to neurons. Just as the upregulated miRNAs, these 74 overlapping miRNAs also might be interesting candidates for further studies evaluating the relevance of miRNAs during neurodevelopment.

Additionally, to validate some of the differentially expressed miRNAs, TaqMan Assays were performed. For this, we focused on three candidate miRNAs that were predicted to be upregulated from E14 to P0 and two miRNAs that were predicted to display a decrease in expression from E14 to P0. MiR-124, which is predominately expressed in mature neurons, showed the highest expression levels at P0. Again, this finding is in accordance with the literature, where it is described, that miR-124 displays this distinct expression pattern in post-mitotic neurons (Kozuka et al., 2019; Han et al., 2020). Many studies state, that the high level of miR-124 in post-mitotic neurons suggests its importance in maintaining the differentiated identity of neurons (Ponomarev et al., 2011). Besides miR-124, two other miRNAs were identified to be more abundantly expressed in later stages of neurodevelopment than in earlier stages: miR-137 and miR-128. This result also coincides with the literature where it is described, that miRNAs -137 and -128 are both frequently expressed in the brain, especially in the cortex with functions in neuronal migration and neuronal development (Mahmoudi & Cairns, 2017; Franzoni et al., 2015). A precise expression of all the three described miRNAs is of utmost importance, as dysregulations of these miRNAs have been described to result in a wide range of neurodevelopmental deficits reaching from impaired neuronal migration to differentiation defects (Sun et al., 2011; Franzoni et al., 2015).

Two miRNAs that were found to have decreasing expression levels across neurodevelopment were miR-15b and miR-130b. Whereas miR-130b has been described to be a tumor promoter in glioma cell lines (Li et al., 2017), miR-15b has been shown to enhance neurogenesis whilst being an inhibitor of neuronal progenitor proliferation during early brain development (Lv et al., 2014). There is only little known about the expression levels of miR130b during brain development, but the decrease in expression from E14 to P0 found in our data might be an indicator for a high relevance during early stages of neurogenesis and decreasing significance in later phases of brain

development. Contrary to the results we found, in the literature miR-15b has been identified to have its peak of expression correlated with the peak of neurogenesis at E15 in the mouse brain (Lv et al., 2014). This discrepancy might have many reasons, one of them could be the analysis of only miR-15b-5p in our data as this is the miRNA preliminary expressed in mouse cells. Lv et al. on the other hand analyzed the overall miR-15b expression level, including miR15b-5p as well as miR-15b-3p. The huge involvement of miR-15b in mechanisms that take place during early stages of neurodevelopment as for example NPC proliferation and neuronal differentiation indicates the necessity of high expression levels of this miRNA at these time points. The increased expression miR-15b displayed in our sequencing data and TaqMan validation reflects this fact.

To sum it up, the miRNA sequencing study in NPCs, neurons and across different time points of neurodevelopment, revealed distinct expression patterns of selected, differentially expressed miRNAs across brain development. The expression profiles of a selection of candidate miRNAs which are crucial for neurogenesis and neurodevelopment were described and discussed. In the following part, this work will focus on miR-16 and its effects on the developing brain.

2. The effect of miRNA 16 on the developing murine neocortex

MiR-16 is a member of the miR-15 miRNA family which is evolutionary conserved and expressed among all vertebrates (Finnerty et al. 2010). All members of the miR-15 miRNA family share the same seed sequence (AGCAGC) and are therefore supposed to share a common set of target mRNAs. Members of the miR-15 miRNA family, including miR-16, have been shown to be involved in cell cycle regulation, proliferation and stress responses to inflammation (Burak et al., 2018; Wang et al., 2019). Furthermore, miR-16 and miR-15a were identified as regulators of serotonin transporters in the mouse brain as well as in human and rat cell lines (Moya et al., 2013).

In my study, I used the in vivo in utero electroporation approach to overexpress miR-16 and its family member miR-15 in the embryonic neocortex of the mouse. We found that the overexpression of miR-16 or miR-15 affected the cellular distribution among the different cortical zones. Cells that, in the control brains, were able to differentiate into

neurons and migrate into the cortical plate, accumulated in the intermediate zone and did not reach the cortical plate in the miR-16 or miR-15 overexpressing brains.

This effect was only seen when the miRNAs were overexpressed under control of the ubiquitous CAG promoter but not when overexpressed under control of the neuron-specific NeuroD promoter which rules out a neuronal migration defect. These results rather suggest that the overexpression of miR-16 and miR-15 causes a defect in neural progenitor biology such as a cell cycle or differentiation defect. The closely related miR-15b has already been shown to regulate cell proliferation, progenitor pool composition and neuronal differentiation in the embryonic brain (Lv et al., 2014).

Indeed, marker staining revealed that miR-16 overexpression increased the proportion of Tbr2 positive intermediate progenitors and reduced the proportion of Satb2 positive neurons. In the literature it can also be seen, that the closely related mir-15b also induced a reduction in Pax6 positive cells and an increase in Tbr2 positive cells in the developing brain (Lv et al., 2014).

The anti-proliferatory effect of miR-16 has already been shown in many studies including developmental and cancer research (Niu et al., 2019, Han et al., 2019; Wei et al., 2020). Han et al., discovered that miR-16 overexpressing mesenchymal cells arrested in G1 phase of the cell cycle and therefore displayed severe proliferation defects. The same study also described a delayed migration ability of miR-16 overexpressing cells. Additionally, miR-16 has been shown to inhibit proliferation in a variety of cancer cell lines (Haghi et al., 2019). The assumption, that miR-16 might not only inhibit proliferation but also promotes differentiation was only recently found, when Papagiannopoulos et al. showed, that miR-16 promotes the maturation of erythroleukemia cells (Papagiannopoulos et al., 2021).

The fact, that miR-16 has been found to be increased during embryonic stem cell differentiation in mice, supports the theory of its role for proliferation and differentiation which we came up with due to the results of miR-16 overexpression in the developing embryonic brain (Aranha et al., 2010).

One hypothesis could be, that by activating differentiation in the NPCs of the ventricular zone and therefore decreasing further proliferation of these cells, miR-16 might cause a

shift from proliferative divisions to neurogenic divisions and therefore increase the number of Tbr2 positive intermediate progenitors in the ventricular and intermediate zone. By this, the stem cell pool of self-renewing NPCs might exceed and IPCs accumulate in the lower areas of the developing cortex. Apparently, these intermediate progenitors are not able to differentiate further into Satb2 positive post mitotic neurons and therefore don't migrate to the upper areas of the cortical plate.

In the literature, miR-16 has already been shown to cause cell cycle arrests by targeting *Cyclin-D1* in cancer cells (Lui et al., 2008). This supports the hypothesis that miR-16 obstructs proliferation and causes a shift from proliferation to differentiation mode in NPCs.

In summary the observed increase in Tbr2 positive progenitors and decrease in Satb2 positive neurons in the miR-16 overexpressing neocortex suggests that miR-16 plays an important role in regulating neural proliferation and differentiation. By displaying anti-proliferative and differentiation enhancing effects at the same time, miR-16 could be the cause for a premature switch of NPCs from proliferation to differentiation mode. This could lead to an early exhaustion of the neuronal stem cell pool and would also explain the increased number of intermediate progenitor cells in the ventricular and intermediate zone. Prematurely differentiated IPCs in the ventricular and intermediate zone on the other hand either further differentiate into neurons and undergo apoptosis or accumulate in the subventricular and intermediate zone of the developing cortex.

To shed more light on potential mechanisms that might cause the observed phenotype, the relevance of possible miR-16 target genes will be discussed in the following chapter.

3. Possible miRNA 16 target genes and mechanisms

The role of miR-16 in a variety of biological processes has been shown in many studies (Yan et al., 2013; Ma et al., 2021). Most of the work has been done in the field of cancer research, where miR-16 was identified as a regulator of many tumorigenesis-related target genes (Aqeilan et al., 2010). Besides its anti-tumorigenic function, there is also evidence, that miR-16 is an important regulator of apoptosis and proliferation. This was shown, when anti-apoptotic genes as *Bcl-2* and cell cycle regulator genes as for example

Cyclin-D1 were identified as miR-16 targets (Cimmino et al., 2005; Linsley et al., 2007). To identify brain specific miR-16 targets, I performed mRNA sequencing with miR-16 overexpressing neocortical cells. The GO term analysis revealed that many of the gene downregulated in the neocortex after miR-16 overexpression and hence putative miR-16 targets were associated with terms such as “cell division”, “chromosome segregation” and others, all related to the broad field of cell cycle and mitosis. Five of these target genes that showed a decrease in expression in cortical cells after electroporation with miR-16 appeared to be of special interest for my study. All of them are predicted to have miR-16 binding sites in their 3’UTRs, are downregulated in the developing brain after miR-16 overexpression and additionally are involved in cell cycle progression, cell cycle checkpoints, DNA damage repair and other related fields. All chosen target genes are well known in the literature and have been shown to play important roles in cell cycle related mechanisms. *Fbxw7* for example has been found to be regulated by miR-25 and is involved in the reprogramming process of somatic cells into induced pluripotent stem cells (iPSCs) (Lu et al., 2012). *Taf15* has also been identified as an important factor for cellular proliferation and is regulated by a number of miRNAs (Ballarino et al., 2013). The cyclin dependent kinase I (*Cdk1*) which is well known for to be a key player in cell cycle progression recently has been found to be regulated by miR-16 in the context of cervical and ovarian cancer (Zubillaga-Guerrero et al., 2020; Schwarzenbach, 2016). The serine/threonine specific protein checkpoint kinase *Chek1* has also been described to be under regulation of the miR-15 miRNA family, including miR-16, and is involved in mitotic arrest of cardiomyocytes (Porrello et al., 2011). The fifth selected target gene of miR-16, the checkpoint kinase *Wee1* is targeted by many miRNAs, including miR-16 and in general is an established target gene for miRNAs in the context of multiple types of cancer, including leukemia (Lezina et al., 2013; Brockway et al., 2015).

The validity of the bioinformatic analyses was proven by transfecting miR-16 and a control into N2A cells, followed by an expression analysis via qPCR analyses of the five target genes. The decreased expression of all five target genes after miR-16 overexpression showed, that there must be a regulatory relation between these genes and miR-16. In order to achieve more insights about possible mechanisms underlying

the miR-16 overexpression phenotype in the developing brain, I decided to study one target gene of miR-16 in more detail.

For this, I chose *Wee1*. As already described above, *Wee1* has already been shown to be post-transcriptionally regulated by miR-16 in a variety of cancer related studies (Du et al., 2021). Besides of this, is has been shown, that *Wee1* is involved in the formation of neuronal polarity in post-mitotic neurons as mis-regulation of *Wee1* leads to disrupted neuronal polarity in these cells (Müller et al., 2010). The regulatory connection between *Wee1* and miR-16 in N2A cells, which is a murine, fast growing neuroblastoma cell line, can be an indicator for the relevance of *Wee1* regulation through miRNAs in brain developmental processes. MiR-16 seems to be one of these regulating miRNAs. This hypothesis is also supported by the studies of Wang et al., who found, that miR-16 is a direct regulator of the *Wee1* G2 checkpoint kinases in Radioresistant non-small cell lung cancer (NSCLC) cell lines (Wang et al., 2020). Here, the protein expression as well as the RNA level and luciferase activity of *Wee1* was also decreased after overexpression of miR-16. Exactly the same effects could be observed in our study.

If miR-16 overexpression causes a downregulation of *Wee1* levels in both RNA as well protein expression in the embryonic developing brain, this could be the cause for many neurodevelopmental deficits, including the phenotype we observed in our experiments after miR-16 overexpression in E13 murine cortices. The switch from proliferative to differentiative modes in neuronal stem cells, observed in miR-16 electroporated cells and discussed earlier, could also be related to a mis-regulation of *Wee1* through miR-16. *Wee1* carefully regulates the G2 checkpoint of the cell cycle and thereby prevents cells from entering mitosis at premature stages. Downregulation of *Wee1* could result in a premature entry of neuronal stem cells into mitosis. When *Wee1* was described for the first time in the 1980s by Nurse and Thuriaux in fission yeast, it was also observed to influence the size of daughter cells by regulating the mother cells timepoint of mitosis entry (Nurse & Thuriaux, 1980). In general, *Wee1* doesn't act alone as a regulator of mitosis entry. *Wee1* itself is influenced by a range of other molecules and is embedded in a complex mitosis-regulating pathway. One interesting finding of our RNA sequencing experiment was also, that *Cdk1* was also identified to be downregulated after miR-16 overexpression in embryonic brain tissue. The G2 checkpoint kinase *Wee1* is a direct

regulator of *Cdk1*, as it inhibits *Cdk1* by phosphorylation and therefore prevents the cell to enter mitosis (Den Haese et al., 1995). The fact that both *Cdk1* as well as its direct inhibitor *Wee1* are regulated by miR-16, again underlines the importance of miR-16's role as a regulator of the cell cycle in the developing brain.

Another evidence for the direct interaction of miR-16 and *Wee1* were the knockdown experiments we performed in the embryonic mouse brain. After the successful verification of the knockdown of miR-16 and its family members miR-15a and miR-15b by siRNA transfection in E13 embryonic mouse brains it was also shown, that the *Wee1* RNA level is significantly increased in cells lacking the miRNAs. This suggests *Wee1* as possible target of all three tested miRNAs. If *Wee1* is targeted by miR-16, miR-15a as well as miR-15b it could be possible that compensatory effects could occur when for example the function of only one miRNA of the miR-15 miRNA family is lost. This hypothesis is supported by the observation, that miR-15 overexpression causes the same phenotype in the developing embryonic brain as it was detected for miR-16. In the literature it is also described, that seed sequence similarity very much correlates with target gene similarity in miRNAs (Kehl et al., 2017).

The final experiments of this study focused on the effect of simultaneous overexpression of *Wee1* and miR-16 in the developing embryonic brain. As an overexpression of miR-16 results in a phenotype strongly aberrant to the control and *Wee1* seems to be a direct target of miR-16, we hypothesized that overexpression of *Wee1* in addition to miR-16 could rescue the phenotype of miR-16 overexpression. This was, however, not the case. There were even less GFP positive cells in the cortical plate of *Wee1* + miR-16 overexpressing neocortex than in the neocortex electroporated with miR-16 only. From these results we concluded, that *Wee1* overexpression causes a phenotype in the developing embryonic neocortex independent of the miR-16 overexpression phenotype. It seems as if an equalization of *Wee1* transcripts in the developing brain together with miR-16 overexpression causes even less cells to differentiate fully into post-mitotic neurons of the cortical plate. This is also supported by the results of the Satb2 stainings which were conducted in *Wee1* + miR-16 overexpressed as well as in control and miR-16 electroporated brains. Here, it was also clear to see, that significantly less electroporated cells reached the status of post-mitotic neurons after miR-16 + *Wee1*

electroporation than after mir-16 only or control electroporation. It is described, that *Wee1* overexpression results in enhanced proliferation and migration in gastric cancer cells (Kim et al., 2016). Although the described effect of increased migration could not be observed in our study, the decrease in Satb2 positive cells suggests that overexpression of *Wee1* could have caused an increased proliferation rate of neuronal stem cells in the ventricular zone of the electroporated brains. In addition to that, *Wee1* has also been identified as potential target for cancer defeat, as inhibition of *Wee1*, due to its cell cycle regulatory properties, results in significant decreases in cancer cell proliferation (Yin et al., 2018). This decrease in proliferation can also be observed in our study after miR-16 overexpression and the subsequent decrease of *Wee1* levels.

Taken together, the G2 checkpoint kinase *Wee1*, which has already been proven to be an important regulator of cell cycle dynamics in a wide range of tissues and in relation to many diseases, seems to be also of huge relevance for embryonic brain development. The connection between *Wee1* and miR-16 in tissue of the developing embryonic brain, made in this work, marks the relevance of miRNA regulation of *Wee1* during proliferation and neurogenesis in general.

However, it is also reasonable, that the phenotype induced by miR-16 overexpression in the developing neocortex, is not only caused by a mis-regulation of *Wee1* alone but by an interaction of many other factors. As already described earlier, besides *Wee1*, I identified many other target genes that are regulated by miR-16 by mRNA sequencing. The genes *Cdk1* as well as *Chk1*, for example, both close interactors of *Wee1* and important regulators of cell cycle and proliferation, have also been found to be targeted by miR-16 and might be involved in the formation of the observed phenotype. This possible interaction, however, still needs to be studied in more detail in the future.

To sum it up, this study provides some so far unknown insights about miRNA regulation in the developing neocortex. With this work, I hope to make a small contribution on the way to a better understanding of the complex process of neurodevelopment, which is highly orchestrated and influenced by many factors and not completely understood yet.

References

Abraira, Victoria E.; Ginty, David D. (2013): The sensory neurons of touch. In: *Neuron* 79 (4), S. 618–639. DOI: 10.1016/j.neuron.2013.07.051.

Agarwal, Vikram; Bell, George W.; Nam, Jin-Wu; Bartel, David P. (2015): Predicting effective microRNA target sites in mammalian mRNAs. In: *eLife* 4. DOI: 10.7554/eLife.05005.

Anderson, S. A.; Marín, O.; Horn, C.; Jennings, K.; Rubenstein, J. L. (2001): Distinct cortical migrations from the medial and lateral ganglionic eminences. In: *Development (Cambridge, England)* 128 (3), S. 353–363.

Aqeilan, R. I.; Calin, G. A.; Croce, C. M. (2010): miR-15a and miR-16-1 in cancer. Discovery, function and future perspectives. In: *Cell death and differentiation* 17 (2), S. 215–220. DOI: 10.1038/cdd.2009.69.

Aranha, Márcia M.; Santos, Daniela M.; Xavier, Joana M.; Low, Walter C.; Steer, Clifford J.; Solá, Susana; Rodrigues, Cecília M. P. (2010): Apoptosis-associated microRNAs are modulated in mouse, rat and human neural differentiation. In: *BMC genomics* 11, S. 514. DOI: 10.1186/1471-2164-11-514.

Armstrong, E.; Schleicher, A.; Omran, H.; Curtis, M.; Zilles, K. (1995): The ontogeny of human gyrification. In: *Cerebral cortex (New York, N.Y. : 1991)* 5 (1), S. 56–63. DOI: 10.1093/cercor/5.1.56.

Association, American Psychiatric (2013): Diagnostic and Statistical Manual of Mental Disorders: American Psychiatric Association.

Ballarino, M.; Jobert, L.; Dembélé, D.; La Grange, P. de; Auboeuf, D.; Tora, L. (2013): TAF15 is important for cellular proliferation and regulates the expression of a subset of cell cycle genes through miRNAs. In: *Oncogene* 32 (39), S. 4646–4655. DOI: 10.1038/onc.2012.490.

Barman, Bahnisikha; Bhattacharyya, Suvendra N. (2015): mRNA Targeting to Endoplasmic Reticulum Precedes Ago Protein Interaction and MicroRNA (miRNA)-mediated Translation Repression in Mammalian Cells. In: *The Journal of biological chemistry* 290 (41), S. 24650–24656. DOI: 10.1074/jbc.C115.661868.

Bartel, David P. (2009): MicroRNAs. Target recognition and regulatory functions. In: *Cell* 136 (2), S. 215–233. DOI: 10.1016/j.cell.2009.01.002.

Baskerville, Scott; Bartel, David P. (2005): Microarray profiling of microRNAs reveals frequent coexpression with neighboring miRNAs and host genes. In: *RNA (New York, N.Y.)* 11 (3), S. 241–247. DOI: 10.1261/rna.7240905.

Baudry, Anne; Mouillet-Richard, Sophie; Schneider, Benoît; Launay, Jean-Marie; Kellermann, Odile (2010): miR-16 targets the serotonin transporter. A new facet for adaptive responses to antidepressants. In: *Science (New York, N.Y.)* 329 (5998), S. 1537–1541. DOI: 10.1126/science.1193692.

Ben-Yehoyada, Merav; Wang, Lily C.; Kozekov, Ivan D.; Rizzo, Carmelo J.; Gottesman, Max E.; Gautier, Jean (2009): Checkpoint signaling from a single DNA interstrand crosslink. In: *Molecular cell* 35 (5), S. 704–715. DOI: 10.1016/j.molcel.2009.08.014.

Bhalala, Oneil G.; Srikanth, Maya; Kessler, John A. (2013): The emerging roles of microRNAs in CNS injuries. In: *Nature reviews. Neurology* 9 (6), S. 328–339. DOI: 10.1038/nrneurol.2013.67.

Bian, Shan; Hong, Janet; Li, Qingsong; Schebelle, Laura; Pollock, Andrew; Knauss, Jennifer L. et al. (2013): MicroRNA cluster miR-17-92 regulates neural stem cell expansion and transition to intermediate progenitors in the developing mouse neocortex. In: *Cell reports* 3 (5), S. 1398–1406. DOI: 10.1016/j.celrep.2013.03.037.

Bielle, Franck; Griveau, Amélie; Narboux-Nême, Nicolas; Vigneau, Sébastien; Sigrist, Markus; Arber, Silvia et al. (2005): Multiple origins of Cajal-Retzius cells at the borders of the developing pallium. In: *Nature neuroscience* 8 (8), S. 1002–1012. DOI: 10.1038/nn1511.

Bienvenu, Frédéric; Jirawatnotai, Siwanon; Elias, Joshua E.; Meyer, Clifford A.; Mizeracka, Karolina; Marson, Alexander et al. (2010): Transcriptional role of cyclin D1 in development revealed by a genetic-proteomic screen. In: *Nature* 463 (7279), S. 374–378. DOI: 10.1038/nature08684.

Blazie, Stephen M.; Geissel, Heather C.; Wilky, Henry; Joshi, Rajan; Newbern, Jason; Mangone, Marco (2017): Alternative Polyadenylation Directs Tissue-Specific miRNA Targeting in Caenorhabditis elegans Somatic Tissues. In: *Genetics* 206 (2), S. 757–774. DOI: 10.1534/genetics.116.196774.

Bonci, Désirée; Coppola, Valeria; Musumeci, Maria; Addario, Antonio; Giuffrida, Raffaella; Memeo, Lorenzo et al. (2008): The miR-15a-miR-16-1 cluster controls prostate cancer by targeting multiple oncogenic activities. In: *Nature medicine* 14 (11), S. 1271–1277. DOI: 10.1038/nm.1880.

Brockway, Sonia; Zeleznik-Le, Nancy J. (2015): WEE1 is a validated target of the microRNA miR-17-92 cluster in leukemia. In: *Cancer genetics* 208 (5), S. 279–287. DOI: 10.1016/j.cancergen.2015.01.001.

Brown, Michael; Keynes, Roger; Lumsden, Andrew (2005): The developing brain. Reprint. Oxford: Oxford Univ. Press.

Brown, Nicholas R.; Korolchuk, Svitlana; Martin, Mathew P.; Stanley, Will A.; Moukhametzianov, Rouslan; Noble, Martin E. M.; Endicott, Jane A. (2015): CDK1 structures reveal conserved and unique features of the essential cell cycle CDK. In: *Nature communications* 6, S. 6769. DOI: 10.1038/ncomms7769.

Buchman, Joshua J.; Tsai, Li-Huei (2007): Spindle regulation in neural precursors of flies and mammals. In: *Nature reviews. Neuroscience* 8 (2), S. 89–100. DOI: 10.1038/nrn2058.

Bukhari, Syed I. A.; Truesdell, Samuel S.; Lee, Sooncheol; Kollu, Swapna; Classon, Anthony; Boukhali, Myriam et al. (2016): A Specialized Mechanism of Translation

Mediated by FXR1a-Associated MicroRNP in Cellular Quiescence. In: *Molecular cell* 61 (5), S. 760–773. DOI: 10.1016/j.molcel.2016.02.013.

Burak, Kristyn; Lamoureux, Lise; Boese, Amrit; Majer, Anna; Saba, Reuben; Niu, Yulian et al. (2018): MicroRNA-16 targets mRNA involved in neurite extension and branching in hippocampal neurons during presymptomatic prion disease. In: *Neurobiology of disease* 112, S. 1–13. DOI: 10.1016/j.nbd.2017.12.011.

Calegari, Federico; Huttner, Wieland B. (2003): An inhibition of cyclin-dependent kinases that lengthens, but does not arrest, neuroepithelial cell cycle induces premature neurogenesis. In: *Journal of cell science* 116 (Pt 24), S. 4947–4955. DOI: 10.1242/jcs.00825.

Cárdenas, Adrián; Borrell, Víctor (2020): Molecular and cellular evolution of corticogenesis in amniotes. In: *Cellular and molecular life sciences : CMLS* 77 (8), S. 1435–1460. DOI: 10.1007/s00018-019-03315-x.

Cheffer, Arquimedes; Tárnok, Attila; Ulrich, Henning (2013): Cell cycle regulation during neurogenesis in the embryonic and adult brain. In: *Stem cell reviews and reports* 9 (6), S. 794–805. DOI: 10.1007/s12015-013-9460-5.

Chen, Jiandong (2016): The Cell-Cycle Arrest and Apoptotic Functions of p53 in Tumor Initiation and Progression. In: *Cold Spring Harbor perspectives in medicine* 6 (3), a026104. DOI: 10.1101/cshperspect.a026104.

Chen, Jun; Zhang, John H.; Hu, Xiaoming (Hg.) (2016): Non-Neuronal Mechanisms of Brain Damage and Repair After Stroke. Cham, s.l.: Springer International Publishing (Springer Series in Translational Stroke Research). Online verfügbar unter http://dx.doi.org/10.1007/978-3-319-32337-4.

Chen, Xi; Ba, Yi; Ma, Lijia; Cai, Xing; Yin, Yuan; Wang, Kehui et al. (2008): Characterization of microRNAs in serum. A novel class of biomarkers for diagnosis of cancer and other diseases. In: *Cell research* 18 (10), S. 997–1006. DOI: 10.1038/cr.2008.282.

Cherone, Jennifer M.; Jorgji, Vjola; Burge, Christopher B. (2019): Cotargeting among microRNAs in the brain. In: *Genome research* 29 (11), S. 1791–1804. DOI: 10.1101/gr.249201.119.

Cho, Kenta Hyeon Tae; Xu, Bing; Blenkiron, Cherie; Fraser, Mhoyra (2019): Emerging Roles of miRNAs in Brain Development and Perinatal Brain Injury. In: *Frontiers in physiology* 10, S. 227. DOI: 10.3389/fphys.2019.00227.

Cimmino, Amelia; Calin, George Adrian; Fabbri, Muller; Iorio, Marilena V.; Ferracin, Manuela; Shimizu, Masayoshi et al. (2005): miR-15 and miR-16 induce apoptosis by targeting BCL2. In: *Proceedings of the National Academy of Sciences of the United States of America* 102 (39), S. 13944–13949. DOI: 10.1073/pnas.0506654102.

Cooper, Jonathan A. (2008): A mechanism for inside-out lamination in the neocortex. In: *Trends in neurosciences* 31 (3), S. 113–119. DOI: 10.1016/j.tins.2007.12.003.

Craig, K. L.; Tyers, M. (1999): The F-box. A new motif for ubiquitin dependent proteolysis in cell cycle regulation and signal transduction. In: *Progress in biophysics and molecular biology* 72 (3), S. 299–328. DOI: 10.1016/s0079-6107(99)00010-3.

Deibler, Richard W.; Kirschner, Marc W. (2010): Quantitative reconstitution of mitotic CDK1 activation in somatic cell extracts. In: *Molecular cell* 37 (6), S. 753–767. DOI: 10.1016/j.molcel.2010.02.023.

Den Haese, G. J.; Walworth, N.; Carr, A. M.; Gould, K. L. (1995): The Wee1 protein kinase regulates T14 phosphorylation of fission yeast Cdc2. In: *Molecular biology of the cell* 6 (4), S. 371–385. DOI: 10.1091/mbc.6.4.371.

Denis, Hélène; Ndlovu, Matladi N.; Fuks, François (2011): Regulation of mammalian DNA methyltransferases. A route to new mechanisms. In: *EMBO reports* 12 (7), S. 647–656. DOI: 10.1038/embor.2011.110.

Desai, D.; Gu, Y.; Morgan, D. O. (1992): Activation of human cyclin-dependent kinases in vitro. In: *Molecular biology of the cell* 3 (5), S. 571–582. DOI: 10.1091/mbc.3.5.571.

Dharap, Ashutosh; Pokrzywa, Courtney; Murali, Shruthi; Pandi, Gopal; Vemuganti, Raghu (2013): MicroRNA miR-324-3p induces promoter-mediated expression of RelA gene. In: *PloS one* 8 (11), e79467. DOI: 10.1371/journal.pone.0079467.

Do, Khanh; Doroshow, James H.; Kummar, Shivaani (2013): Wee1 kinase as a target for cancer therapy. In: *Cell cycle (Georgetown, Tex.)* 12 (19), S. 3159–3164. DOI: 10.4161/cc.26062.

Du, Ran; Jiang, Feng; Yin, Yanhua; Xu, Jinfen; Li, Xia; Hu, Likuan; Wang, Xiuyu (2021): Knockdown of lncRNA X inactive specific transcript (XIST) radiosensitizes non-small cell lung cancer (NSCLC) cells through regulation of miR-16-5p/WEE1 G2 checkpoint kinase (WEE1) axis. In: *International journal of immunopathology and pharmacology* 35, 2058738420966087. DOI: 10.1177/2058738420966087.

Fabbri, Muller (2018): MicroRNAs and miRceptors. A new mechanism of action for intercellular communication. In: *Philosophical transactions of the Royal Society of London. Series B, Biological sciences* 373 (1737). DOI: 10.1098/rstb.2016.0486.

Finnerty, John R.; Wang, Wang-Xia; Hébert, Sébastien S.; Wilfred, Bernard R.; Mao, Guogen; Nelson, Peter T. (2010): The miR-15/107 group of microRNA genes. Evolutionary biology, cellular functions, and roles in human diseases. In: *Journal of molecular biology* 402 (3), S. 491–509. DOI: 10.1016/j.jmb.2010.07.051.

Franzoni, Eleonora; Booker, Sam A.; Parthasarathy, Srinivas; Rehfeld, Frederick; Grosser, Sabine; Srivatsa, Swathi et al. (2015): miR-128 regulates neuronal migration, outgrowth and intrinsic excitability via the intellectual disability gene Phf6. In: *eLife* 4. DOI: 10.7554/eLife.04263.

Freissmuth, Michael; Offermanns, Stefan; Böhm, Stefan (2020): Pharmakologie und Toxikologie. Von den molekularen Grundlagen zur Pharmakotherapie. 3., überarbeitete Auflage. Berlin: Springer (Lehrbuch).

Friedman, Jeffrey M.; Jones, Peter A. (2009): MicroRNAs. Critical mediators of differentiation, development and disease. In: *Swiss medical weekly* 139 (33-34), S. 466–472.

Fu, Guodong; Brkić, Jelena; Hayder, Heyam; Peng, Chun (2013): MicroRNAs in Human Placental Development and Pregnancy Complications. In: *International journal of molecular sciences* 14 (3), S. 5519–5544. DOI: 10.3390/ijms14035519.

Gallo, Alessia; Tandon, Mayank; Alevizos, Ilias; Illei, Gabor G. (2012): The majority of microRNAs detectable in serum and saliva is concentrated in exosomes. In: *PloS one* 7 (3), e30679. DOI: 10.1371/journal.pone.0030679.

Gao, Fen-Biao (2010): Context-dependent functions of specific microRNAs in neuronal development. In: *Neural development* 5, S. 25. DOI: 10.1186/1749-8104-5-25.

Ghiasi, Naghmeh; Habibagahi, Mojtaba; Rosli, Rozita; Ghaderi, Abbas; Yusoff, Khatijah; Hosseini, Ahmad et al. (2014): Tumour suppressive effects of WEE1 gene silencing in breast cancer cells. In: *Asian Pacific journal of cancer prevention : APJCP* 14 (11), S. 6605–6611. DOI: 10.7314/apjcp.2013.14.11.6605.

Gibb, Robbin; Kolb, Bryan (2018): The neurobiology of brain and behavioral development. Saint Louis: Elsevier Science. Online verfügbar unter https://www.sciencedirect.com/science/book/9780128040362

Godlewski, Jakub; Lenart, Jacek; Salinska, Elzbieta (2019): MicroRNA in Brain pathology. Neurodegeneration the Other Side of the Brain Cancer. In: *Non-coding RNA* 5 (1). DOI: 10.3390/ncrna5010020.

Gonzalez, Susana; Pisano, David G.; Serrano, Manuel (2008): Mechanistic principles of chromatin remodeling guided by siRNAs and miRNAs. In: *Cell cycle (Georgetown, Tex.)* 7 (16), S. 2601–2608. DOI: 10.4161/cc.7.16.6541.

Götz, Magdalena; Huttner, Wieland B. (2005): The cell biology of neurogenesis. In: *Nature reviews. Molecular cell biology* 6 (10), S. 777–788. DOI: 10.1038/nrm1739.

Haghi, Mehdi; Taha, Masoumeh F.; Javeri, Arash (2019): Suppressive effect of exogenous miR-16 and miR-34a on tumorigenesis of breast cancer cells. In: *Journal of cellular biochemistry* 120 (8), S. 13342–13353. DOI: 10.1002/jcb.28608.

Han, Dong; Dong, Xiaoyu; Zheng, Dongming; Nao, Jianfei (2019): MiR-124 and the Underlying Therapeutic Promise of Neurodegenerative Disorders. In: *Frontiers in pharmacology* 10, S. 1555. DOI: 10.3389/fphar.2019.01555.

Han, Tao; Wu, Ni; Wang, Youjing; Shen, Weimin; Zou, Jijun (2019): miR-16-2-3p inhibits cell proliferation and migration and induces apoptosis by targeting PDPK1 in maxillary primordium mesenchymal cells. In: *International journal of molecular medicine* 43 (3), S. 1441–1451. DOI: 10.3892/ijmm.2019.4070.

Hanzlik, Emily; Gigante, Joseph (2017): Microcephaly. In: *Children (Basel, Switzerland)* 4 (6). DOI: 10.3390/children4060047.

Hatten, M. E. (1999): Central nervous system neuronal migration. In: *Annual review of neuroscience* 22, S. 511–539. DOI: 10.1146/annurev.neuro.22.1.511.

He, Qingmei; Ren, Xianyue; Chen, Jiewei; Li, Yingqin; Tang, Xinran; Wen, Xin et al. (2016): miR-16 targets fibroblast growth factor 2 to inhibit NPC cell proliferation and invasion via PI3K/AKT and MAPK signaling pathways. In: *Oncotarget* 7 (3), S. 3047–3058. DOI: 10.18632/oncotarget.6504.

Hevner, Robert F.; Haydar, Tarik F. (2012): The (not necessarily) convoluted role of basal radial glia in cortical neurogenesis. In: *Cerebral cortex (New York, N.Y. : 1991)* 22 (2), S. 465–468. DOI: 10.1093/cercor/bhr336.

Hicks, Steven D.; Middleton, Frank A. (2016): A Comparative Review of microRNA Expression Patterns in Autism Spectrum Disorder. In: *Frontiers in psychiatry* 7, S. 176. DOI: 10.3389/fpsyt.2016.00176.

Huang, Weili (2017): MicroRNAs. Biomarkers, Diagnostics, and Therapeutics. In: *Methods in molecular biology (Clifton, N.J.)* 1617, S. 57–67. DOI: 10.1007/978-1-4939-7046-9_4.

Huang, Xiao A.; Yin, Hang; Sweeney, Sarah; Raha, Debasish; Snyder, Michael; Lin, Haifan (2013): A major epigenetic programming mechanism guided by piRNAs. In: *Developmental cell* 24 (5), S. 502–516. DOI: 10.1016/j.devcel.2013.01.023.

Huang, Zhen (2009): Molecular regulation of neuronal migration during neocortical development. In: *Molecular and cellular neurosciences* 42 (1), S. 11–22. DOI: 10.1016/j.mcn.2009.06.003.

Hussein, Mona; Magdy, Rehab (2021): MicroRNAs in central nervous system disorders. Current advances in pathogenesis and treatment. In: *Egypt J Neurol Psychiatry Neurosurg* 57 (1), S. 197. DOI: 10.1186/s41983-021-00289-1.

Jackson, R. J.; Howell, M. T.; Kaminski, A. (1990): The novel mechanism of initiation of picornavirus RNA translation. In: *Trends in biochemical sciences* 15 (12), S. 477–483. DOI: 10.1016/0968-0004(90)90302-r.

Jakovcevski, Mira; Akbarian, Schahram (2012): Epigenetic mechanisms in neurological disease. In: *Nature medicine* 18 (8), S. 1194–1204. DOI: 10.1038/nm.2828.

Jones-Rhoades, Matthew W.; Bartel, David P.; Bartel, Bonnie (2006): MicroRNAS and their regulatory roles in plants. In: *Annual review of plant biology* 57, S. 19–53. DOI: 10.1146/annurev.arplant.57.032905.105218.

Juan Romero, Camino de; Borrell, Víctor (2015): Coevolution of radial glial cells and the cerebral cortex. In: *Glia* 63 (8), S. 1303–1319. DOI: 10.1002/glia.22827.

Kay, Matthew Krivacka; Zhang, Jian; Choudhury, Mahua (2021): Screening for alternative splicing of lncRNA Dleu2 in the mouse liver cell line AML-12. In: *Biomedical reports* 14 (6), S. 50. DOI: 10.3892/br.2021.1426.

Kehl, Tim; Backes, Christina; Kern, Fabian; Fehlmann, Tobias; Ludwig, Nicole; Meese, Eckart et al. (2017): About miRNAs, miRNA seeds, target genes and target pathways. In: *Oncotarget* 8 (63), S. 107167–107175. DOI: 10.18632/oncotarget.22363.

Kellogg, Douglas R. (2003): Wee1-dependent mechanisms required for coordination of cell growth and cell division. In: *Journal of cell science* 116 (Pt 24), S. 4883–4890. DOI: 10.1242/jcs.00908.

Kim, Hye-Young; Cho, Yunhee; Kang, HyeokGu; Yim, Ye-Seal; Kim, Seok-Jun; Song, Jaewhan; Chun, Kyung-Hee (2016): Targeting the WEE1 kinase as a molecular targeted therapy for gastric cancer. In: *Oncotarget* 7 (31), S. 49902–49916. DOI: 10.18632/oncotarget.10231.

Klein, Ulf; Lia, Marie; Crespo, Marta; Siegel, Rachael; Shen, Qiong; Mo, Tongwei et al. (2010): The DLEU2/miR-15a/16-1 cluster controls B cell proliferation and its deletion leads to chronic lymphocytic leukemia. In: *Cancer cell* 17 (1), S. 28–40. DOI: 10.1016/j.ccr.2009.11.019.

Klungland, Arne; Robertson, Adam B. (2017): Oxidized C5-methyl cytosine bases in DNA. 5-Hydroxymethylcytosine; 5-formylcytosine; and 5-carboxycytosine. In: *Free radical biology & medicine* 107, S. 62–68. DOI: 10.1016/j.freeradbiomed.2016.11.038.

Ko, L. J.; Prives, C. (1996): p53. Puzzle and paradigm. In: *Genes & development* 10 (9), S. 1054–1072. DOI: 10.1101/gad.10.9.1054.

Kozuka, Takashi; Omori, Yoshihiro; Watanabe, Satoshi; Tarusawa, Etsuko; Yamamoto, Haruka; Chaya, Taro et al. (2019): miR-124 dosage regulates prefrontal cortex function by dopaminergic modulation. In: *Scientific reports* 9 (1), S. 3445. DOI: 10.1038/s41598-019-38910-2.

Kriegstein, Arnold; Alvarez-Buylla, Arturo (2009): The glial nature of embryonic and adult neural stem cells. In: *Annual review of neuroscience* 32, S. 149–184. DOI: 10.1146/annurev.neuro.051508.135600.

Krishnan, Harish R.; Sakharkar, Amul J.; Teppen, Tara L.; Berkel, Tiffani D. M.; Pandey, Subhash C. (2014): The epigenetic landscape of alcoholism. In: *International review of neurobiology* 115, S. 75–116. DOI: 10.1016/B978-0-12-801311-3.00003-2.

Kumar, Suresh; Chinnusamy, Viswanathan; Mohapatra, Trilochan (2018): Epigenetics of Modified DNA Bases. 5-Methylcytosine and Beyond. In: *Frontiers in genetics* 9, S. 640. DOI: 10.3389/fgene.2018.00640.

Kyzar, Evan J.; Banerjee, Ritabrata (2016): Targeted Epigenetic Modulation of Gene Expression in the Brain. In: *The Journal of neuroscience : the official journal of the Society for Neuroscience* 36 (36), S. 9283–9285. DOI: 10.1523/JNEUROSCI.1990-16.2016.

Lagos-Quintana, M.; Rauhut, R.; Lendeckel, W.; Tuschl, T. (2001): Identification of novel genes coding for small expressed RNAs. In: *Science (New York, N.Y.)* 294 (5543), S. 853–858. DOI: 10.1126/science.1064921.

Lang, Ming-Fei; Shi, Yanhong (2012): Dynamic Roles of microRNAs in Neurogenesis. In: *Frontiers in neuroscience* 6, S. 71. DOI: 10.3389/fnins.2012.00071.

Lee, Jihui; Heo, Jeongyeon; Kang, Hara (2019): miR-92b-3p-TSC1 axis is critical for mTOR signaling-mediated vascular smooth muscle cell proliferation induced by hypoxia. In: *Cell death and differentiation* 26 (9), S. 1782–1795. DOI: 10.1038/s41418-018-0243-z.

Lee, R. C.; Feinbaum, R. L.; Ambros, V. (1993): The C. elegans heterochronic gene lin-4 encodes small RNAs with antisense complementarity to lin-14. In: *Cell* 75 (5), S. 843–854. DOI: 10.1016/0092-8674(93)90529-y.

Letzen, Brian S.; Liu, Cyndi; Thakor, Nitish V.; Gearhart, John D.; All, Angelo H.; Kerr, Candace L. (2010): MicroRNA expression profiling of oligodendrocyte differentiation from human embryonic stem cells. In: *PloS one* 5 (5), e10480. DOI: 10.1371/journal.pone.0010480.

Levine, A. J. (1997): p53, the cellular gatekeeper for growth and division. In: *Cell* 88 (3), S. 323–331. DOI: 10.1016/s0092-8674(00)81871-1.

Lew, D. J.; Kornbluth, S. (1996): Regulatory roles of cyclin dependent kinase phosphorylation in cell cycle control. In: *Current opinion in cell biology* 8 (6), S. 795–804. DOI: 10.1016/s0955-0674(96)80080-9.

Lezina, L.; Purmessur, N.; Antonov, A. V.; Ivanova, T.; Karpova, E.; Krishan, K. et al. (2013): miR-16 and miR-26a target checkpoint kinases Wee1 and Chk1 in response to p53 activation by genotoxic stress. In: *Cell death & disease* 4, e953. DOI: 10.1038/cddis.2013.483.

Li, B.; Liu, Y-H; Sun, A-G; Huan, L-C; Li, H-D; Liu, D-M (2017): MiR-130b functions as a tumor promoter in glioma via regulation of ERK/MAPK pathway. In: *European review for medical and pharmacological sciences* 21 (12), S. 2840–2846.

Lindner, Silke E.; Lohmüller, Michael; Kotkamp, Bianka; Schuler, Fabian; Knust, Zeynep; Villunger, Andreas; Herzog, Sebastian (2017): The miR-15 family reinforces the transition from proliferation to differentiation in pre-B cells. In: *EMBO reports* 18 (9), S. 1604–1617. DOI: 10.15252/embr.201643735.

Lindqvist, Arne; Rodríguez-Bravo, Verónica; Medema, René H. (2009): The decision to enter mitosis. Feedback and redundancy in the mitotic entry network. In: *The Journal of cell biology* 185 (2), S. 193–202. DOI: 10.1083/jcb.200812045.

Linsley, Peter S.; Schelter, Janell; Burchard, Julja; Kibukawa, Miho; Martin, Melissa M.; Bartz, Steven R. et al. (2007): Transcripts targeted by the microRNA-16 family cooperatively regulate cell cycle progression. In: *Molecular and cellular biology* 27 (6), S. 2240–2252. DOI: 10.1128/MCB.02005-06.

Liscovitch, Noa; Chechik, Gal (2013): Specialization of gene expression during mouse brain development. In: *PLoS computational biology* 9 (9), e1003185. DOI: 10.1371/journal.pcbi.1003185.

Liu, Qin; Fu, Hanjiang; Sun, Fang; Zhang, Haoming; Tie, Yi; Zhu, Jie et al. (2008): miR-16 family induces cell cycle arrest by regulating multiple cell cycle genes. In: *Nucleic acids research* 36 (16), S. 5391–5404. DOI: 10.1093/nar/gkn522.

Lu, Dong; Davis, Matthew P. A.; Abreu-Goodger, Cei; Wang, Wei; Campos, Lia S.; Siede, Julia et al. (2012): MiR-25 regulates Wwp2 and Fbxw7 and promotes reprogramming of mouse fibroblast cells to iPSCs. In: *PloS one* 7 (8), e40938. DOI: 10.1371/journal.pone.0040938.

Lukaszewicz, Agnès; Savatier, Pierre; Cortay, Véronique; Kennedy, Henry; Dehay, Colette (2002): Contrasting effects of basic fibroblast growth factor and neurotrophin 3 on cell cycle kinetics of mouse cortical stem cells. In: *The Journal of neuroscience : the official journal of the Society for Neuroscience* 22 (15), S. 6610–6622.

Lv, Xiaohui; Jiang, Huihui; Liu, Yanli; Lei, Xuepei; Jiao, Jianwei (2014): MicroRNA-15b promotes neurogenesis and inhibits neural progenitor proliferation by directly repressing TET3 during early neocortical development. In: *EMBO reports* 15 (12), S. 1305–1314. DOI: 10.15252/embr.201438923.

Ma, Li; Liu, Junping; Xiao, Erhui; Ning, Huibin; Li, Kuan; Shang, Jia; Kang, Yi (2021): MiR-15b and miR-16 suppress TGF-β1-induced proliferation and fibrogenesis by regulating LOXL1 in hepatic stellate cells. In: *Life sciences* 270, S. 119144. DOI: 10.1016/j.lfs.2021.119144.

Mahmoudi, E.; Cairns, M. J. (2017): MiR-137. An important player in neural development and neoplastic transformation. In: *Molecular psychiatry* 22 (1), S. 44–55. DOI: 10.1038/mp.2016.150.

Malumbres, Marcos (2014): Cyclin-dependent kinases. In: *Genome biology* 15 (6), S. 122. DOI: 10.1186/gb4184.

Marín, O.; Rubenstein, J. L. (2001): A long, remarkable journey. Tangential migration in the telencephalon. In: *Nature reviews. Neuroscience* 2 (11), S. 780–790. DOI: 10.1038/35097509.

McIntosh, J. Richard (2016): Mitosis. In: *Cold Spring Harbor perspectives in biology* 8 (9). DOI: 10.1101/cshperspect.a023218.

McNeely, S.; Beckmann, R.; Bence Lin, A. K. (2014): CHEK again. Revisiting the development of CHK1 inhibitors for cancer therapy. In: *Pharmacology & therapeutics* 142 (1), S. 1–10. DOI: 10.1016/j.pharmthera.2013.10.005.

Mira, Helena; Morante, Javier (2020): Neurogenesis From Embryo to Adult - Lessons From Flies and Mice. In: *Frontiers in cell and developmental biology* 8, S. 533. DOI: 10.3389/fcell.2020.00533.

Miyata, Takaki; Kawaguchi, Ayano; Okano, Hideyuki; Ogawa, Masaharu (2001): Asymmetric Inheritance of Radial Glial Fibers by Cortical Neurons. In: *Neuron* 31 (5), S. 727–741. DOI: 10.1016/s0896-6273(01)00420-2.

Moazed, Danesh (2009): Small RNAs in transcriptional gene silencing and genome defence. In: *Nature* 457 (7228), S. 413–420. DOI: 10.1038/nature07756.

Moiseeva, Tatiana N.; Qian, Chenao; Sugitani, Norie; Osmanbeyoglu, Hatice U.; Bakkenist, Christopher J. (2019): WEE1 kinase inhibitor AZD1775 induces CDK1 kinase-dependent origin firing in unperturbed G1- and S-phase cells. In: *Proceedings of the National Academy of Sciences of the United States of America* 116 (48), S. 23891–23893. DOI: 10.1073/pnas.1915108116.

Moreno, Nerea; González, Agustín (2011): The non-evaginated secondary prosencephalon of vertebrates. In: *Frontiers in neuroanatomy* 5, S. 12. DOI: 10.3389/fnana.2011.00012.

Morgan, D. O. (1995): Principles of CDK regulation. In: *Nature* 374 (6518), S. 131–134. DOI: 10.1038/374131a0.

Morohoshi, Fumiko; Ootsuka, Yoshiko; Arai, Kyoko; Ichikawa, Hitoshi; Mitani, Sachiyo; Munakata, Nobuo; Ohki, Misao (1998): Genomic structure of the human RBP56/hTAFII68 and FUS/TLS genes. In: *Gene* 221 (2), S. 191–198. DOI: 10.1016/S0378-1119(98)00463-6.

Morris-Rosendahl, Deborah J.; Crocq, Marc-Antoine (2020): Neurodevelopmental disorders-the history and future of a diagnostic concept. In: *Dialogues in clinical neuroscience* 22 (1), S. 65–72. DOI: 10.31887/DCNS.2020.22.1/macrocq.

Moya, Pablo R.; Wendland, Jens R.; Salemme, Jennifer; Fried, Ruby L.; Murphy, Dennis L. (2013): miR-15a and miR-16 regulate serotonin transporter expression in human placental and rat brain raphe cells. In: *The international journal of neuropsychopharmacology* 16 (3), S. 621–629. DOI: 10.1017/S1461145712000454.

Müller, Myriam; Lutter, Daniela; Püschel, Andreas W. (2010): Persistence of the cell-cycle checkpoint kinase Wee1 in SadA- and SadB-deficient neurons disrupts neuronal polarity. In: *Journal of cell science* 123 (Pt 2), S. 286–294. DOI: 10.1242/jcs.058230.

Mulrane, Laoighse; McGee, Sharon F.; Gallagher, William M.; O'Connor, Darran P. (2013): miRNA dysregulation in breast cancer. In: *Cancer research* 73 (22), S. 6554–6562. DOI: 10.1158/0008-5472.CAN-13-1841.

Nadarajah, Bagirathy; Parnavelas, John G. (2002): Modes of neuronal migration in the developing cerebral cortex. In: *Nature reviews. Neuroscience* 3 (6), S. 423–432. DOI: 10.1038/nrn845.

Niu, Yingying; Zhou, Hongbo; Liu, Yancui; Wang, Yunfeng; Xie, Jinding; Feng, Chong; An, Ning (2019): miR-16 regulates proliferation and apoptosis of pituitary adenoma cells by inhibiting HMGA2. In: *Oncology letters* 17 (2), S. 2491–2497. DOI: 10.3892/ol.2018.9872.

Noctor, Stephen C.; Martínez-Cerdeño, Verónica; Kriegstein, Arnold R. (2008): Distinct behaviors of neural stem and progenitor cells underlie cortical neurogenesis. In: *The Journal of comparative neurology* 508 (1), S. 28–44. DOI: 10.1002/cne.21669.

Nurse, P.; Thuriaux, P. (1980): Regulatory genes controlling mitosis in the fission yeast Schizosaccharomyces pombe. In: *Genetics* 96 (3), S. 627–637. DOI: 10.1093/genetics/96.3.627.

Nurse, Paul (2004): Wee beasties. In: *Nature* 432 (7017), S. 557. DOI: 10.1038/432557a.

O'Brien, Jacob; Hayder, Heyam; Zayed, Yara; Peng, Chun (2018): Overview of MicroRNA Biogenesis, Mechanisms of Actions, and Circulation. In: *Frontiers in endocrinology* 9, S. 402. DOI: 10.3389/fendo.2018.00402.

Ozkul, Yusuf; Taheri, Serpil; Bayram, Kezban Korkmaz; Sener, Elif Funda; Mehmetbeyoglu, Ecmel; Öztop, Didem Behice et al. (2020): A heritable profile of six miRNAs in autistic patients and mouse models. In: *Scientific reports* 10 (1), S. 9011. DOI: 10.1038/s41598-020-65847-8.

Papagiannopoulos, Christos I.; Theodoroula, Nikoleta F.; Vizirianakis, Ioannis S. (2021): miR-16-5p Promotes Erythroid Maturation of Erythroleukemia Cells by Regulating Ribosome Biogenesis. In: *Pharmaceuticals (Basel, Switzerland)* 14 (2). DOI: 10.3390/ph14020137.

Paraskevopoulou, Maria D.; Hatzigeorgiou, Artemis G. (2016): Analyzing MiRNA-LncRNA Interactions. In: *Methods in molecular biology (Clifton, N.J.)* 1402, S. 271–286. DOI: 10.1007/978-1-4939-3378-5_21.

Patil, Mallikarjun; Pabla, Navjotsingh; Dong, Zheng (2013): Checkpoint kinase 1 in DNA damage response and cell cycle regulation. In: *Cellular and molecular life sciences : CMLS* 70 (21), S. 4009–4021. DOI: 10.1007/s00018-013-1307-3.

Peng, Yong; Croce, Carlo M. (2016): The role of MicroRNAs in human cancer. In: *Signal transduction and targeted therapy* 1, S. 15004. DOI: 10.1038/sigtrans.2015.4.

Pines, J. (1995): Cyclins and cyclin-dependent kinases. Theme and variations. In: *Advances in cancer research* 66, S. 181–212. DOI: 10.1016/s0065-230x(08)60254-7.

Plotnikova, Olga; Baranova, Ancha; Skoblov, Mikhail (2019): Comprehensive Analysis of Human microRNA-mRNA Interactome. In: *Frontiers in genetics* 10, S. 933. DOI: 10.3389/fgene.2019.00933.

Ponomarev, Eugene D.; Veremeyko, Tatyana; Barteneva, Natasha; Krichevsky, Anna M.; Weiner, Howard L. (2011): MicroRNA-124 promotes microglia quiescence and suppresses EAE by deactivating macrophages via the C/EBP-α-PU.1 pathway. In: *Nature medicine* 17 (1), S. 64–70. DOI: 10.1038/nm.2266.

Ponting, Chris P.; Oliver, Peter L.; Reik, Wolf (2009): Evolution and functions of long noncoding RNAs. In: *Cell* 136 (4), S. 629–641. DOI: 10.1016/j.cell.2009.02.006.

Porrello, Enzo R.; Johnson, Brett A.; Aurora, Arin B.; Simpson, Emma; Nam, Young-Jae; Matkovich, Scot J. et al. (2011): MiR-15 family regulates postnatal mitotic arrest of cardiomyocytes. In: *Circulation research* 109 (6), S. 670–679. DOI: 10.1161/CIRCRESAHA.111.248880.

Prantner, Andrew M.; Ord, Teri; Medvedev, Sergey; Gerton, George L. (2016): High-throughput sexing of mouse blastocysts by real-time PCR using dissociation curves. In: *Molecular reproduction and development*, S. 6–7. DOI: 10.1002/mrd.22595.

Prieto-Colomina, Anna; Fernández, Virginia; Chinnappa, Kaviya; Borrell, Víctor (2021): MiRNAs in early brain development and pediatric cancer. At the intersection between healthy and diseased embryonic development. In: *BioEssays : news and reviews in molecular, cellular and developmental biology* 43 (7), e2100073. DOI: 10.1002/bies.202100073.

Radhakrishnan, Balachandar; Alwin Prem Anand, A. (2016): Role of miRNA-9 in Brain Development. In: *Journal of experimental neuroscience* 10, S. 101–120. DOI: 10.4137/JEN.S32843.

Rajman, Marek; Schratt, Gerhard (2017): MicroRNAs in neural development. From master regulators to fine-tuners. In: *Development (Cambridge, England)* 144 (13), S. 2310–2322. DOI: 10.1242/dev.144337.

Rakic, P. (1972): Mode of cell migration to the superficial layers of fetal monkey neocortex. In: *The Journal of comparative neurology* 145 (1), S. 61–83. DOI: 10.1002/cne.901450105.

Rakic, Pasko (2009): Evolution of the neocortex. A perspective from developmental biology. In: *Nature reviews. Neuroscience* 10 (10), S. 724–735. DOI: 10.1038/nrn2719.

Rice, D. S.; Curran, T. (2001): Role of the reelin signaling pathway in central nervous system development. In: *Annual review of neuroscience* 24, S. 1005–1039. DOI: 10.1146/annurev.neuro.24.1.1005.

Rie, Derek de; Abugessaisa, Imad; Alam, Tanvir; Arner, Erik; Arner, Peter; Ashoor, Haitham et al. (2017): An integrated expression atlas of miRNAs and their promoters in human and mouse. In: *Nature biotechnology* 35 (9), S. 872–878. DOI: 10.1038/nbt.3947.

Romero-Cordoba, Sandra L.; Salido-Guadarrama, Ivan; Rodriguez-Dorantes, Mauricio; Hidalgo-Miranda, Alfredo (2014): miRNA biogenesis. Biological impact in the development of cancer. In: *Cancer biology & therapy* 15 (11), S. 1444–1455. DOI: 10.4161/15384047.2014.955442.

Russo, Vincenzo E. A. (Hg.) (1996): Epigenetic mechanisms of gene regulation. Plainview, NY: Cold Spring Harbor Laboratory Press (Cold Spring Harbor monograph series, 32).

Sárközy, Márta; Kahán, Zsuzsanna; Csont, Tamás (2018): A myriad of roles of miR-25 in health and disease. In: *Oncotarget* 9 (30), S. 21580–21612. DOI: 10.18632/oncotarget.24662.

Sauer, Mareike; Fleischmann, Thea; Lipiski, Miriam; Arras, Margarete; Jirkof, Paulin (2016): Buprenorphine via drinking water and combined oral-injection protocols for pain relief in mice. In: *Applied Animal Behaviour Science* 185 (5), S. 103–112. DOI: 10.1016/j.applanim.2016.09.009.

Schepici, Giovanni; Cavalli, Eugenio; Bramanti, Placido; Mazzon, Emanuela (2019): Autism Spectrum Disorder and miRNA. An Overview of Experimental Models. In: *Brain sciences* 9 (10). DOI: 10.3390/brainsci9100265.

Schwarzenbach, Heidi (2016): Clinical significance of miR-15 and miR-16 in ovarian cancer. In: *Transl. Cancer Res* 5 (S1), S50-S53. DOI: 10.21037/tcr.2016.04.14.

Sempere, Lorenzo F.; Freemantle, Sarah; Pitha-Rowe, Ian; Moss, Eric; Dmitrovsky, Ethan; Ambros, Victor (2004): Expression profiling of mammalian microRNAs uncovers a subset of brain-expressed microRNAs with possible roles in murine and human neuronal differentiation. In: *Genome biology* 5 (3), R13. DOI: 10.1186/gb-2004-5-3-r13.

Sen, Chandan K. (2014): MicroRNA in regenerative medicine [Elektronische Ressource]. Amsterdam: Academic Press. Online verfügbar unter http://www.sciencedirect.com/science/book/9780124055445.

Sessa, Alessandro; Mao, Chai-An; Hadjantonakis, Anna-Katerina; Klein, William H.; Broccoli, Vania (2008): Tbr2 directs conversion of radial glia into basal precursors and guides neuronal amplification by indirect neurogenesis in the developing neocortex. In: *Neuron* 60 (1), S. 56–69. DOI: 10.1016/j.neuron.2008.09.028.

Shenoy, Archana; Danial, Muhammad; Blelloch, Robert H. (2015): Let-7 and miR-125 cooperate to prime progenitors for astrogliogenesis. In: *The EMBO journal* 34 (9), S. 1180–1194. DOI: 10.15252/embj.201489504.

Shi, Yanhong; Zhao, Xinyu; Hsieh, Jenny; Wichterle, Hynek; Impey, Soren; Banerjee, Sourav et al. (2010): MicroRNA regulation of neural stem cells and neurogenesis. In: *The Journal of neuroscience : the official journal of the Society for Neuroscience* 30 (45), S. 14931–14936. DOI: 10.1523/JNEUROSCI.4280-10.2010.

Soriano, Eduardo; Del Río, José Antonio (2005): The cells of cajal-retzius. Still a mystery one century after. In: *Neuron* 46 (3), S. 389–394. DOI: 10.1016/j.neuron.2005.04.019.

Stefani, Giovanni; Slack, Frank J. (2008): Small non-coding RNAs in animal development. In: *Nature reviews. Molecular cell biology* 9 (3), S. 219–230. DOI: 10.1038/nrm2347.

Stiles, Joan; Jernigan, Terry L. (2010): The basics of brain development. In: *Neuropsychology review* 20 (4), S. 327–348. DOI: 10.1007/s11065-010-9148-4.

Sun, GuoQiang; Ye, Peng; Murai, Kiyohito; Lang, Ming-Fei; Li, Shengxiu; Zhang, Heying et al. (2011): miR-137 forms a regulatory loop with nuclear receptor TLX and LSD1 in neural stem cells. In: *Nature communications* 2, S. 529. DOI: 10.1038/ncomms1532.

Sun, Tao; Hevner, Robert F. (2014): Growth and folding of the mammalian cerebral cortex. From molecules to malformations. In: *Nature reviews. Neuroscience* 15 (4), S. 217–232. DOI: 10.1038/nrn3707.

Takada, Mamoru; Zhang, Weiguo; Suzuki, Aussie; Kuroda, Taruho S.; Yu, Zhouliang; Inuzuka, Hiroyuki et al. (2017): FBW7 Loss Promotes Chromosomal Instability and

Tumorigenesis via Cyclin E1/CDK2-Mediated Phosphorylation of CENP-A. In: *Cancer research* 77 (18), S. 4881–4893. DOI: 10.1158/0008-5472.CAN-17-1240.

Takahashi, T.; Nowakowski, R. S.; Caviness, V. S. (1995): The cell cycle of the pseudostratified ventricular epithelium of the embryonic murine cerebral wall. In: *J. Neurosci.* 15 (9), S. 6046–6057. DOI: 10.1523/JNEUROSCI.15-09-06046.1995.

Taverna, Elena; Götz, Magdalena; Huttner, Wieland B. (2014): The cell biology of neurogenesis. Toward an understanding of the development and evolution of the neocortex. In: *Annual review of cell and developmental biology* 30, S. 465–502. DOI: 10.1146/annurev-cellbio-101011-155801.

Therrien, Martine; Parker, J. Alex (2014): Worming forward. Amyotrophic lateral sclerosis toxicity mechanisms and genetic interactions in Caenorhabditis elegans. In: *Frontiers in genetics* 5, S. 85. DOI: 10.3389/fgene.2014.00085.

Therrien, Martine; Rouleau, Guy A.; Dion, Patrick A.; Parker, J. Alex (2016): FET proteins regulate lifespan and neuronal integrity. In: *Scientific reports* 6, S. 25159. DOI: 10.1038/srep25159.

Vahia, Vihang N. (2013): Diagnostic and statistical manual of mental disorders 5. A quick glance. In: *Indian journal of psychiatry* 55 (3), S. 220–223. DOI: 10.4103/0019-5545.117131.

Valiente, Manuel; Marín, Oscar (2010): Neuronal migration mechanisms in development and disease. In: *Current opinion in neurobiology* 20 (1), S. 68–78. DOI: 10.1016/j.conb.2009.12.003.

Verlinden, Lieve; Vanden Bempt, Isabelle; Eelen, Guy; Drijkoningen, Maria; Verlinden, Ilse; Marchal, Kathleen et al. (2007): The E2F-regulated gene Chk1 is highly expressed in triple-negative estrogen receptor /progesterone receptor /HER-2 breast carcinomas. In: *Cancer research* 67 (14), S. 6574–6581. DOI: 10.1158/0008-5472.CAN-06-3545.

Vermeulen, Katrien; van Bockstaele, Dirk R.; Berneman, Zwi N. (2003): The cell cycle. A review of regulation, deregulation and therapeutic targets in cancer. In: *Cell proliferation* 36 (3), S. 131–149. DOI: 10.1046/j.1365-2184.2003.00266.x.

Vo, Ngan K.; Cambronne, Xiaolu A.; Goodman, Richard H. (2010): MicroRNA pathways in neural development and plasticity. In: *Current opinion in neurobiology* 20 (4), S. 457–465. DOI: 10.1016/j.conb.2010.04.002.

Wang, Chi Chiu (2004): Development of the Rhombencephalon. Molecular Evolution and Genetic Regulation. In: *Neuroembryol and Aging* 3 (2), S. 78–91. DOI: 10.1159/000088208.

Wang, Chunlei; Mei, Lin (2013): In utero electroporation in mice. In: *Methods in molecular biology (Clifton, N.J.)* 1018, S. 151–163. DOI: 10.1007/978-1-62703-444-9_15.

Wang, Qi; Chen, Yaokun; Lu, Haijun; Wang, Haiji; Feng, Hui; Xu, Jinpeng; Zhang, Biyuan (2020): Quercetin radiosensitizes non-small cell lung cancer cells through the regulation of miR-16-5p/WEE1 axis. In: *IUBMB life* 72 (5), S. 1012–1022. DOI: 10.1002/iub.2242.

Wang, Si; Zhu, Wenhua; Xu, Jing; Guo, Yuanxu; Yan, Jidong; Meng, Liesu et al. (2019): Interpreting the MicroRNA-15/107 family. Interaction identification by combining network based and experiment supported approach. In: *BMC medical genetics* 20 (1), S. 96. DOI: 10.1186/s12881-019-0824-9.

Wei, Jianghong; Jia, Aijun; Ma, Libing; Wang, Yueling; Qiu, Lulu; Xiao, Bing (2020): MicroRNA-16 inhibits the proliferation and metastasis of human lung cancer cells by modulating the expression of YAP1. In: *Journal of B.U.ON. : official journal of the Balkan Union of Oncology* 25 (2), S. 862–868.

Wei, Jian-Wei; Huang, Kai; Yang, Chao; Kang, Chun-Sheng (2017): Non-coding RNAs as regulators in epigenetics (Review). In: *Oncology reports* 37 (1), S. 3–9. DOI: 10.3892/or.2016.5236.

Weinhold, Bob (2006): Epigenetics. The science of change. In: *Environmental health perspectives* 114 (3), A160-7. DOI: 10.1289/ehp.114-a160.

Welcker, Markus; Orian, Amir; Grim, Jonathan E.; Grim, Jonathan A.; Eisenman, Robert N.; Clurman, Bruce E. (2004): A nucleolar isoform of the Fbw7 ubiquitin ligase regulates c-Myc and cell size. In: *Current biology : CB* 14 (20), S. 1852–1857. DOI: 10.1016/j.cub.2004.09.083.

Winter, Julia; Jung, Stephanie; Keller, Sarina; Gregory, Richard I.; Diederichs, Sven (2009): Many roads to maturity. MicroRNA biogenesis pathways and their regulation. In: *Nature cell biology* 11 (3), S. 228–234. DOI: 10.1038/ncb0309-228.

Xu, Wenlong; San Lucas, Anthony; Wang, Zixing; Liu, Yin (2014): Identifying microRNA targets in different gene regions. In: *BMC bioinformatics* 15 Suppl 7, S4. DOI: 10.1186/1471-2105-15-S7-S4.

Yan, Xin; Liang, Hongwei; Deng, Ting; Zhu, Kegan; Zhang, Suyang; Wang, Nan et al. (2013): The identification of novel targets of miR-16 and characterization of their biological functions in cancer cells. In: *Molecular cancer* 12, S. 92. DOI: 10.1186/1476-4598-12-92.

Yang, Fan; Deng, Xinxian; Ma, Wenxiu; Berletch, Joel B.; Rabaia, Natalia; Wei, Gengze et al. (2015): The lncRNA Firre anchors the inactive X chromosome to the nucleolus by binding CTCF and maintains H3K27me3 methylation. In: *Genome biology* 16, S. 52. DOI: 10.1186/s13059-015-0618-0.

Yeh, Chien-Hung; Bellon, Marcia; Nicot, Christophe (2018): FBXW7. A critical tumor suppressor of human cancers. In: *Molecular cancer* 17 (1), S. 115. DOI: 10.1186/s12943-018-0857-2.

Yin, Yunping; Shen, Qian; Tao, Ruikang; Chang, Weilong; Li, Ruidong; Xie, Gengchen et al. (2018): Wee1 inhibition can suppress tumor proliferation and sensitize p53 mutant

colonic cancer cells to the anticancer effect of irinotecan. In: *Molecular medicine reports* 17 (2), S. 3344–3349. DOI: 10.3892/mmr.2017.8230.

Zaratiegui, Mikel; Irvine, Danielle V.; Martienssen, Robert A. (2007): Noncoding RNAs and gene silencing. In: *Cell* 128 (4), S. 763–776. DOI: 10.1016/j.cell.2007.02.016.

Zeng, Y.; Forbes, K. C.; Wu, Z.; Moreno, S.; Piwnica-Worms, H.; Enoch, T. (1998): Replication checkpoint requires phosphorylation of the phosphatase Cdc25 by Cds1 or Chk1. In: *Nature* 395 (6701), S. 507–510. DOI: 10.1038/26766.

Zhang, Ran; Huang, Min; Cao, Zhijuan; Qi, Jieyu; Qiu, Zilong; Chiang, Li-Yang (2015): MeCP2 plays an analgesic role in pain transmission through regulating CREB / miR-132 pathway. In: *Molecular pain* 11, S. 19. DOI: 10.1186/s12990-015-0015-4.

Zhang, Youwei; Hunter, Tony (2014): Roles of Chk1 in cell biology and cancer therapy. In: *International journal of cancer* 134 (5), S. 1013–1023. DOI: 10.1002/ijc.28226.

Zhu, Jie; Zhang, Bin; Song, Wenfeng; Zhang, Xie; Wang, Lei; Yin, Bowei et al. (2016): A literature review on the role of miR-370 in disease. In: *Gene Reports* 4 (Suppl. B), S. 37–44. DOI: 10.1016/j.genrep.2016.02.005.

Zubillaga-Guerrero, Ma Isabel; Illades-Aguiar, Berenice; Flores-Alfaro, Eugenia; Castro-Coronel, Yaneth; Jiménez-Wences, Hilda; Patiño, Esther Ivonne López-Bayghen et al. (2020): An increase of microRNA-16-1 is associated with the high proliferation of squamous intraepithelial lesions in the presence of the integrated state of HR-HPV in liquid cytology samples. In: *Oncology letters* 20 (4), S. 104. DOI: 10.3892/ol.2020.11965.

Attachment

1. Table of abbreviations

NPCs: neuronal progenitor cells

RGCs: radial glia cells

IPCs: intermediate progenitor cells

ASD: autism spectrum disorder

miRNAs: micro ribonucleic acids

et al.: et alii

E XY: embryonic day XY of mouse development

P XY: postnatal day XY of mouse development

EGF: epidermal growth factor

FGF: fibroblast growth factor

RT: room temperature

GFP: green fluorescent protein

FACS: Fluorescent activated cell sorting

EtOH: Ethanol

H_2O: water

DEGs: differentially expressed genes

XY h: XY hours

XY min: XY minutes

N2A cells: neuroblastoma cell line, murine

HEK293 cells: human embryonic kidney cells, human

g: G- Force

rpm: rounds per minute

V: volt

SCR: scrambled control

2. Target genes of miR-16 with predicted miR-16 binding sites in TargetScan

Abbreviation	Gene Name
Actr2	Actin Related Protein 2
Asf1b	Anti-Silencing Function Protein 1
Atp5g1	ATP Synthase, H+ Transporting, Mitochondrial F0 Complex, Subunit C1
Atxn7l3b	Ataxin-7-Like Protein 3B
Capns1	Calcium-Dependent Protease Small Subunit 1
Cdca7l	Cell Division Cycle Associated 7 Like
Cdk1	Cyclin Dependent Kinase 1
Chek1	Checkpoint Kinase 1
Clspn	Claspin
Ddx39	DExD-Box Helicase 39A
Fbxw7	F-Box and WD Repeat Domain Containing 7
Mob3b	MOB Kinase Activator 3B
Myb	MYB Proto-Oncogene, Transcription Factor
Mybl1	MYB Proto-Oncogene Like 1
Nucks1	Nuclear Casein Kinase and Cyclin Dependent Kinase Substrate 1
Rad51	RAD51 Recombinase
Sgk1	Serum/Glucocorticoid Regulated Kinase 1
Shcbp1	SHC Binding and Spindle Associated 1
Stk33	Serine/Threonine Kinase 33
Taf15	TATA-Box Binding Protein Associated Factor 15
Tmem183a	Transmembrane Protein 183A
Ubfd1	Ubiquitin Family Domain Containing 1
Wee1	WEE1 G2 Checkpoint Kinase
Wnt7a	Wnt Family Member 7A
Ywhah	Tyrosine 3-Monooxygenase/Tryptophan 5-Monooxygenase Activation Protein Eta
Zfp367	Zinc Finger Protein 367

Table 40: List of downregulated miR-16 target genes with miR-16 binding site in TargetScan. Genes display decreased expression after miR-16 overexpression in the developing neocortex. Data obtained from mRNA sequencing.

3. List of figures and tables

4. Statement of Authorship (Selbstständigkeitserklärung)

Hiermit erkläre ich, Laura Schlichtholz (geboren am 14.06.1992 in Freiburg im Breisgau), die hier vorliegende Arbeit selbstständig und ohne unerlaubte Hilfe angefertigt zu haben und alle verwendeten Hilfsmittel und Inhalte aus anderen Quellen als solche kenntlich gemacht zu haben. Zudem versichere ich, dass die vorliegende Arbeit noch an keiner anderen Fakultät oder Universität zur Prüfung vorgelegen hat.

Mir ist der Inhalt der Promotionsordnung bekannt.

Laura Schlichtholz